



HAL
open science

Osteological revision of the holotype of the Middle Jurassic sauropod dinosaur *Patagosaurus fariasi* (Sauropoda: Cetiosauridae) BONAPARTE 1979

Femke Holwerda, Oliver W.M. Rauhut, Pol Diego

► **To cite this version:**

Femke Holwerda, Oliver W.M. Rauhut, Pol Diego. Osteological revision of the holotype of the Middle Jurassic sauropod dinosaur *Patagosaurus fariasi* (Sauropoda: Cetiosauridae) BONAPARTE 1979. 2020. hal-02977029

HAL Id: hal-02977029

<https://hal.science/hal-02977029>

Preprint submitted on 27 Oct 2020

HAL is a multi-disciplinary open access archive for the deposit and dissemination of scientific research documents, whether they are published or not. The documents may come from teaching and research institutions in France or abroad, or from public or private research centers.

L'archive ouverte pluridisciplinaire **HAL**, est destinée au dépôt et à la diffusion de documents scientifiques de niveau recherche, publiés ou non, émanant des établissements d'enseignement et de recherche français ou étrangers, des laboratoires publics ou privés.

1 **Osteological revision of the holotype of the Middle Jurassic sauropod**
2 **dinosaur *Patagosaurus fariasi* (Sauropoda: Cetiosauridae)**

3 **BONAPARTE 1979**

4

5 **Femke M Holwerda¹²³⁴, Oliver W M Rauhut¹⁵⁶, Diego Pol⁷⁸**

6

7 1 Staatliche Naturwissenschaftliche Sammlungen Bayerns (SNSB), Bayerische Staatssammlung für
8 Paläontologie und Geologie, Richard-Wagner-Strasse 10, 80333 München, Germany

9

10 2 Department of Geosciences, Utrecht University, Princetonlaan, 3584 CD Utrecht, 10 Netherlands

11

12 3 Royal Tyrrell Museum of Palaeontology, Drumheller, AlbertaT0J 0Y0, Canada (current)

13

14 4 Fachgruppe Paläoumwelt, GeoZentrum Nordbayern, Friedrich-Alexander-Universität Erlangen-
15 Nürnberg, Loewenichstr. 28, 91054 Erlangen, Germany

16

17 5 Department für Umwelt- und Geowissenschaften, Ludwig-Maximilians-Universität München, Richard-
18 Wagner-Str. 10, 80333 München, Germany

19

20 6 GeoBioCenter, Ludwig-Maximilians-Universität München, Richard-Wagner-Str. 10, 80333 16 München,
21 Germany

22

23 7 Consejo Nacional de Investigaciones Científicas y Técnicas (CONICET), Argentina

24

25 8 Museo Paleontológico Egidio Feruglio, Avenida Fontana 140, Trelew, Argentina

26

27

28

29

30 **ABSTRACT**

31 Middle Jurassic sauropod taxa are poorly known, due to a stratigraphic bias of localities
32 yielding body fossils. One such locality is Cerro Cóndor North, Cañadón Asfalto Formation,
33 Patagonia, Argentina, dated to latest Early–Middle Jurassic. From this locality, the holotype
34 of *Patagosaurus fariasi* Bonaparte 1986 is revised. The material consists of the axial
35 skeleton, the pelvic girdle, and the right femur. *Patagosaurus* is mainly characterised by a
36 combination of features mainly identified on the axial skeleton, including the following: (1)
37 cervical centra with low Elongation Index, (2) high projection of the postzygodiapophyseal
38 lamina, (3) deep anterior pleurocoels that are sometimes compartmentalized in cervicals, (4)
39 high projection of the neural arch and spine in dorsal vertebrae and anterior(most) caudal
40 vertebrae, (5) deep pneumatic foramina in posterior dorsals which connect into an internal
41 pneumatic chamber, (6) anterior caudal vertebrae with ‘saddle’ shaped neural spines.
42 Diagnostic features on the appendicular skeleton include (7) a transversely wide and
43 anteroposteriorly short femur, (8) a medial placement of the fourth trochanter on the
44 femur, and (9) an anteroposteriorly elongated ilium with a rounded dorsal rim, with hook-
45 shaped anterior lobe. The characters that are diagnostic for *Patagosaurus* are discussed, and
46 the osteology of *Patagosaurus* is compared to that of Early and Middle Jurassic
47 (eu)sauropods from both Laurasia and Gondwana.

48

49 **Keywords:** Sauropoda, Eusauropoda, *Patagosaurus*, Gondwana, Middle Jurassic,
50 pneumaticity

51

52 INTRODUCTION

53 The late Early to Middle Jurassic is an important time window for sauropod evolution, as
54 phylogenetic studies indicate this was the time when most major lineages diversified and
55 spread worldwide. Even though the Late Jurassic shows a diversity peak, the earlier stages of
56 the Jurassic (or perhaps even the latest Triassic) seem to have been the time of the start of

57 this rise in sauropods (Yates 2003; Barrett & Upchurch 2005; Irmis *et al.* 2007; Allain &
58 Aquesbi 2008; Mannion & Upchurch 2010; Yates *et al.* 2010; McPhee *et al.* 2014, 2015,
59 2016; Xu *et al.* 2018). Not many terrestrial deposits remain from the specific time window
60 that is the Early - Middle Jurassic, and fewer still contain diagnostic basal sauropod or basal
61 non-neosauropod eusauropod material.

62 Notable Early Jurassic examples are *Isanosaurus attavipachi* from Thailand Buffetaut *et al.*,
63 2002, (Laoyumpon *et al.* 2017); *Sanpasaurus yaoi* McPhee *et al.*, 2016 from China;
64 *Barapasaurus tagorei* Jain *et al.*, 1975, *Kotasaurus yamanpalliensis* Yadagiri, 1988 from India,
65 (Yadagiri 2001; Bandyopadhyay *et al.* 2010); and indeterminate non-neosauropodan
66 material from Morocco (Nicholl *et al.* 2018); *Vulcanodon karibaensis* Raath, 1972 from
67 Zimbabwe (Cooper 1984); and the Elliot Formation ?sauropodiform/sauropodomorph
68 fauna from South Africa and Lesotho (McPhee *et al.* 2017).

69 Notable Middle Jurassic examples are the cetiosaurs from the UK, e.g. *Cetiosaurus*
70 *oxoniensis* Phillips, 1871, the Rutland *Cetiosaurus* and cetiosaurid and gravisaurian material
71 from England, Scotland and Germany (von Huene 1927; Upchurch and Martin 2002, 2003;
72 Liston 2004; Galton 2005; Barrett 2006; Buffetaut *et al.* 2011; Brusatte *et al.* 2015; Stumpf *et*
73 *al.* 2015; Clark and Gavin 2016; Holwerda *et al.* 2019); *Datousaurus bashanensis* Dong &
74 Tang 1984, *Nebulasaurus taito* Xing *et al.*, 2015, *Lingwulong shenqi* Xu *et al.*, 2018, and
75 the mamenchisaur fauna from China (Young and Zhao 1972; Russell and Zheng 1993; Pi *et al.*
76 1996; Moore *et al.* 2018; Wang *et al.* 2018); *Tazoudasaurus naimi* Allain *et al.*, 2004,
77 *Spinophorosaurus nigerensis* Remes *et al.*, 2009 and *Chebsaurus algeriensis* Mahammed *et*
78 *al.*, 2005 from North Africa (Allain and Aquesbi 2008); indeterminate non-neosauropodan
79 material and *Lapparentosaurus madagascariensis* Bonaparte 1986a from Madagascar (Läng
80 2008; Mannion 2010), and finally, *Patagosaurus fariasi* Bonaparte, 1979, *Volkheimeria*

81 *chubutensis* Bonaparte 1979 and *Amygdalodon patagonicus* Cabrera, 1947 (Bonaparte
82 1986b; Rauhut 2003) from Argentina.

83 Some sauropods that were traditionally considered to be Middle Jurassic might originate
84 from the Late Jurassic; (*Rhoetosaurus brownei* Longman, 1926 from Australia (Nair and
85 Salisbury 2012; Todd et al. 2019), *Shunosaurus lii* Dong et al., 1983 and *Omeisaurus*
86 *junghsiensis* Young, 1939 from China (He et al. 1984, 1988; Zhang 1988; Tang et al. 2001;
87 Chatterjee and Zheng 2002; Peng et al. 2005; and see Wang et al. 2018 for refined ages). For
88 a short overview of some of these Early and Middle Jurassic sauropods, see Holwerda and
89 Pol (2018).

90

91 In Patagonia, Argentina, the Cañadón Asfalto Formation (Stipanicic et al. 1968; Tasch and
92 Volkheimer 1970), is one of the few geological units worldwide to contain several latest
93 Early to early Middle Jurassic eusauropod fossils. It crops out in west-central Patagonia,
94 Argentina, and has recently been dated as ranging from the Toarcian to the
95 Aalenien/Bajocian (Cúneo et al. 2013). The sauropod fauna of this unit includes
96 *Patagosaurus fariasi*, *Volkheimeria chubutensis* (Bonaparte 1979), and at least two
97 undescribed taxa (Rauhut 2002, 2003; Pol et al. 2009; Holwerda et al. 2015; Becerra et al.
98 2016; Carballido et al. 2017a).

99 Patagonia first came under the attention of vertebrate palaeontologists by the discovery of
100 the basal sauropod *Amygdalodon patagonicus* by Cabrera (1947), and later by Casamiquela
101 (1963) from the Pampa de Agnia locality, Cerro Carnerero Formation (Rauhut 2003a). These
102 beds were revisited in 1976, but no further discovery was made, until another excursion in
103 Patagonia, about 50 Km further away in the Cañadón Asfalto Formation, in 1977, was
104 successful. José Bonaparte led numerous additional expeditions to the region between 1977
105 and 1986, during which *Patagosaurus fariasi*, *Volkheimeria chubutensis* and the theropod
106 *Piatnitzkysaurus floresi* Bonaparte, 1979 were found and described (Bonaparte 1979, 1986b,

107 1996; Rauhut 2004). Since then, numerous other dinosaurs and other vertebrates have been
108 discovered in the Cañadón Asfalto Formation; see Escapa et al. (2008), Cuneo et al (2013)
109 and Olivera et al. (2015). The MPEF in Trelew has more recently visited the locality of Cerro
110 Cóndor South to uncover more material, of which only one element has been described
111 (Rauhut 2003b).

112 Thus far, *Patagosaurus* is the only well-known sauropod taxon from this area, and one of the
113 few sauropods from the Middle Jurassic outside of China, known from abundant material. It
114 was coined by Bonaparte in 1979; *Patagosaurus* for Patagonia, and *fariasi* to honour the
115 owners of the Farias farmland, on which it was discovered. It has been included in numerous
116 phylogenetic studies (e.g. Upchurch 1998; Wilson 2002; Upchurch et al. 2004; Harris 2006;
117 Allain and Aquesbi 2008; Wilson and Upchurch 2009; Carballido et al. 2011, 2012; Holwerda
118 and Pol 2018). However, the only description of this taxon published so far (Bonaparte,
119 1986b) is not only based on the holotype, but also draws information from a selection of
120 associated material, representing several individuals from different localities, therefore not
121 guaranteeing these are all *Patagosaurus* individuals. Some of the associated material comes
122 partially from the same bonebed as the holotype, but others come from a nearby bonebed
123 (Bonaparte 1979; Bonaparte 1986a). Since this description, new sauropod finds from the
124 Cañadón Asfalto Formation show a higher sauropod diversity for this unit than previously
125 assumed (Pol et al. 2009). Furthermore, recent studies of *Patagosaurus* material revealed
126 the probable presence of another taxon in the associated material (Rauhut 2002; Rauhut
127 2003). In light of this, a revision of *Patagosaurus* is needed.

128

129 **MATERIAL AND METHODS**

130

131 **ANATOMICAL ABBREVIATIONS**

132

133 *Terminology:* Wilson (1999) is followed for the terminology of vertebral laminae, with some
134 modifications based on Carballido and Sander (2014). The terminology of vertebral fossae
135 follows Wilson *et al.* (2011).

136 As was already pointed out by Wedel (2003) and Carballido and Sander (2014), the term
137 pleurocoel has not been rigourously defined. The term, however, was used in that paper for
138 a lateral excavation on the vertebral centrum with clearly defined anterior, ventral and
139 dorsal margins, and a usually less clearly defined but still visible posterior margin (Carballido
140 and Sander 2014). As this description is applicable for the lateral pneumatopores found in
141 *Patagosaurus*, it will be used in this sense.

142 The use of 'anterior' and 'posterior' is preferred instead of 'cranial' and 'caudal'. This is to
143 avoid confusion when describing, for instance, the caudal vertebrae.

144

145 *Laminae:* **acdl:** anterior centrodiapophyseal lamina; **acpl:** anterior centroparapophyseal
146 lamina; **cpol:** centropostzygapophyseal lamina; **cpri:** centroprezygapophyseal lamina; **pcdl:**
147 posterior centrodiapophyseal lamina; **podl:** postzygadiapophyseal lamina; **posl:** postspinal
148 lamina; **ppdl:** parapodiapophyseal lamina; **prdl:** prezygodiapophyseal lamina; **prsl:** prespinal
149 lamina; **spdl:** spinodiapophyseal lamina; **spol:** spinopostzygapophyseal lamina; **sprl:**
150 spinoprezygapophyseal lamina; **stpol:** single intrapostzygapophyseal lamina; **stprl:** single-
151 intraprezygapophyseal laminal; **tpri:** intraprezygapophyseal lamina; **tpol:**
152 intrapostzygapophyseal lamina;

153

154 *Fossae:* **cdf,** centrodiapophyseal fossa (fenestrae for some posterior dorsals); **cpof,**
155 centropostzygapophyseal fossa; **cprf,** centroprezygapophyseal fossa; **ivf,** intervertebral
156 fossa; **pocdf,** postzygapophyseal centrodiapophyseal fossa; **posdf,** postzygapophyseal
157 spinodiapophyseal fossa; **prcdf,** prezygapophyseal centrodiapophyseal fossa; **prsdof,**

158 prezygospinodiapophyseal fossa; **sdf**, spinodiapophyseal fossa; **spof**, spinopostzygapophyseal
159 fossa; **sprf**, spinoprezygapophyseal fossa

160

161 *Institutional abbreviations:* LEICT: New Walk Museum and Art Gallery, Leicester Arts and
162 Museum Service, Leicester, UK. MACN: Museo Argentino de Ciencias Naturales ‘Bernardino
163 Rivadavia’, Buenos Aires, Argentina. MNHN-MAA: Musee National d’Histoire Naturelle,
164 Paris, France. OUMNH: Oxford University Museum of Natural History, Oxford, UK. PVL:
165 Paleovertebrados, Instituto Miguel Lillo, Tucuman, Argentina.

166

167 **SYSTEMATIC PALEONTOLOGY**

168 SAURISCHIA SEELEY 1887

169 SAUROPODA MARSH 1878

170 EUSAUROPODA UPCHURCH 1995

171 CETIOSAURIDAE LYDEKKER 1888

172 *PATAGOSAURUS* BONAPARTE 1979

173 *PATAGOSAURUS FARIASI* BONAPARTE 1979

174

175 *Holotype:* PVL 4170, consisting of several anterior, middle and posterior cervical vertebrae,
176 PVL 4170 1-9, anterior, mid- and posterior dorsals, PVL 4170 10-17, anterior caudals 19-25
177 and middle to posterior caudals 26-32, sacrum, PVL 4170 18, fused ischia, PVL 4170 36, right
178 ilium, PVL 4170 34, right pubis, PVL 4170 35, and right femur, PVL 4170 37. See Table 1 and 2
179 for vertebral measurements, and Table 3 for appendicular measurements. The holotype was
180 said to also contain a scapula and coracoid (Bonaparte, 1986a), but these could
181 unfortunately not be located in the collections. In the collections of the MACN we found two
182 elements labelled as MACN-CH 1986 scapula ‘A’ and coracoid ‘B’, which might be these
183 holotypic elements; however, at present the association of these bones with the holotype is

184 uncertain, and the association with another *Patagosaurus* specimen, MACN-CH 935, is also
185 likely, due to close association of these elements with MACN-CH 935 on the excavation map.
186 A large humerus is also indicated in the original quarry map for the holotype, however, the
187 only large humerus retrieved from the PVL collections is from another locality, Cerro C6ndor
188 South. Originally, associated teeth with typical eusauropod wrinkled enamel were
189 mentioned (Bonaparte 1986b). However, no directly associated teeth or tooth-bearing
190 bones are known for the holotype specimen, so that these teeth are not regarded as part of
191 the holotype here and were not used in the diagnosis, even though some are ascribed to
192 *Patagosaurus* (Holwerda et al. 2015). Ribs and chevrons appear on the quarry map of the
193 holotype, but are mixed in with ribs and chevrons of other *Patagosaurus* specimens, and will
194 therefore be omitted from the holotype description.

195

196 *Original Diagnosis (Bonaparte 1986b):* Cetiosaurid of large size, with tall dorsal vertebrae;
197 posterior dorsals with elevated neural arches and well-developed neural spines, formed
198 from 4 divergent laminae and with a massive dorsal region; dorsoventrally-oriented neural
199 spine cavities, more expanded than in *Barapasaurus*. Anterior and lateral regions of the
200 neural arch similar to that of *Cetiosaurus* and *Barapasaurus*. Sacrum with 5 vertebrae,
201 elevated neural spines, and a large dilation of the neural canal forming a neural cavity. Pelvis
202 with pubis showing distal and proximolateral expansions, more developed than
203 in *Barapasaurus*, and a less expanded pubic symphysis than in *Amygdalodon*. Ischium
204 slightly transversely compressed, with a ventromedial ridge of sublaminar type, and with a
205 clear distal expansion. Ratio of tibia-femur lengths from 1:1.5 in juveniles, reaching 1:1.7 in
206 adults. Mandible with weak medial torsion. Spatulate teeth with occlusal traces.

207

208 *Emended diagnosis: Patagosaurus fariasi* is a non-neosauropodan eusauropod dinosaur that
209 can be diagnosed on the basis of the following morphological features, and the following

210 combination of characters (features with * are tentatively considered autapomorphies): 1)
211 cervical and anterior dorsal vertebrae with marked pleurocoel, which is deep in cervicals but
212 shallower in dorsals. In cervical vertebrae, the pleurocoel is deeper anteriorly with well
213 defined margins, but becomes shallow posteriorly and has only well defined dorsal and
214 ventral margins. 2) In several cervicals, a faint oblique accessory lamina is present, dividing
215 the pleurocoel into an anterior deeper part and a posteriorly shallower part. 3) The cervicals
216 have a relatively high neural spine, accompanied by high dorsal placement of
217 postzygapophyses, which results in a high angle between the postzygodiapophyseal and
218 posterior centrodiaepophyseal laminae of about 55°. 4) Posterior dorsal neural arches with a
219 centrodiaepophyseal fossa that extends internally as a pneumatic structure, which is
220 separated by the mirroring structure by a thin septum, and both of which connect into a
221 ventral, oval shaped internal pneumatic chamber, which is dorsal to and well separated from
222 the neural canal*. 5) Posterior dorsals with small round excavations on the posterior side of
223 the distal extremity of the diapophyses*. 6) Posteriormost dorsals have rudimentary aliform
224 processes. 6) All dorsals display an absence of the spinodiapophyseal lamina in all dorsals,
225 with a contact between the lateral spol and podl in posterior-most dorsals instead. 7) Sacrals
226 with dorsoventrally high neural spine. 8) Ilium with round dorsal rim, hooks-shaped anterior
227 lobe and dorsoventrally elongated pubic peduncle. 9) Fused distal ischia with the paired
228 distal shafts creating an angle of 110° to the horizontal, 10) pubis with torsion and kidney-
229 shaped pubic foramen. 11) Femur with posteromedially placed fourth trochanter, and
230 laterally convex surface of femoral shaft.

231

232 *Horizon, locality and age: Patagosaurus fariasi* was found in what are now considered latest
233 Early to early Middle Jurassic beds of the Cañadón Asfalto Formation in west-central Chubut,
234 Patagonia, South Argentina (Cúneo et al., 2013). The Cañadón Asfalto Formation is a
235 continental unit, consisting mainly of lacustrine deposits. *Patagosaurus* was found in the

236 Cerro Cóndor area. The type locality of the holotype of *Patagosaurus fariasi* is Cerro Cóndor
237 North, which lies approximately 2 Km north-east of the first discovery site of *Patagosaurus*
238 remains: Cerro Cóndor South, close to the village of Cerro Cóndor, near the Chubut river, not
239 far from the town of Paso de Indios (Figure 1).

240

241 **GEOLOGICAL SETTING**

242 The Cañadon Asfalto Formation (west-central Chubut province, Patagonia, Argentina, see
243 Figure 1) was first studied by Piatnitzky (1936), after which it was formally described and
244 named by Stipanovic et al. (1968) and further described by Nullo (1983). It is part of the
245 sedimentary infill of the eponymous Cañadón Asfalto Basin, which consists of different
246 subunits of Lower Jurassic to Upper Cretaceous sediments. The Cañadon Asfalto Formation
247 is the uppermost unit of the lower megasequence of the Cañadón Asfalto basin, which has
248 sedimentary infill of the Lower Jurassic (Figari *et al.* 2015). This unit is exposed between the
249 Chubut province towns of Paso del Sapo and Paso de Indios (Olivera et al. 2015). The early
250 Middle Jurassic (Toarcian-Bajocian, possibly earliest Bathonian) Cañadón Asfalto Formation
251 conformably overlies the Early Jurassic (Pliensbachian-early Toarcian; Cúneo et al. 2013;
252 Figari et al. 2015; Volkheimer et al. 2015) Lonco Trapial Formation. It has been the subject of
253 numerous geological studies in recent years to determine its sedimentology and age, since
254 the age of the Cañadón Asfalto Formation has long been considered to be Callovian-
255 Oxfordian (and thus the South American equivalent of several other Jurassic beds
256 worldwide, such as the Oxford Clay; Frenguelli 1949; Bonaparte 1979; Bonaparte 1986;
257 Rauhut 2003). However, a recent detailed chronostratigraphic study showed otherwise,
258 using zircon grains from several tuff samples from the Cañadón Asfalto Formation (Cuneo et
259 al. 2013). These were pre-treated by the chemical abrasion, or CA-TIMS technique, in order
260 to constrain radiation-induced Pb loss. This method (using U/Pb isotopes) is considered to
261 be one of the most precise dating methods (Mattinson 2005). The U/Pb isotope ratios show

262 a latest Early (early-mid Toarcian), to early Middle Jurassic age range (Aalenian or Bajocian,
263 Cúneo et al. 2013), although the youngest radiometric age for this formation has been given
264 as Bajocian-Bathonian (Cabaleri et al. 2010a). This much older age of the formation is also
265 consistent with palynological and other radiometric studies (e.g. Volkheimer et al. 2008;
266 Cabaleri et al. 2010; Zavattieri et al. 2010; Olivera et al., 2015; Hauser et al. 2017).

267 Moreover, this new age also puts the vertebrate fossils found in the Cañadón Asfalto
268 Formation in a new light.

269

270 Since its discovery, over twenty species of different taxonomic groups (including sauropod,
271 theropod, and ornithischian dinosaurs, pterosaurs, sphenodontians, mammals, fishes, frogs,
272 turtles and crocodiles) have been discovered (Sterli et al. 2010; Olivera et al. 2015). This
273 makes it an important unit for the study of Middle Jurassic tetrapods, and the diversification
274 of Middle Jurassic dinosaurs in particular.

275

276 The outcrops of the Cañadón Asfalto Formation are dominated by microbial limestones,
277 often tuffaceous mudstones and shales with conchostracans, and conglomeratic
278 intercalations (Silva Nieto et al. 2002; Tasch and Volkheimer 1970). They provide mainly
279 disarticulated dinosaur remains, as well as a few articulated skeletons, as shown in the
280 quarry map of the sauropod bonebed of Cerro Cóndor North (Figure 1). The Cañadón Asfalto
281 Formation shows evidence of both folding and faulting, which makes correlation of the
282 different localities impossible, until further study is performed.

283 The region was dominated by a warm and relatively humid climate in the Middle Jurassic,
284 evidenced by palynology (Volkheimer et al. 2001) and by macrofloral remains (e.g.
285 Cheirolepidiaceae and Araucariaceae; Volkheimer et al. 2008, Volkheimer et al. 2015).

286 Lacustrine sedimentation cycles found in paleolakes in the Cañadón Asfalto Formation
287 provide evidence of climatic fluctuations and cyclicity (Cabaleri and Armella 2005; Cabaleri

288 et al. 2005).

289

290 José Bonaparte started excavations in the Cañadón Asfalto Formation with a team of
291 scientists and preparators, and with funding from the National Geographic Society, in 1977.
292 They found bones, on the Farias farm estate close to the river Chubut. After this, in 1978,
293 they found a sauropod skeleton 4-5 km north of Cerro Condor. This site was then dubbed
294 Cerro Cóndor Norte (North), and the original site Cerro Cóndor Sur (South). The Cerro
295 Cóndor North site was excavated until 1982; in 1980, however, most material was
296 uncovered and visible, as demonstrated in the quarry map of Figure 1. From this site, the
297 holotype PVL 4170 originates, as well as at least seven other individuals, most likely of
298 *Patagosaurus*.

299

300 The sediments of Cerro Cóndor North are dark grey, and hard. The bones from this quarry
301 are similarly dark grey or dark brown in colour. The sediments of Cerro Cóndor North were
302 interpreted by Bonaparte as fluvial deposits; however, they have more recently been
303 interpreted as mainly lacustrine deposits.

304 Cerro Cóndor South was thought to be fluvial, but from observations by O.R. is now thought
305 to be originating from an alluvial fan within a shallow lacustrine environment. Sediments
306 from Cerro Cóndor South are fine-grained to paraconglomeratic, light-coloured and contain
307 small freshwater shell fragments of invertebrates. Bonaparte also hinted that this locality
308 consists of multiple layers of sediment with fossils.

309 **RESULTS**

310

311 **AXIAL SKELETON**

312

313 *Cervicals*: PVL 4170 has seven cervical vertebrae preserved, ranging from anterior to
314 posterior cervicals. The most anterior cervical preserved (PVL 4170 1) is probably the third or
315 fourth cervical, based on comparisons with the Rutland *Cetiosaurus* (LEICT 468.1968.40;
316 Upchurch and Martin 2002).

317 Given the incomplete preservation of the neck in *Patagosaurus*, the exact cervical count in
318 this taxon cannot be established. At the very least, the atlas, axis and first one or two
319 postaxial cervicals are missing, given the high projection of the neural spine in the first
320 cervical preserved, and compared to the Rutland *Cetiosaurus*, where neural arches and
321 spines are low in the first 2-3 cervicals after the axis. Only very few non-neosauropodan
322 sauropods with complete cervical series are known, making a comparison of the preserved
323 elements difficult. Of the basal eusauropods with complete cervical series, *Shunosaurus* and
324 *Jobaria tiguidensis* Sereno et al., 1999 have 12 cervicals (Zhang 1988; Sereno et al. 1999),
325 whereas *Spinophorosaurus* has 13 (Remes et al. 2009). The Rutland *Cetiosaurus* was said to
326 have 14 cervicals by Upchurch and Martin (2002), but several of these vertebrae, including
327 the possibly last two cervicals, have only parts of the neural arch preserved, so that it cannot
328 be established with certainty if these two last vertebrae are cervicals or might already be
329 anterior dorsals (Upchurch & Martin 2002). The derived non-neosauropodan
330 mamenchisaurids apomorphically increased the cervical vertebral count to as much as 18
331 cervicals (Ouyang & Ye 2002). The primitive number of cervicals in basal eusauropods thus
332 seems to be either 12 or 13, and this is the condition we assume for *Patagosaurus*. As the
333 exact position of the different cervicals preserved can thus not be established, the
334 numbering used here starts with the first element preserved, therefore what is actually Cv 3

335 or 4 is numbered cervical 1 in the PVL collections. For convenience we will adhere to this
336 numbering.

337 The cervical centra are longer than high (see Table 1) and opisthocoelous, as in most
338 sauropods. In comparison with other sauropods, cervicals are rather stout, with an average
339 elongation index (aEI; Chure *et al.*, 2010) ranging from 1.9-2 in anterior to 1.2-1.4 in
340 posterior cervicals and the 'traditional' elongation index (EI, Upchurch 1998) ranging from
341 2.1 in anterior to 1.2 in posterior cervicals, compared to ~3.5 on average in
342 *Spinophorosaurus* (Remes *et al.* 2009b), ~3.1 in the only cervical known from *Amygdalodon*
343 (Rauhut 2003, MLP 46-VIII-21-1/8), and 2,1 in anterior to 5,3 in mid cervicals in an
344 undescribed sauropod from the Bagual site in the Cañadón Asfalto Formation (MPEF-PV
345 'Bagual' C2-4; Pol *et al.* 2009). This index is thus on average lower if compared to other non-
346 neosauropod eusauropods (see Table 1). The condyle has an anterior protrusion slightly
347 dorsal to its center, and the condyle is 'cupped' by a ca. 1-2 cm thick rugose layer, similar to
348 that in the Rutland *Cetiosaurus* (see Upchurch and Martin 2003, LEICT 468.1968 cervical
349 series). The cotyles are concave; with the deepest concavity slightly dorsal to the midpoint.

350 As in most saurischians, the parapophyses are placed on the anteroventral end of the
351 centra. In lateral view, the centra are ventrally concave posterior to the parapophysis. The
352 posteriormost 1/3rd of the ventral side of the centra is convex, and the dorsoventral height
353 of the centra increases posteriorly. Pleurocoels are developed as large, but only partially
354 well-defined lateral depressions on the centra. In anterior cervicals, the pleurocoel is deeper
355 than in posterior cervicals, and has a well-defined anterior, dorsal and ventral margin. In
356 mid- and posterior cervicals the posterior margin of the pleurocoel is less clearly defined and
357 the depression gradually fades into the lateral surface of the centrum. In some mid- to
358 posterior cervicals, the left and right pleurocoels are only separated by thin septa (which are
359 damaged or broken in some elements), but they do not invade the centrum and ramify
360 within the bone, as is the case in neosauropods, (Wedel *et al.* 2005). Some cervicals show a

361 faint compartmentalization of anterior and posterior pleurocoels, but they generally lack the
362 oblique lateral lamina that subdivides the cervical pleurocoels in neosauropods and some
363 derived basal eusauropods.

364 In ventral view, the centra are constricted directly posterior to the condyle, as in most
365 sauropods. A prominent ventral keel is present, which extends to about 2/3rd of the length
366 of the ventral axial midline of the cervicals, after which it fades and disappears into the
367 ventral surface of the centrum. It is present in all cervicals preserved (and possibly in the
368 first dorsal as well as a marginally developed keel). The keel is developed as a thin, ventrally
369 protruding ridge, with a very small hypapophysis anteriorly. The latter is developed as a
370 transversely thin, rounded, sail-like ventral protrusion present immediately behind the
371 ventral rim of the condylar 'cup'. This structure is accompanied by elliptical lateral fossae, as
372 in *Amygdalodon* (Rauhut 2003), *Tazoudasaurus* (MNHM To1-64; 81; 112; 354)
373 *Lapparentosaurus* (MNHM MAA 13; 172; 5) and *Spinophorosaurus* (NMB-1699-R), but in
374 contrast to the Rutland *Cetiosaurus* (Leicht 468.1968.40; 42; 7) and *Mamenchisaurus*
375 *hochuanensis* (Young and Zhao 1972) and derived sauropods. At the posterior end, the
376 cotyle extends further ventrally than it does dorsally, also seen in *Lapparentosaurus*,
377 *Amygdalodon*, *Tazoudasaurus*, and *Spinophorosaurus*. The dorsal side of the cotyle shows a
378 U-shaped notch in middle and posterior cervicals.

379 Neurocentral sutures are visible on the lateral side of the centrum in some cervical
380 vertebrae, a possible sign of morphological immaturity in archosaurs (Brochu 1996; Irmis
381 2007). The neural arches of the cervicals are axially elongated, transversely narrow and
382 higher posteriorly than the vertebral centrum, as in most sauropods. The diapophyses are
383 placed on ventrolaterally directed transverse processes, which are attached to the neural
384 arch by bony laminae, which are described in detail below for the individual vertebrae. The
385 prezygapophyses are more prominent than the postzygapophyses, being placed on stout,
386 elongated, beam-like stalks projecting anteriorly from the neural arch. They consistently

387 project anteriorly beyond the centrum in anterior cervical vertebrae, and show an increasing
388 incline towards posterior cervicals, as in basal sauropods *Tazoudasaurus*, the Rutland
389 *Cetiosaurus*, and in basal neosauropods such as *Haplocanthosaurus priscus* Hatcher, 1903.
390 Well-developed prezygapophyses apparently have a pre-epiphysis, however, a similar
391 structure is mentioned in a basal non-neosauropodan sauropod from the Early Jurassic of
392 Morocco, (Nicholl et al. 2018). The postzygapophyses are less prominent as they do not
393 project much posteriorly from the neural arch. With the increasing height of the neural arch
394 in more posterior cervicals, the postzygodiapophyseal lamina becomes more steeply
395 inclined. A relatively high posterior cervical neural arch is shared with mamenchisaurids
396 (Mannion et al. 2019). In mid cervicals, this inclination of the postzygodiapophyseal lamina is
397 approximately 45-50°, measured from the axial plane, which is larger than in most basal
398 sauropods, but comparable to the situation in diplodocids (see also McPhee et al 2015).
399 At the anterior end of the cervical neural arches the intraprezygapophyseal laminae are
400 separated medially, as in *Tazoudasaurus* (Allain and Aquesbi 2008) and the Rutland
401 *Cetiosaurus* (LEICT 468.1968). The intrapostzygapophyseal laminae (tpol) do meet at the
402 midline. However, there are no centropostzygapophyseal laminae, as in *Tazoudasaurus*
403 (Allain and Aquesbi 2008), but unlike the Rutland *Cetiosaurus* (Leict 468.1968). Cervical
404 vertebra PVL 4170 (7) is the only cervical with a single centropostzygapophyseal lamina
405 (stpol). This lamina is found more commonly in middle and posterior cervicals of
406 neosauropods, *Haplocanthosaurus* and *Cetiosaurus* (Upchurch et al. 2004). As this is the last
407 cervical before the cervico-dorsal transition (which happens at cervical PVL 4170 (8), this
408 could be a feature enabling ligament attachment for stability and strength at the base of the
409 neck, however, this would need more investigation with e.g. biomechanical modeling.
410 The cervical neural spines project higher than in most basal sauropods, especially in the
411 middle and posterior cervicals. The spines are connected to the zygapophyses by well-
412 developed spinopre- and spinopostzygapophyseal laminae. Whereas the summit of the

413 spine is more or less flush with the spinopostzygapophyseal lamina (spol) in the
414 anteriormost vertebra, it protrudes dorsally beyond that lamina in more posterior elements.
415 The spol are robust in all cervicals, but the sprl is only extensive in anterior elements and
416 becomes short and thin in more posterior cervicals. From cervical 4 onwards the neural
417 spine forms a rounded protrusion which is transversely wider than long anteroposteriorly.
418 The neural spine is slightly anteriorly inclined in anterior cervicals (to at least the fifth
419 preserved element), but becomes more erect towards the end of the cervical series, with a
420 straight anterior margin; this is also seen in *Shunosaurus* (Zhang 1988, T5402).

421

422 *Cervical vertebra PVL 4170 (1)*: This is the smallest and anteriormost of the cervical
423 vertebrae preserved. The element is generally complete and well-preserved, but the right
424 prezygapophysis is broken off at the base (see Fig. 2). A lump of sediment is still attached to
425 the anterior part of the neural arch, above the condyle.

426 The centrum is relatively shorter than in the mid-cervicals, with an EI of 1,55 and an aEI of
427 1,43. The articular ends are notably offset from each other, with the anterior end facing
428 anteroventrally in respect to the posterior cotyle (Fig. 2E, F). The cotyle is not as concave as
429 in the other cervicals of the series. The ventral keel is strongly developed in the anterior
430 1/3rd of the centrum, after which it gradually fades into ventral surface. In ventral view, the
431 parapophyses are visible as lateral oval bulges, the articular surfaces of which are confluent
432 with the condyle rim (Figure 2E).

433 The centrum shows a distinct pleurocoel, present laterally on the vertebral body (Figure 2A,
434 B). It is deeper anteriorly than posteriorly and developed as a rounded concavity that follows
435 the rim of the condyle on the lateral anterior side of the centrum. Posteriorly it extends
436 almost to the posterior end of the centrum; however, it fades gently into the lateral surface
437 from about 2/3rd of the centrum axial length. Within the pleurocoel there appears to be a
438 slight bulge at about the height of the diapophysis, which is similar to the oblique accessory

439 lamina in neosauropods (Upchurch 1998), dividing the pleurocoel in two subdepressions.
440 This subdivision is also seen to some extent in mamenchisaurids (e.g. Ouyang and Ye 2002;
441 Tang et al. 2001; Young 1939; Young and Zhao 1972; Zhang et al. 1998), and also in the
442 Rutland *Cetiosaurus* (Upchurch and Martin 2003). This incipient subdivision is also present in
443 some other cervicals of *Patagosaurus*, but it is best developed in this element. The
444 parapophysis is positioned anteroventrally on the lateral side of the centrum, and is
445 connected to the rugose rim of the condyle. The dorsal side is excavated, with the recess
446 being confluent with the deep anterior part of the pleurocoel. A stout lamina extends
447 horizontally posteriorly from the parapophysis and forms the ventral border of the
448 pleurocoel and the border between the lateral and the ventral side of the centrum. This
449 lamina becomes less prominent posteriorly (Figure 2A, B).

450 The posterior region of the neural arch is approximately as high as the posterior end of the
451 centrum. It extends over most of the length of the centrum, but is slightly offset anteriorly
452 from the posterior end of the latter. The neural canal is rather small and round in outline,
453 but only its posterior opening is visible, as the anterior end is still covered in matrix. Despite
454 the anterior position of the vertebrae, lateral neural arch lamination is well-developed, with
455 prominent prdl, podl and pcdl. The diapophysis is developed as a small, lateroventrally
456 projecting process on the anterior third of the neural arch (Figure 2A, C, D). It is connected
457 to the prezygapophysis by a slightly anterodorsally directed prezygadiapophyseal lamina
458 (prdl). The latter is in line with the pcdl, which meets the diapophysis from posteroventral.
459 The postygyadiapophyseal lamina (podl) is steeply anteroventrally inclined and meets the
460 prdl just anterior to the diapophysis. A short and stout acdl is present, but hidden in lateral
461 view by the diapophysis.

462 The prezygapophysis is placed on a stout, anteriorly and slightly dorsally directed process
463 that slightly overhangs the anterior condyle of the centrum (Figure 2A, C). The base of this
464 process is connected to the centrum by a short and almost vertical centroprezygapophyseal

465 lamina (cprl), which here meets the prdl in an acute angle; from this point onwards only a
466 single, very robust lateroventral lamina continues anteriorly onto the stall and braces the
467 prezygapophysis from lateroventral. The prezygapophyseal articular surface is flat, triangular
468 to elliptic in shape and measures about 3 by 3 cm. It is inclined dorsomedially at an angle of
469 approximately 30-40° from the horizontal. The intraprezygapophyseal lamina is very short
470 and widely separated from its counterpart in the middle of the anterior surface of the neural
471 arch.

472 A slightly asymmetrical centroprezygapophyseal fossa (cprf) is present below the
473 intraprezygapophyseal (tpri) and centroprezygapophyseal laminae on either side of the
474 neural arch, with the right fossa being hidden by sediment (Figure 2C). Anteroventral to the
475 diapophysis an axially elongated prezygapophyseal centrodiaepophyseal fossa (prcdf) is
476 visible, contra Upchurch and Martin (2003), who reported this to be absent in *Patagosaurus*.
477 A slightly larger centrodiaepophyseal fossa (cdf) is present posteroventral to the diapophysis,
478 and a very large, triangular pocdf is present between the pcdl and podl.

479 The postzygapophysis is placed on the posterodorsal edge of the neural arch, above the
480 posterior end of the centrum, which it does not overhang it posteriorly. It is developed as a
481 large, lateroventrally facing facet which is dorsally bordered by the slightly curved podl and
482 dorsally braced by the stout spinopostzygapophyseal lamina (spol). The stout and almost
483 vertical cpol connects the centrum to the medial margin of the postzagypophysis. The
484 intrapostzygapophyseal lamina (tpol) is directed ventromedially and connects the medial
485 side of the postzygapophysis to the dorsal margin of the neural canal, where it is separated
486 from its counterpart.

487 The neural spine is relatively low, barely extending dorsally beyond the postzygapophysis,
488 but it is anteroposteriorly elongate and robust, becoming wider transversely posteriorly
489 (Figure 2A, B, C, D). It is placed more over the anterior side of the centrum and is almost 2/3
490 of the length of the latter. Its anterior margin is inclined anterodorsally. The spine is

491 connected to the medial side of the prezygapophyseal process by a short
492 spinoprezygapophyseal lamina (sprl), which meets its counterpart at about one third of the
493 height of the neural spine, thus defining a small sprf. The spol is robust, but also short and
494 connects the posterior end of the spine with the dorsal surface of the postzygapophysis. A
495 large, diamond-shaped spof is bordered by the spols and tpols, with the latter being longer
496 than the former. The entire dorsal surface of the neural spine is rugose.

497

498 *Cervical vertebra PVL 4170 (2)*: This anterior cervical vertebra is the second element
499 preserved after the anteriormost cervical, and appears to be directly sequential based on
500 the size similarity in cotylar and condylar size between PVL 4170 (1) and (3). It is incomplete,
501 missing the neural arch and neural spine, which are broken off (Fig 3). The centrum,
502 prezygapophyses and the right postzygapophysis, however, are complete. The left
503 postzygapophysis is also broken. The vertebra is slightly flattened/displaced towards the
504 right lateral side, most likely due to compression.

505 The centrum is stout and robust, although slightly more elongated than that of the previous
506 cervical PVL 4170 (1). Its EI is 1,64 and its aEI is 1,97. The overall shape is not as curved as in
507 PVL 4170 (1), but rather straight along the axial plane, with a slight concave curvature of the
508 ventral side of the centrum. The condyle is convex, although slightly more dorsoventrally
509 flattened than in the previous cervical. In lateral view it shows a slightly pointy 'nose', i.e. a
510 pointed protrusion, on its dorsal side (Fig. 3A, B). The cotyle is slightly flattened
511 dorsoventrally as well, and it is wider transversely than dorsoventrally. Because the condyle
512 and cotyle show a high amount of osteological detail, this flattening might be natural, and
513 not caused by compression. On the ventral side of the cotyle, a lateral flange extends on the
514 left side but not on the right (Fig. 3E). This flange extends further posteriorly than the dorsal
515 rim of the cotyle, extending posteriorly and laterally. The dorsal side of the rim of the cotyle
516 shows a U-shaped indentation in dorsal and posterior view, posterior to the neural canal. As

517 in the first preserved cervical, the parapophyses are placed at the anteroventral end of the
518 centrum and extend from the thick condylar rim to the lateral and posterior sides of the
519 condyle. They are generally conical in shape and elongated towards the rest of the centrum.
520 The parapophyseal articular surfaces are more elongated axially than in the previous cervical
521 (PVL 4170 1). In ventral view, the ventral keel on the centrum is clearly present anteriorly on
522 the vertebral body, but fades after about 2/3rd of the vertebral length towards the posterior
523 side where it is not clearly visible (Fig. 3E).

524 On the lateral sides of the centrum, pleurocoels are clearly visible as deep round anterior
525 depressions, directly behind the rim of the anterior condyle (Fig. 3A, C). These depressions
526 fade into the lateral side of the centrum posteriorly. In this cervical, as in the first preserved
527 cervical, the right pleurocoel slightly ramifies anteriorly near the right parapophysis;
528 however, this is not visible on the left side of the centrum. As in the previous cervical, the
529 ventrolateral side of the centrum and ventral border of the pleurocoel is formed by a stout
530 lamina that extends from the posterior edge of the parapophyses to the posterior end of the
531 cotyle.

532 The neural arch is only partially preserved (Fig. 3A, B). Its height is similar to the height of
533 the cotyle. The neural arch in this element is limited to the middle/posterior end of the
534 vertebra; however, this is probably due to the fact that the neural spine is missing. The
535 neural canal, however, is clearly visible in this vertebra, being round to oval in anterior view
536 and more rounded triangular in posterior view. As in the previous vertebra, the lateral
537 neural arch lamination is well-developed, with the stoutest laminae being the prdl, the
538 posterior centrodiaepophyseal lamina (pcdl), and the right podl. The anterior
539 centrodiaepophyseal lamina (acdl) is also visible; however, it is smaller and shorter than the
540 pcdl. Both diapophyses are present on the neural arch, and are positioned dorsal and slightly
541 posterior to the parapophyses. The diapophyses are developed as small, lateroventrally
542 projecting protrusions of bone, being oval in shape in lateral view and conical in anterior

543 view. The left diapophysis is flexed more towards the centrum than the right, this is probably
544 due to deformation. The right prdl runs straight in a slight anterodorsal slope from the
545 diapophysis towards the prezygapophysis, where it meets with the cpri. Similarly, the right
546 sprl runs more or less parallel to the prdl. The left prdl, however, forms a much steeper
547 angle from the left diapophysis to the left prezygapophysis, due to the taphonomical
548 deformation. Towards the posterior end of the neural arch, the pcpl is in alignment with the
549 prdl. However, the former is directed slightly posteroventrally. The right podl is visible but is
550 damaged. It is a stout lamina and it forms a steep angle of 50° from the horizontal axis in its
551 course from the right diapophysis towards the right postzygapophysis.

552
553 The prezygapophyses are much more elongated than in the previous cervical PVL 4170 (1),
554 (Fig. 3B, C). They project further anteriorly from the vertebral condyle than PVL 4170 (1) by
555 about 9 cm. Moreover, unlike in PVL 4170 (1), they project mostly anteriorly and only slightly
556 dorsally from the neural arch. Once more the taphonomical deformation of this cervical is
557 apparent, as the left prezygapophysis is displaced and bent towards the vertebral body,
558 while the right projects more lateral and away from the vertebral body. The
559 prezygapophyses are supported by very stout stalks, which are formed by the prdl on the
560 dorsolateral side, the cpri on the lateral, and, partially, the sprl on their dorsal side. The prdl
561 meets the cpri in an acute angle, which is obscured from view by the prezygapophyseal
562 articular surfaces. A small, short, pair of tpri is present, which meet in a wide acute angle,
563 dorsal to the neural canal (Fig. 3C). Lateral to these laminae, small, paired, rounded to oval
564 prcds are visible underneath the prezygapophyses. They are also transversely convex.
565 The only preserved, right postzygapophysis is flexed slightly medially in dorsal view, and has
566 its articular surface directed dorsally and tipped slightly anteriorly and laterally (Figure 3B,
567 D). It is supported by the stout podl and an acutely angled, thin cpol, which together with
568 the pcpl creates a triangular, wing-like structure, which is offset from the neural arch

569 dorsally and posteriorly. The thin sheet of bone between the podl and the pcdl is pierced.

570 The distal end of the postzygapophysis is rounded to triangular in shape. A relatively deep

571 right pocdf is visible between the cpol and the podl. No tpol is visible here.

572

573

574 *Cervical vertebra PVL 4170 (3)*: This is the third cervical preserved in the series; it probably

575 corresponds to the 5-6th cervical (compared to the Rutland *Cetiosaurus* Leict LEICT

576 468.1968). It is well-preserved, but lacks both diapophyses, see Figure 4. The cervical is

577 stout, and is similar to PVL 4170 (2) in that the centrum is generally straight, and the anterior

578 and posterior ends are not as offset from each other as in the first preserved cervical.

579 Nevertheless, the cotyle is slightly offset to the ventral side, and the condyle bends slightly

580 ventrally from the relatively straight vertebral body (Fig. 4A, B). The prezygapophyses are

581 slightly displaced, the right projects further laterally than the left; this might be caused by

582 deformation.

583 Both the condyle and cotyle are larger in this cervical than in the previous two (Fig. 4A, B).

584 The condyle is oval in shape, and is transversely wider than dorsoventrally. It has a small

585 rounded protrusion, visible slightly dorsal to the midpoint of the condyle (Fig. 4E). A thick

586 rugose rim surrounds the condyle, from which the parapophyses protrude at the

587 lateroventral sides. The cotyle is more or less equally wide transversely as high

588 dorsoventrally. It has its deepest depression slightly dorsal to the midpoint. The cotyle does

589 not have a rugose rim; however, its ventral rim projects further posterior and slightly lateral

590 than its dorsal rim. In ventral view, (as well as in lateral view) the parapophyses are clearly

591 visible as rugose, oval structures that protrude from behind the condylar rim to the posterior

592 and lateral sides. Also emerging from this condylar rim is the ventral keel, which is

593 prominently visible for about 2/3rds of the length of the centrum, after which it fades into

594 the ventral body of the centrum. At the onset of the keel, a small round hypapophysis

595 protrudes ventrally from the centrum. Two oval depressions are visible on the lateral sides
596 of the hypapophysis.

597 In lateral view, the centrum shows neurocentral sutures between the lower part of the
598 centrum and the upper part of the vertebral body (Fig. 4A, B). The suture is better preserved
599 on the right side than on the left side of the centrum. On both lateral sides of the centrum, a
600 prominent pleurocoel is visible as a deep oval depression, which becomes shallower
601 posteriorly but spans almost the entire length of the vertebral body. Unlike in the previous
602 two cervicals, no compartmentalization of the pleurocoel is visible in this element. The
603 dorsal and ventral rim of the pleurocoels are marked by two stout laminae that define the
604 ventral and dorsal sides of the centrum.

605 The neural arch becomes more dorsoventrally elevated in this cervical, with the neural arch
606 being slightly higher than the dorsoventral height of the cotyle (Fig. 4A, B). The neural canal
607 is triangular to slightly teardrop-shaped in anterior view, in contrast to the previous two
608 cervicals. In posterior view, the neural canal is oval, with a flat ventral surface. Because the
609 diapophyses are damaged, the lamination underneath the diapophyses is clearly visible in
610 lateral view. The acdl is developed as a short lamina, running anteroventrally in an oblique
611 slope towards the anterodorsal end of the pleurocoel. The pcdl is a very stout, elongated
612 lamina in this cervical. It runs from directly underneath the diapophysis to the posterior end
613 of the vertebral body, but fades into the centrum shortly before the rim of the cotyle. The
614 acdl and pcdl delimit a small triangular centrodiaepophyseal fossa (cdf), while a much wider
615 postzygapophyseal centrodiaepophyseal fossa (pocdf) is bordered by the slightly convex,
616 stout podl (Figure 4A, B, C). This lamina runs at an oblique angle of about 40 degrees to the
617 horizontal from the diapophysis to the postzygapophysis. Shortly before reaching the
618 postzygapophysis, the curvature of the lamina changes from straight to slightly concave
619 (ventrally), giving the podl a slight sinusoidal appearance. The prdl runs from the
620 diapophyses to the prezygapophyses in an oblique angle similar to the podl. The four major

621 laminae on this cervical, prdl, acdl, pcdl, and podl, together create an X shape (in near
622 symmetrical oblique angles) on the midpoint of this cervical.

623 The prezygapophyses project anteriorly, dorsally, and slightly laterally, with the angle
624 between each prezygapophyseal summit being about 110-120° (Fig. 4D). They project
625 asymmetrically; this is probably due to taphonomical deformation. The stout stalks
626 supporting the prezygapophyses are concave ventrally, and convex dorsally, and project 9
627 cm anterior from the vertebral body (Fig. 4A, B, D). The articular surfaces are triangular in
628 shape. The prezygapophyses are supported by the prdl from the dorsolateral side, and by
629 the cprls ventrally. The cprls extend in a near vertical axis from the ventral side of the neural
630 arch, but at about the height of the neural canal project laterally towards the
631 prezygapophyseal articular surface in an angle of about 30°. In anterior view, the stout,
632 sinusoidal tprl join together from the medial articular surface of the prezygapophyses to the
633 ventral side of the prezygapophyses, just dorsal to the neural canal. Here a very short, stout,
634 single intraprezygapophyseal lamina (stprl) is present. The paired prcdfs, seen as triangular
635 depressions, bordered by the tprls and the cprls, are larger than in previous cervicals PVL
636 4170 (1) and (2).

637 The postzygapophyses are triangular in shape in posterior view, and their articular surfaces
638 in posterior/ventral view are rounded to triangular in shape (Fig. 4C). There is a slight V-
639 shaped indentation on the medial side of each postzygapophysis between the posterior
640 termination of the podl and the cpol at the postzygapophyses. The cpols run in a curved,
641 oblique angle of about 55° to the horizontal, from the postzygapophyseal articular surfaces
642 to the dorsal rim of the posterior neural canal. No stpol is visible here. On each lateral side
643 of the paired cpols, large triangular paired pocdf are visible, bordered by the vertically
644 aligned podls.

645 The neural spine is already prominent in this cervical, more so than in PVL 4170 (1) and (2)
646 (Fig. 4A, B, F). In dorsal view, the neural spine appears solid, and is rounded in shape, and

647 the anterior, posterior and lateral rims are clearly visible and protrude slightly dorsally
648 (Figure 4F). The dorsalmost part shows rugosities, probably for ligament attachment. In
649 anterior view, the neural spine is kite-shaped, and shows rugosities on the anterior surface.
650 Relatively thin, paired sprl curve down from the anterior lateral sides of the neural spine,
651 where they extend in an inverted V-shape to the lateral sides of the prezygapophyses.
652 Medial to these laminae, an oval sprf is visible, ventrally bordered by the tprls. Similarly, in
653 posterior view, the spols form an inverted V towards the postzygapophyses, dorsally
654 bordering the spof, which is clearly visible as a deep and large fossa, which in turn is
655 bordered laterally by the paired cpols. The neural spine in lateral view as well as in posterior
656 view is seen to incline anteriorly, making the neural spine summit less prominent in
657 posterior view (Fig. 4A, B, C).

658

659

660 *Cervical vertebrae PVL 4170 (4)*: The fourth preserved cervical is generally well-preserved.

661 However, the left diapophysis and part of the neural arch are missing, and the right neural
662 arch, between the neural spine and the diapophysis, is partially reconstructed, see Figure 5.
663 The left prezygapophysis, and the articular surface of the postzygapophysis are also partially
664 missing. This cervical could have been more robust than the next one, and the neural spine
665 could have projected further dorsally, making this cervical in fact cervical (5), however, as it
666 is reconstructed, this cannot be ascertained for certain.

667 The centrum is more elongated than that of the previous cervical (Fig. 5A, B). The centrum
668 only shows a mild curvature, and the cotyle and condyle are not offset from one another;
669 the condyle bends slightly ventrally and the cotyle also mildly curves ventrally. The
670 lateroventral rims of the cotyle flare out slightly laterally and posteriorly, and are more
671 elongated ventrally than dorsally. In anterior view, the condyle is oval and slightly
672 dorsoventrally flattened (Fig. 5D). It has a thick, prominent rim surrounding it, from which
673 the parapophyses are offset in anterior view. In posterior view, the cotyle is larger than the

674 condyle, and more or less equally wide transversely as dorsoventrally. In ventral view, the
675 thick rim that cups the condyle is clearly visible (Fig. 5E). From this rim, the hypapophysis
676 protrudes ventrally as a small rounded bulge. The ventral keel is prominently visible, and
677 runs along the ventral surface of the centrum until it fades into the posterior 1/3rd of the
678 centrum, where it widens transversely towards its posterior end. This is also seen to some
679 extent in *Lapparentosaurus* (MNHM MAA 13; 172; 5), although this fanning includes a
680 dichotomous branching of the posterior end of the ventral keel in the latter taxon. In lateral
681 view, the ventral keel protrudes slightly more ventrally than the stout lamina that defines
682 the ventral lateral end of the centrum. In lateral view, the pleurocoels are visible as deep
683 depressions on the lateral side of the centrum, being deepest behind the rim of the condyle,
684 and fading into the posterior 1/3rd of the lateral centrum. Interestingly, this cervical shows
685 pleurocoels with well-defined posterior margins (as well as anterior, dorsal and ventral),
686 which differs from the pleurocoels in the previous cervicals (Fig. 5A, B). Moreover, the
687 pleurocoels in this element are slightly compartmentalized (a deeper depression of the
688 pleurocoel is visible anteriorly and posteriorly, while the mid section is less deep in the
689 lateral body of the centrum), as in the first two cervicals.

690 As in the previous three cervicals, the neural arch extends over most of the length of the
691 centrum, but ends a short way anterior to the posterior end of the centrum. The neural
692 canal is rounded to teardrop-shaped in anterior view, and oval to triangular in posterior
693 view, with an abrupt transverse ventral rim, as in PVL 4170 (3). The configuration of the four
694 prominent laminae on the lateral neural arch is similar to that of PVL 4170 (3) in that pcdl,
695 prdl, podl and acdl form an X-shaped structure. However, the right diapophysis (the left is
696 missing) of this element is larger than in the previous cervicals. The right diapophysis is
697 developed as a ventrolaterally projecting process, which is supported posteriorly by the very
698 stout pcdl, and anteriorly by a smaller, shorter acdl. The diapophysis is oval in shape and is
699 axially shorter than dorsoventrally.

700 The right prezygapophysis is supported laterally and dorsally by the stout prdl, which
701 extends from the anterodorsal side of the diapophysis to approximately 2/3rds of the length
702 of the stalk of the prezygapophysis (Fig. 5B, D). Ventrally, the prezygapophysis is supported
703 by the cpri, which is nearly vertically positioned on the neural arch. The prezygapophysis has
704 a triangular articular surface. As in the previous cervicals, the cpri and tpri meet at the distal
705 end of the prezygapophysis in an acute angle of approximately 30 degrees. The paired tpri
706 slope steeply down and meet on the dorsal rim of the anterior neural canal. The cpri and
707 tpri enclose paired, rhomboid prcdf.

708 In posterior view, the left postzygapophysis is only partially preserved, as the articular
709 surface is missing, but the right structure is present, showing a flattened articular surface
710 (Fig. 5C). The intrapostzygapophyseal laminae form a V shape with an angle of about 55°
711 from the sagittal plane of the centrum, which is similar to PVL 4170 (3). They meet only on
712 the dorsal rim of the posterior neural canal. The paired, triangular pocdfs, which are
713 demarcated by the cpols and the podls, are also similar to the third preserved cervical.

714 The neural spine is robust in anterior view (Fig. 5D). It is narrower at the base (at the onset
715 of the spinoprezygapophyseal lamina) and expands transversely towards the summit, which
716 in anterior view is shaped like a rounded hexagon. The right sprl is a near-vertically
717 positioned, prominent structure that extends from about 1/3rd under the neural spine
718 summit to the ventral pairing of the tpri. In lateral view, the neural spine is
719 anteroposteriorly shorter, with respect to the length of the centrum, than in previous
720 cervicals. Its anterior margin is slightly inclined anteriorly. In posterior view, the neural spine
721 summit has a more rounded, rectangular shape, and is clearly inclined towards the anterior
722 side of the cervical. The (only preserved) right spol curves concavely towards the
723 postzygapophysis (Figure 5A,B,C). The spinopostzygapophyseal fossa is deep and triangular
724 in shape.

725 In dorsal view, the neural spine summit is roughly quadrangular in outline, although it is
726 slightly wider transversely than long anteroposteriorly (Figure 5F). On the anterior rim of the
727 summit, the spine slightly bulges out convexly, with an indent on the midline, rendering the
728 anterior rim slightly heart-shaped. The posterior side of the neural spine summit is slightly
729 concave in dorsal view, with the spool sharply protruding from each lateral side.

730
731

732 *Cervical vertebra PVL 4170 (5)*: This is a mid-posterior cervical, which is well-preserved, with
733 all zygapophyses and diapophyses intact, although the neural spine is slightly
734 taphonomically deformed, and the diapophyses are slightly asymmetrical, also probably due
735 to deformation. The left parapophysis is also missing (Fig. 6A).

736 The centrum is different from the previous cervicals in that it is more robust, less axially
737 elongated and the condyle, cotyle and neural spine are dorsoventrally larger (Fig. 6A, B). The
738 anterior condyle is rounded, robust and slightly dorsoventrally flattened. The anterior end of
739 the condyle has a rounded protrusion on the midpart. The rim of the condyle is clearly
740 visible and protrudes slightly dorsally (Fig. 6C). Posteriorly, the cotyle is deeply concave and
741 is larger transversely and dorsoventrally than the condyle. The posterior end of the centrum,
742 ventral to the cotyle, flares out laterally, however, it shows a U-shaped indent in the
743 midpart, seen in posterior view (Fig. 6D). In lateral view, the centrum is concavely
744 constricted anteriorly, directly posterior to the rim of the condyle. As in the other cervicals,
745 the dorsal end of the posterior cotyle extends a little further posteriorly from the neural
746 canal in lateral and ventral view. The right parapophysis is visible in lateral view at the
747 ventrolateral end of the condylar rim (Fig. 6B). It is oval in shape and protrudes ventrally and
748 posteriorly. The pleurocoel on the lateral side of the centrum is deeper anteriorly than
749 posteriorly, and spans almost the entire lateral side of the condyle anteriorly (Fig. 6A, B).
750 Posteriorly it fades into the centrum. In ventral view, the ventral keel is clearly visible, and

751 stretches over the entire length of the centrum, but flattens in the posteriormost part (Fig.
752 6E). The hypapophysis protrudes less in this cervical than in the previous ones. The
753 parapophysis is more elongated axially than transversely in ventral view, and less rounded
754 than in the previous cervicals; rather than having a rounded rectangular shape in ventral
755 view, it is more elliptical in shape, and is slightly more offset to the lateral sides of the
756 centrum (Fig. 6E). Both posterior centroparapophyseal laminae are clearly visible in this
757 element as short but strong laminae that are confluent with the ventrolateral edges of the
758 vertebral body.

759 The neural arch is higher dorsoventrally in this element than in the previous ones. In lateral
760 view, the neural arch spans almost the entire axial length of the centrum, however, as in the
761 previous cervicals, it is slightly offset from the anterior dorsal end of the centrum (Fig. 6A, B).
762 In anterior view, the neural canal is slightly teardrop-shaped, and dorsoventrally is more
763 elongated than transversely. In posterior view, the neural canal is also teardrop-shaped,
764 however here it is more dorsoventrally flattened and transversely widened at the base. The
765 diapophyses, in lateral view, appear as rounded appendices, which are offset from the
766 vertebral body as ventral and lateral projection. They are transversely thin and flattened. In
767 anterior view they are more complex in shape, created by a conjoining of the acdl, pcdl and
768 prdl in a triangular shape, which shows a ventral hook-shaped distal protrusion. In posterior
769 view the diapophyses are enclosed in sheets of bone. The prezygapophyses on this cervical
770 rest on more dorsoventrally elongate stalks than in previous cervicals (Fig. 6A, B, C). These
771 stalks have a pedestal-like appearance, and show lateral rounded bulges at their base, dorsal
772 and lateral to the thick condylar rim. The prezygapophyses project anteriorly and slightly
773 medially and dorsally, and are anteriorly triangular in shape. There are deep rhomboid
774 prcdfs visible as dorsoventrally narrow, slit-like fossae, ventral to the prezygapophyses. The
775 centroprezygapophyseal laminae form an oblique angle towards the centrum. The
776 prezygodiapophyseal laminae run ventrally from the prezygapophyses in a sharp angle.

777 These laminae meet dorsally in an acute angle. The tpri meet dorsal to the neural canal in a
778 wider angle than in the previous cervicals, showing a widening of the space between the
779 prezygapophyses towards more posterior cervicals in *Patagosaurus*.

780 The postzygapophyses and prezygapophyses are both more aligned with the axial column
781 than in previous cervicals (Fig. 6F). In lateral view, the articular surface of the
782 postzygapophyses is aligned with the horizontal axis, and in dorsal and posterior view the
783 articular surfaces are triangular in shape (Fig. 6A, B). In lateral view, the podl form a wide
784 angle with the axial column, owing to the further elongation of the cpol (producing more
785 elevated postzygapophyses). The cpols show an acute angle from the postzygapophyses to
786 the anterior and ventral side, and are slightly ragged in appearance. They meet the centrum
787 anteriorly to the dorsal rim of the cotyle. In posterior view, the cpol run at an acute angle,
788 and in a slightly concave way, to the ventral side of the postzygapophysis (Figure 6D). This
789 angle is smaller than in previous cervicals, being about 35°, due to the elongation of the
790 neural arch and higher dorsal position of the postzygapophyses. Between the cpol and podl,
791 large, triangular pocdf are visible.

792 The neural spine in anterior view is slightly sinusoidal, probably due to taphonomic
793 deformation (Fig. 6C). In lateral view, the neural spine is further reduced in its axial length
794 compared to the previous cervicals (Fig. 6A, B). The spine summit is prominent; it is seen to
795 protrude dorsally and anteriorly, clearly separated from the vertebral body as a rounded
796 rectangular bony mass. In dorsal view, the neural spine summit is wider than the neural
797 spine body, and is of a teardrop-shaped protuberant shape (Fig. 6F). It is also expanded
798 transversely. Anteriorly on the neural spine, a prominent protuberance is visible anteriorly,
799 possibly an attachment site for ligaments. The sprls are seen, in dorsal view, to protrude
800 from the anterior side of the neural spine summit (Fig. 6C). They run nearly vertically
801 towards the dorsal base of the prezygapophyseal stalks. At the base of the neural spine they

802 are slightly transversely constricted. The spool are positioned as near-horizontally aligned
803 with the axial plane of the cervical. They are thin, prominent laminae.

804

805 *Cervical vertebrae PVL 4170 (6)*: This is a well-preserved posterior cervical with some
806 damaged/broken thin septa. The centrum is robust, as in PVL 4170 (5), but unlike the more
807 elongated anterior cervicals. The cervical is further distinguished by having an axially more
808 elongated neural arch than in the previous cervical, see Figure 7.

809 The centrum is shorter than in previous cervicals, and stouter, with a transversely flattened
810 condyle with a small rounded protrusion slightly higher than the midpoint (Fig. 7A, B). The
811 cotyle is slightly larger and higher dorsoventrally than the condyle, as in the other cervicals.
812 In ventral view, the ventral keel is developed as a protruding ridge between two concavities,
813 which are flanked by the ventrolateral ridges of the centrum (Fig. 7E). This keel flattens
814 towards the caudal end into a bulge and is no longer visible at the posterior end of the
815 ventral side of the centrum. Instead there is a slight depression on the distal end of the keel.

816 The centrum is constricted directly posterior to the parapophyses, which shows a deep
817 concavity of the centrum in lateral view, after which the centrum curves more gently
818 towards a convex posterior end of the centrum (Fig. 7A, B). The pleurocoel is anteriorly
819 deep, and the thin septum that separated it from its mirroring pleurocoel is broken, creating
820 an anterior fenestra. On the left side of the centrum the neurocentral suture is visible. In
821 anterior view, the neural canal is oval, being higher dorsoventrally than wide transversely,
822 and in posterior view, the neural canal is subcircular with a pointed dorsal side.

823 In anterior view, the prezygapophyses are a triangular shape, due to the tapering of both
824 cprl and prdl towards the dorsal tip of the prezygapophyses, where they meet in an inverted
825 V-shape, as in PVL 4170 (5), see Fig. 7C. The cprf are not as deep as in the previous cervicals.
826 The dorsal end of the prezygapophyses is not as convex as in the previous cervicals. In
827 ventral and posterior view, the postzygapophyseal articular surfaces are triangular (Fig. 7D,

828 E). In lateral view, the sprl is positioned less vertical than in PVL 4170 5, and instead slopes in
829 a gentle curve towards the prezygapophyses (Fig. 7A, B). In posterior view, the thick cpols
830 and the spols support the laterally canted, 'wing-tip'-shaped sheet of bones that are
831 supported by the podl and pcdl on the lateral side (Fig. 7D). The cpol do not meet, while
832 there is no tpol. In dorsal view, the postzygapophyses and spol expand further beyond the
833 centrum than the prezygapophyses overhang the centrum anteriorly, which is the reversed
834 condition compared to the more anterior cervicals in PVL 4170. The
835 spinopostzygapophyseal lamina is also less oblique than in previous cervicals, and curves
836 gently concavely towards the postzygapophyses (Fig. 7D).

837 The neural spine is craniocaudally flattened but transversely broader than PVL 4170 (5). The
838 base of the neural spine is only supported by a rather thin bony sheet, both anteriorly and
839 posteriorly, as can be seen due to a break. The dorsal end and summit of the neural spine,
840 however, are formed by solid bone. In anterior view, the spine is not as teardrop-shaped as
841 in PVL 4170 (5), but is more rectangular, and widens towards its summit. The neural spine
842 does not tilt notably forward as in PVL 4170 (5), but cants only slightly anteriorly. The neural
843 spine summit extends dorsally beyond the spol as an oval to rhomboid protuberance. The
844 neural spine and the postzygapophyses, together with the podl are more axially elongated
845 and dorsally elevated in this cervical than in the previous ones. In dorsal view, the neural
846 spine summit is a stout, transverse strut. It is slightly transversely expanded, and thicker at
847 the lateral ends.

848

849

850 *Cervical vertebra PVL 4170 (7)*: This is a partially reconstructed posterior cervical, with the
851 left diapophysis missing (Fig. 8). The vertebra is shorter axially and higher dorsoventrally
852 than previous cervicals (Fig. 8A, B). The centrum is stout. In anterior view, the condyle is
853 dorsoventrally compressed and transversely widened (Fig. 8 F). The 'cup' is very distinct. The
854 cotyle is larger than the condyle, more rounded, and shows an indentation dorsally for the

855 neural canal, making the cotyle slightly heart-shaped (Fig. 8E). In ventral view, this centrum
856 is less elongated and transversely wider than previous cervicals. The keel is still well
857 developed, as are the lateral concavities coinciding with the hypapophysis, which is present
858 as a sharp ridge (Fig. 8C). The posterior ventral side of the centrum is ventrally offset from
859 the anterior ventral side, due to the larger size of the cotyle in this specimen, and due to the
860 ventral bulge of the distal half of the centrum. The parapophyses are more aligned with the
861 centrum, in that they do not project ventrolaterally, but more posteriorly, in contrast to
862 previous cervicals (Fig. 8C). The parapophyses are oval in ventral view and more triangular in
863 lateral view. The neural canal is dorsoventrally flattened and teardrop-shaped (Fig. 8E, F).
864 The prezygapophyses differ from previous cervicals in that they form a more acute angle
865 with the vertebral body and have a flat, dorsally directed articular surface in lateral view
866 (Fig. 8A, B). The beams supporting the prezygapophyseal articular surface are stout, as in the
867 previous cervicals. The prezygapophyses are inverted V-shaped in anterior view (Fig. 8F).
868 However, this structure is wider transversely than in previous cervicals. The
869 intraprezygapophyseal laminae tilt ventromedially, whereas the distal tips of the
870 prezygadiapophyseal laminae tilt ventrolaterally, creating an inverted V-shape in anterior
871 view of each prezygapophysis, as in the previous cervical. The *stprl* is not present (see Table
872 2). In dorsal view, the articular surface of the prezygapophysis is more rounded than in
873 previous cervicals. The postzygapophyses are supported from the lateral and ventral sides
874 by the prominent *podl*, which project in a wide angle of about 70 degrees from the posterior
875 side of the diapophysis to the postzygapophyses; this lamina curves gently convexly (Figure
876 8A, B, E). In lateral view, the postzygapophyses are present as triangular structures at the
877 distal end of the thick *podl*. Dorsal to the postzygapophyses, triangular epipophyses are
878 visible (Fig. 8A, B, E). Also, in lateral view, the *tpols* run ventral to the postzygadiapophyses
879 in a vertical line towards a U-shaped recess, formed by the *stpol*. In posterior view, the
880 intrapostzygapophyseal laminae form a V-shape. The *tpol* are much shorter than in PVL 4170

881 (6), which also limits the size of the spinopostzygapophyseal fossa (spof). The stpol is
882 present as a thin lamina that recedes towards the neural arch (Figure 8E). This is the only
883 cervical that has an stpol that is longer than 1 cm. It separates paired rhomboid cpof. These
884 are flanked by the thick podl, which are more elongated in this vertebra than in cervical PLV
885 4170 (6). The right diapophysis expands from the lateral side of the neural arch, and shows a
886 strong ventral bend towards its distal end. This strong bend could be the product of
887 deformation. The left diapophysis also bends ventrally and laterally, but not as strongly as
888 the right one (Fig. 8A, B, E, F). The diapophyses are clearly visible both in anterior and
889 posterior view. Ventrally and anteriorly they are concave, with elongated but axially short
890 prcdfs. They are dorsally supported by the convergence of the prdl and the podl, which form
891 a thick rugose, rounded plate of bone on the dorsal tips of the diapophyses.

892 The neural spine is transversely broad and axially short, and rectangular in shape (Fig. 8F). In
893 dorsal view, it fans out transversely at the apex, but, together with the sprl, becomes
894 constricted ventrally (Fig. 8D). This cervical is further distinguished from the previous
895 cervicals by the dorsoventral elongation of the neural spine, and the accompanying
896 elongation of the tpol in lateral view (Fig. 8A, B).

897

898 *Cervicodorsal PVL 4170 (8)*: The neural arch is dorsoventrally elongated in this transitional
899 vertebra between cervicals and dorsals; a trend that persists throughout the anterior and
900 posterior dorsals. The posterior articular surface (cotyle) is dorsoventrally higher than the
901 anterior condyle, (Fig. 9).

902 The condyle is of similar shape to that in PVL 4170 (7) (Fig. 9A, B, C). The cotyle of this
903 vertebra is well-preserved and has an oval, slightly dorsoventrally flattened shape, with a
904 small concave recess at the base of the neural canal (Fig. 9D).

905 On the ventral side of the centrum, the ventral keel and adjacent fossae are still clearly
906 visible (Fig. 9F). In lateral view, the ventral margin of the centrum is strongly concave in the
907 first half of its length (slightly damaged but still visible) and in the posterior part becomes
908 more convex and robust (Fig. 9F). The ventral keel extends over the first 1/3 of the length, as
909 in the other vertebrae, and then becomes a bulge, adding to the convexity of the posterior
910 ventral end of the centrum. In lateral view, the pleurocoels of either side show a cut through
911 the centrum, creating a foramen (Fig. 9A, B). This supports the observation that the
912 pleurocoels are very deep in the cervicals of *Patagosaurus*, and that they are normally only
913 separated from the adjacent pleurocoel by a very thin midline septum (Carballido and
914 Sander 2014), which in this vertebra is not preserved. The parapophyses are present as
915 rounded to triangular extensions on the lateral sides of the condylar rim (Fig. 9F). They are
916 not clearly visible in anterior or lateral view, but are visible in ventral view. At the base of the
917 prezygapophyseal stalks, however, similar triangular protrusions exist (Fig. 9C).

918 The *cpri* project slightly laterally from the centrum (Figure 9A, B). The *prdcf* are larger than in
919 previous vertebrae, due to the wider lateral projection of the diapophyses. These fossae are
920 triangular in shape (Figure 9C). The prezygapophyses are roughly square with rounded edges
921 in dorsal view. The spinoprezygapophyseal fossa (*sprf*) is very deep. The *prdl* are
922 prominently developed as sinusoidal thick laminae, supporting the *prdl* from below and
923 from the lateral side, and supporting the diapophyses anteriorly. The prezygapophyseal
924 articular surfaces are flat and axially longer than in previous vertebrae (Fig. 9E). The angle of
925 lateral expansion of the *spri* however, is greater than in previous vertebrae.

926 In posterior view, the postzygapophyses project to the lateral side (Fig. 9D). The *tpols* do not
927 meet, but run down parallel in the dorsoventral plane to the neural canal. A faint right *cpol*
928 seems to be present in this vertebra, however, it could also be an anomaly of the *pocdf*. This
929 elongates the *spof*. The *podl* project dorsally and posteriorly in a high angle. Towards about

930 2/3rd of the total vertebral height. These project in a straight line, after which they bend in a
931 convex curve to the posterior side. The pcdl make a similar bending curve towards the
932 centrum, due to the elongation of the posterior neural arch. Prominent pocdf are present as
933 shallow triangular fossae.

934 In dorsal view, as in PVL 4170 (7), the neural spine is transversely wide and axially short (Fig.
935 9E). It is constricted towards the postzygapophyses so that it 'folds' posteriorly. In anterior
936 view, the neural spine is ventrally more constricted than in the previous vertebra (Fig. 9C). It
937 is more elongated dorsoventrally, and the neural spine is transversely overall less wide than
938 the previous vertebra.

939

940 *Dorsals*: the holotype specimen has nine dorsals preserved, including a transitional
941 cervicodorsal vertebra. Dorsals are numbered PVL 4170 (9) – (17). Most of the anterior and
942 mid-dorsals are preserved, however, some may be missing, seen in the sudden transition
943 from anterior-mid dorsals PVL 4170 (10) – (11) and mid-posterior dorsals PVL 4170 (12) –
944 (13). Most neural arches and spines are relatively complete; except dorsal PVL 4170 (15) has
945 only the centrum preserved. The number of missing dorsals can only be estimated. The
946 Rutland *Cetiosaurus*, thus far morphologically the closest sauropod to *Patagosaurus* (see
947 Holwerda and Pol 2018), shows the disappearance of the acdl at around vertebra nr 15. As
948 the acdl seems to disappear in anteriormost dorsals of *Patagosaurus*, assuming the
949 anteriormost dorsal is preserved, both sauropods could have had as few as 10 dorsal
950 vertebrae (see Table 2). However, (approximately) contemporaneous non-neosauropodan
951 eusauropods are reported to have 12 dorsals (*Jobaria*, mamenchisaur) or 13 (*Shunosaurus*).
952 *Barapasaurus* is estimated to have had even 14 dorsal vertebrae. Diplodocids *Apatosaurus*
953 Marsh, 1877, *Diplodocus* Marsh, 1878, and *Barosaurus* Marsh, 1890 all had 10 dorsal

954 vertebrae, and basal neosauropod *Haplocanthosaurus* 13-14 (Hatcher 1903; Carballido et al.
955 2017).

956 The dorsal centra in PVL 4170 become axially shorter and dorsoventrally higher towards the
957 posterior dorsals, with mediolateral width increasing proportionally with height towards
958 posterior dorsals. Anterior-mid dorsal centra are therefore more rectangular in anterior and
959 posterior view, and the posteriormost dorsals more round with a higher mediolateral width.

960 The centra also change from being opisthocoelous to amphicoelous between anterior-mid
961 dorsals PVL 4170 (11)-(13), see Fig. 12 - 14. Opisthocoelus anterior dorsals are shared with
962 *Cetiosaurus*, *Tazoudasaurus*, and diplodocids (Tschopp et al. 2015). The pleurocoel on dorsal
963 vertebral centra in *Patagosaurus* remains visible on the lateral side of the centrum
964 throughout the dorsal series, but does gradually become more of an oval depression. The
965 ventral surface of the centra in anterior dorsals is similar to posterior cervicals in that there
966 is a vestigial ventral keel in anteriormost dorsals, but also in the constriction of the centrum
967 anteriorly, right behind the condyle. The cotyle flares out laterally. Towards mid and
968 posterior dorsals, the centrum in ventral view becomes more symmetrical, with a
969 constriction at the midpoint and flaring out of the centrum towards anterior and posterior
970 articular surfaces. In lateral view, the posterior dorsal centra show a strong curving inwards
971 more anteriorly than posteriorly. Towards the posterior end of the dorsal column, the neural
972 arches increase in height to twice that of the posterior cervicals. The neural spines become
973 axially shorter and transversely broader, however, the posteriormost dorsals have
974 protuberant neural spines that are nearly as high as the combined length of the neural arch
975 and centrum. The neural canal becomes elongated dorsoventrally in the elongated neural
976 arches, and is oval.

977 Anteriormost dorsals (PVL 4170 9-10) are already more elongated dorsoventrally than the
978 cervicals, however, they are still opisthocoelous, and are morphologically distinct from the

979 posterior dorsals, in that they have transversely wide neural spines, which are flattened
980 axially. The neural canal is transversely wide and oval. The diapophyses are bent ventrally as
981 in the cervicals, and the prezygapophyses are placed higher dorsally than the diapophyses.
982 Prezygapophyses are also directed obliquely dorsally. The spol flare out ventrally, giving the
983 neural spine a broad exterior. As in the cervicals, the angle made between the podl and the
984 pcdl is high.

985 Middle dorsals (PVL 4170 11-12) become more transversely slender in the neural arch, and
986 the prezygapophyses have a more horizontally positioned articular surface. The transverse
987 processes are also more elongated than the anterior dorsals. The pedicels become more
988 elevated, and the neural spine more elongated dorsoventrally. spol still flare out, but less
989 posteriorly than in anterior dorsals, creating a more 'compact' neural spine complex.

990 At the transition from middle to posterior dorsals, anteriorly, cpri lengthen as the neural
991 arch and the pedicels elongate. Posteriorly, first the intrapostzygapophyseal laminae meet,
992 then the centropostzygapophyseal laminae disappear, and instead an stpol appears (see
993 Table 2).

994 The posterior dorsals (PVL 4170 13-17) possess the most discriminating combination of
995 features for *Patagosaurus*. The holotype posterior dorsals show an extensive elongation of
996 the neural arch, both at the pedicels as well as at the neural spine. Elongation of the neural
997 spine towards posterior dorsals is common for sauropods (e.g. *Cetiosaurus*, *Barapasaurus*,
998 *Haplocanthosaurus*, *Omeisaurus*, (Hatcher 1903; He et al. 1984; Upchurch and Martin 2003;
999 Bandyopadhyay et al. 2010), however this in combination with the elevation of the pedicels
1000 is not seen to this degree, save for *Cetiosaurus*, and then the elongation is still higher in
1001 *Patagosaurus*. The elongation of the neural arch and pedicels is only seen in
1002 *Mamenchisaurus youngi* (Pi et al. 1996). The lateral elongation of the transverse processes is
1003 reduced. Next to being elongated, the pedicels also show a lateral, ragged sheet of bone
1004 that stretches from the base of the prezygapophyses to the ventral end of the cpri. This is

1005 seen in a more rudimentary form in *Cetiosaurus oxoniensis* (Upchurch and Martin 2003,
1006 OUMNH J13644/2). The relatively horizontal lateral projection of the transverse processes
1007 also distinguishes *Patagosaurus* from many (more or less) contemporary basal non-
1008 neosauropodan eusauropods, as these tend to project more dorsally in *Cetiosaurus*,
1009 *Mamenchisaurus*, *Omeisaurus*, and also in the basal neosauropod *Haplocanthosaurus*
1010 (Hatcher 1903; Young and Zhao 1972; Pi et al. 1996; Tang et al. 2001; Upchurch and Martin
1011 2002, 2003). In anterior view, the neural arch is characterized by two dorsoventrally
1012 elongated oval excavations; the cprf, which are separated by a stprl. The stprl runs down to
1013 the dorsal rim of the neural canal. This is also seen in *Cetiosaurus oxoniensis* OUMNH
1014 J13644/2, and to some extent in *Tazoudasaurus* (Allain and Aquesbi 2008), and
1015 *Spinophorosaurus* (Remes et al. 2009). However, in these taxa, this lamina is shorter, as the
1016 neural arch is less dorsoventrally elongated. In *Patagosaurus* dorsals, the neural canal itself
1017 is also dorsoventrally elongated and oval, this is also seen in *Cetiosaurus oxoniensis* OUMNH
1018 J13644/2, although not to the extent of *Patagosaurus*. It is not slit-like, as seen in
1019 *Amygdalodon* (Rauhut 2003a; Carballido et al. 2011) and *Barapasaurus* ISIR 700
1020 (Bandyopadhyay et al. 2010). In posterior view, the spol remain close to the body of the
1021 neural spine, i.e. they do not flare out laterally as in the anterior and mid-dorsals. The
1022 hyposphene appears here as a small, rhomboid structure, accompanied by very faint
1023 centropostzygapophyseal laminae which are embedded in the posterior neural arch. The
1024 hyposphene is a few cm more dorsal to the neural canal (about 5 cm). It is prominently
1025 visible below the postzygapophyses, which now are aligned at 90° with the neural spine, and
1026 have a horizontal articular surface. Posteriorly, during the transition from mid- to posterior
1027 dorsals, the tpol becomes shorter, and eventually disappears as the postzygapophyses
1028 approach each other medially. Instead, the stpol split into the medial and lateral
1029 spinopostzygapophyseal laminae (m.spol and l.spol, see Table 2). The podl include the l.spol.

1030 The stpol continues to run down to the hyposphene. Posterior dorsals have a very
1031 rudimentary aliform process, sensu Carballido and Sander (2014).

1032 The most noted autapomorphy of *Patagosaurus* is the presence of paired cdf, or fenestrae,
1033 which appear from dorsals PVL 4170 13 onwards. It was long thought that these were
1034 connected to the neural canal, however, recent CT data reveals that a thin septum which
1035 separates the adjacent fenestrae from each other, and from the neural canal. Ventrally
1036 these fenestrae form a central chamber, still well above the neural canal (see PVL 4170 13).

1037 The cpof is present in posterior dorsals of *Patagosaurus*, however it is only weakly
1038 developed. It is more developed in *Cetiosaurus*.

1039

1040 *Dorsal PVL 4170 (9)*: Anterior-mid dorsal with the centrum drastically reduced in
1041 anteroposterior length, making it stouter than the cervicals, but still clearly opisthocoelous.,
1042 see Fig. 10. The left diapophysis, neural arch and part of the neural spine are partially
1043 reconstructed. The condyle has a slightly pointed protrusion on the midpoint, as in the
1044 cervicals (See Fig. 10A, B, F). Ventrally, the centrum constricts strongly immediately
1045 posterior to the anterior condyle (Fig. 10F). The ventral keel marginally visible, and exists
1046 more as a scar running down the midline from the small hypapophysis. The ventral side of
1047 the posterior cotyle is slightly deformed, with the left lateral end projecting further than the
1048 right. As in the other ventral posterior surfaces of the vertebrae, the lateral ends flare out
1049 slightly further posteriorly than the axial midpart (Fig. 10 A, B, F).

1050 The neural canal in anterior view is subtriangular in shape, and transversely wider than
1051 dorsoventrally high (Fig. 10C). Directly above it, there is a small protrusion present of the
1052 hypapophysis. In posterior view, the shape of the neural canal is similar, however, the
1053 posterior opening is less triangular and more rounded (Fig. 10D).

1054 The neural arch of this vertebra is still transversely wide, as in the cervicals. However, it is
1055 also becoming dorsoventrally higher (see Fig. 10A, B, C, D). Because of this, the

1056 centroprezygapophyseal fossae, which are placed medially to the prezygapophyseal stalks,
1057 are not as deep as in the cervicals (Fig. 10C). In lateral view, the prezygapophyseal pedestals
1058 are directed nearly vertically in the dorsoventral plane (Fig. 10A, B).

1059 The prezygapophyses are leaning slightly medially and ventrally towards the single
1060 intraprezygapophyseal lamina that runs along the midline of the vertebral neural arch on the
1061 anterior side (Fig. 10C). In dorsal view, the prezygapophyses are subtriangular in shape and
1062 are widely spaced apart, with about 1/3rd of the spinal summit width between them (Fig.
1063 10E).

1064 The postzygapophyses are raised even higher dorsally in this anterior dorsal than in the
1065 cervicals, at about 2/3rd of the height of the neural spine (Fig. 10A, B, D). Consequently, the
1066 podl are more elongated and makes a high angle, of about 130°, with respect to the axial
1067 plane and to the pcdl. Both podl's are slightly arched towards the postzygapophyses (Figure
1068 10A, B). Because of the extension of the podl, the posdf takes in a large portion of the
1069 posterior lateral surface of the vertebra (Fig. 10A, B). The tpols in posterior view are
1070 prominent, convexely curving laminae, which meet right above the posterior neural canal. In
1071 lateral view, the tpols show a triangular recess below the postzygapophyses, after which the
1072 tpols expand posteriorly before meeting the hyposphene dorsal to the neural canal (Fig.
1073 10D).

1074 In this vertebra, the cpol's are no longer clearly visible, and indeed, only the left cpol is seen
1075 as a thin lamina on the neural arch, lateral and ventral to the left tpol (Fig. 10D). Here, a
1076 rudimentary hyosphene is present as a small teardrop-shape ventral to the ventral fusion
1077 of the tpols. The fusion of the tpols and the hyosphene are also visible as a triangular
1078 protruding complex in dorsal view.

1079 The right diapophysis is prominent in anterior, posterior and lateral view as a stout,
1080 lateroventrally positioned element (Figure 10A, B, C, D). It is transversely broader than in the
1081 cervicals. In anterior view, the prdl and acdl/pcdl are all positioned in an inverted V-shape

1082 with oblique angles of about 45° to the horizontal. In anterior view, the cprl divides the cprf
1083 neatly from the prcdf, which is similarly inverted V-shaped as the outline of the
1084 diapophyseal laminae (Fig. 10C). In posterior view, the pocdf is confluent with the posterior
1085 flat surface of the diapophysis (Fig. 10D). The posterior centrodiaophyseal lamina in
1086 posterior view, curves convexly towards the ventral side of the vertebra.

1087 The articular surface of the diapophysis is flat to concave, and rounded to rectangular in
1088 shape. Posteriorly, they show small, elliptic depressions, on the distal end of the
1089 diapophyses (Fig. 10D).

1090 Note that the sprl are reconstructed, and will not be discussed here. The spol are clearly
1091 seen in anterior view; they flare out transversely in a steep sloping line (Fig. 10C). The spol
1092 are rugose, and the tpol as well, these appear ragged in lateral view. In this anterior dorsal,
1093 the spinopostzygapophyseal fossae (spof) are more rectangular than in the cervicals, and
1094 also deeper (Fig. 10D).

1095

1096 The neural spine is constricted transversely around the dorsoventral midlength, and fans out
1097 transversely towards the summit. The spine summit consists of a thick transverse ridge,
1098 which folds posteriorly on each lateral side, before smoothly transitioning to the spols (Fig.
1099 10E). The neural spine summit is positioned higher dorsally in this anterior dorsal than in the
1100 cervicals (so that the spol are consequently more elongated).

1101

1102

1103 *Dorsal PVL 4170 (10)*: This partially reconstructed anterior-middle dorsal (Fig. 11) is slightly
1104 taphonomically distorted, in that the right transverse process is bent slightly more ventrally,
1105 and the neural spine is slightly tilted to the left side (see Fig. 11). Parts of the centrum, the
1106 middle anterior part of the neural arch, and ventral parts of the diapophyses are partially
1107 reconstructed.

1108 The centrum is still slightly opisthocoelous in lateral view, as in PVL 4170 (9), and as in the
1109 cervicals, with the characteristic stout rim cupping the anterior condyle (Fig. 11A, B). It is
1110 noteworthy however, that the centrum and neural arch do not entirely match, possibly due
1111 to this vertebra being partially reconstructed. The centrum in ventral view is transversely
1112 constricted posterior to the rim that cups the condyle (Fig. 11F). The rim stands out
1113 transversely from the centrum body. The parapophyses are located dorsal to this this
1114 expansion, as triangular protrusions. The cotyle in posterior view is concave, and is slightly
1115 transversely wider than dorsoventrally high.

1116 The neural arch transversely narrows slightly, dorsal to the parapophyses (both at its
1117 anterior and posterior side; Fig. 11C). The anterior neural canal is embedded in this
1118 narrowing, and is rounded to rectangular in shape. It is less wide transversely as in the
1119 posterior cervicals (Fig. 11C). The posterior neural canal is equally rectangular to rounded in
1120 shape. About 5 cm dorsal to it, the hyosphene is present as a rhomboid, small structure
1121 (Fig. 11D).

1122 The diapophyses in this dorsal are creating a wider angle with respect to the horizontal than
1123 in the last dorsal PVL 4170 (9), see Fig. 11C, D. The prdl, the acdl, and posteriorly, the pcdl,
1124 all arch into a less oblique angle, creating an inverted V-shape of about 50° (note that the
1125 right diapophysis is slightly distorted due to taphonomical damage). The diapophyseal
1126 articular surface is triangular, with the tip pointing ventrally, and the flat surface pointing
1127 dorsally, in lateral view (Fig. 11A, B). Ventral to the diapophyses, in lateral view, the anterior
1128 and pcdl are more or less equally distributed in length and spacing on the lateral surface of
1129 the neural arch. A roughly triangular but deep cdf can be seen between these laminae.

1130 The prezygapophyses in dorsal view make a wide wing-like structure together with the
1131 diapophyses and the prdls (Fig. 11E). There is a U-shaped, wide recess between the
1132 prezygapophyses. In anterior view, the prezygapophyses stand widely apart from one
1133 another, and are supported by stout cpri, creating thick pedicels that expand laterally above

1134 the centrum, dorsal to a slight recess right above the centrum (Fig. 11C). The articular
1135 surface of the prezygapophyses is rounded to rectangular in shape, and in anterior view is
1136 tilted ventrally towards the midline of the vertebra (Fig. 11C, E). The prezygapophyseal
1137 spinodiapophyseal fossae (prsd) are present between the prezygapophyseal pedicels, on
1138 the neural arch. They are rounded to rectangular in shape, dorsoventrally elongated, and
1139 shallow, the deepest point being near the onset of the sprl (Fig. 11C).

1140 The postzygapophyseal articular surfaces are obliquely offset from the hyposphene. The
1141 articular surfaces are roughly triangular in shape (Fig. 11D). In posterior view, the tpol are
1142 distinctly flaring out from the dorsal end of the hyposphene to the postzygapophyses. The
1143 cpols are present only as very faint, low ridges embedding the hyposphene on the lateral
1144 side (Fig. 11D). The postzygodiapophyseal lamina is short and stout, therefore dramatically
1145 reduced in length and angle compared to dorsal PVL 4170 (9), (Fig. 11A, B), leading to
1146 believe at least one dorsal between PVL 4170 (9) and (10) should have existed. The spof is
1147 deeply excavated, occupying about 1/3rd of the transverse length of the neural spine (Figure
1148 11D,E). The postzygapophyseal centriadiapophyseal fossae (pocdf) are shallow, and only a bit
1149 more excavated near the ventral rim of the postzygapophyseal pedicels.

1150 The sprl run from the top of the spine to the prezygapophyses in an oblique angle of about
1151 40°. They flank the entire length of the neural spine, creating roughly a V-shape (Fig. 11C, E).

1152 The spol are clearly visible in anterior view in this vertebra, as they flare out laterally from
1153 the neural spine, giving the neural arch and spine a triangular appearance.

1154 In anterior view, the neural spine is roughly V-shaped, with a transversely broad dorsalmost
1155 rim (Fig. 11C). In posterior view, the neural spine combined with spol and postzygapophyses
1156 are slightly bell-shaped. The neural spine tapers dorsally to a point, exposing a stout rim. In
1157 dorsal view, the neural spine summit is clearly seen as an anteroposteriorly thin rim,
1158 transversely wide, reaching to the level of the onset of the postzygapophyses (Fig. 11E).

1159

1160 *Dorsal PVL 4170 (11)*: Partially reconstructed dorsal; the centrum is a replica, which will not
1161 be described. The neural arch and spine and transverse processes, however, are original, see
1162 Figure 12. The diapophyses of this vertebra are elongated laterally compared to the other
1163 dorsals, and the transition between this and the previous and next vertebrae, leads to
1164 believe a transitional dorsal could have existed originally.

1165

1166 The neural arch is mainly shaped by the acdl in anterior view, and the pcdl in posterior view.
1167 It is about as long and wide, as PVL 4170 (10), see Fig. 12A, B. The neural canal in anterior
1168 view is rounded to rectangular in shape, with a dorsoventral elongation (Fig. 12C). The
1169 posterior neural canal is more flattened, and triangular to round in shape. The hyosphene
1170 is seen as a small rhomboid structure, about 5 cm dorsal to the posterior neural canal (Fig.
1171 12D).

1172 In this dorsal, the diapophyses are more prominent and extend wider transversely than in
1173 previous dorsals (Fig. 12C, D). Their shape in anterior and posterior view is near rectangular.
1174 They are directed laterally and slightly ventrally in anterior view (Fig. 12C). The articular
1175 surface of the diapophyses is more rounded than triangular (Fig. 12A, B). The diapophyses in
1176 posterior view are slightly expanded towards their extremities (Fig. 12D). The pcdl are
1177 slightly damaged and have a frayed appearance, but arch convexly towards the transverse
1178 processes.

1179 The prezygapophyses are more or less perpendicularly placed towards the neural spine, and
1180 slightly canted medially in anterior view (Fig. 12C). Their articular surface lies in the dorsal
1181 plane. The articular surface of the prezygapophyses is roughly square in shape (Fig. 12E). In
1182 dorsal view, a U-shaped recess is seen between the prezygapophyseal articular surfaces. The
1183 prdl are stout and run in a convex arch transversely to the diapophyses. In this vertebra, the
1184 single intraprezygapophyseal lamina (stprl) is visible, as the interprezygapophyseal laminae
1185 (tprl) run down in a curved V-shape towards the neural canal (Fig. 12C). The paired cprf,

1186 positioned laterally to the stprl, are more excavated than in previous dorsals, and also have
1187 a more defined rim.

1188 The postzygapophyses are more pronounced in this vertebra than in previous dorsals, and
1189 also protrude posteriorly more than in previous dorsals (Fig. 12D). Their articular surface is
1190 triangular in shape. There is a similar U-shaped recess between the postzygapophyses,
1191 though not as wide, as with the prezygapophyses (Fig. 12C, D). The tpols are shorter in this
1192 vertebra, as they do not reach as far down ventrally to reach the hyposphene. Below the
1193 tpols, two cpols are seen to strut the hyposphene on lateral sides. The triangular and
1194 shallow pocdf's are positioned on each lateral side of the cpols, and ventral to the tpols (Fig.
1195 12D).

1196 The neural spine is transversely wide and anteroposteriorly short, but protrudes out
1197 posteriorly at both lateral sides and on the midline (Fig. 12D). This midline could be a
1198 rudimentary scar of a postspinal lamina (posl), but that is not clearly visible. In anterior view,
1199 the neural spine resembles that of PVL 4170 10, however the neural spine is more
1200 dorsoventrally elongated, and the spol are more dented than straight as they run down to
1201 the postzygapophyses. The morphology of the neural spine posteriorly, towards the
1202 postzygapophyses is similar to PVL 4170 10 in that the composition looks bell-shaped in
1203 posterior view, and the posterior half contains a deep V-shaped spof. The neural spine is
1204 more dorsally elevated however, and the summit is less transversely broad than in the
1205 previous dorsal (Fig. 12E).

1206

1207

1208 *Dorsal PVL 4170 (12):* Mid-posterior dorsal with partially reconstructed neural spine (which
1209 will therefore be omitted from description). The transition from middle to posterior dorsals
1210 is perhaps the most drastic morphological transition in *Patagosaurus*, and hints at missing
1211 vertebrae (Fig. 13).

1212 The centrum is clearly opisthocoelous, though the condyle is not as convex as in previous
1213 anterior dorsals (Fig. 13A, B). The centrum is posteriorly still wider transversely than
1214 anteriorly. The condyle still has a rugose rim, as in the cervicals. The parapophyses are
1215 positioned on the dorsolateral side of this rim, and are visible as rounded rugose
1216 protrusions. The pleurocoel is still clearly visible, and has a deep, rounded dorsal rim, and a
1217 clear rectangular posterior rim. The ventral side of the cotyle extends further posteriorly
1218 than the dorsal side (Fig. 13E). The cotyle is heart-shaped in posterior view, with a rounded
1219 'trench' below the neural canal (Fig. 13D). In ventral view, the centrum is not as constricted
1220 as in previous vertebrae; even though there is still a slight constriction posterior to the rim
1221 of the condyle. The ventral keel is no longer present.

1222 The neural canal in anterior view is elongated to an oval to teardrop shape, which is
1223 dorsoventrally longer than transversely wide (Fig. 13C). The neural canal in posterior view is
1224 oval to rectangular in shape, and is also dorsoventrally elongated.

1225 The neural arch in this dorsal is rather rectangular and straight in anterior and posterior
1226 view, widens axially in lateral view, towards the prezygapophyses (Figure 13 A, B, C, D). A
1227 fenestra is formed instead of the cdf. The centriadiapophyseal laminae run smoothly in a
1228 convex curve towards the centrum.

1229 The pedicels of the prezygapophyses are stout, and expand laterally towards the ventral side
1230 of the prezygapophyses (Fig. 13C). The tpri meet ventrally and at the midpoint between the
1231 prezygapophyses, where a rudimentary hypantrum is formed, below which a stpri runs
1232 down to the dorsal roof of the neural canal. This lamina separates two parallel, rhomboid,
1233 deep cprf.

1234 In posterior view, the postzygapophyses form a wide V-shape, and the tpols meet dorsal to a
1235 small diamond-shaped possible rudimentary hyposphene, below which a stpol runs down to
1236 the neural canal, which is oval and dorsoventrally elongated (Fig. 13D). The podl is a sharply
1237 curved, short lamina, not to be confused with the spd, which is not present in this vertebra

1238 (Fig. 13A, B). Two parallel cpols might be present, but this is not entirely clear as the
1239 posterior part of this vertebra is partially reconstructed (Fig. 13D).
1240 In anterior view, the diapophyses are no longer ventrally and laterally positioned, but
1241 dorsally and laterally, in an oblique angle dorsally (Figure 13C). In lateral view, pcdl runs in a
1242 sinusoidal shape down from the diapophysis to the neural arch, while the prdl is convex (Fig.
1243 13A, B). The diapophyses extend a bit further ventrally in a subtriangular protrusion. The
1244 diapophyses are slightly excavated between the podl and the pcdl. In dorsal view, the
1245 diapophyses are seen to extend to nearly the entire width of the centrum (Fig. 13F). They
1246 are slightly pointed posteriorly as well.

1247

1248

1249 *Dorsal PVL 4170 (13)*: This is the most complete posterior dorsal of the holotype (Fig. 14,
1250 15). It has consequently been scanned in order to elucidate on the pneumatic features
1251 present in the holotype (Fig. 14). The pneumatic opening ventral to the diapophyses, on the
1252 lateral surface of the neural arch, opens into an internal pneumatic chamber (Fig. 14 B, C),
1253 but is separated from the opening on the opposite neural arch by a thin septum (Fig. 14 I, J).
1254 The pneumatic chamber is situated ventral to this septum, and is round to squared in shape.
1255 It remains separated from the neural canal (see Discussion).

1256 The anterior articular surface of the centrum is oval in anterior view, with a slight
1257 constriction at about two-thirds of the dorsoventral height (Fig. 15C). Consequently, the
1258 ventral side is transversely wider than the dorsal side. In posterior view, the posterior
1259 articular surface of the centrum is heart-shaped at its dorsal side, and flattened on its
1260 ventral side. The articular surface itself is slightly oval, and is constricted towards the upper
1261 1/3rd as in the anterior side. In ventral view, the centrum is more or less equally flaring out
1262 at each articular surface, and slightly constricted in the midpoint. No keel is visible, but on
1263 the anterior ventral side of the centrum, a small triangular 'lip' is seen. In lateral view, the
1264 centrum is ventrally concave, with the posterior ventral side expanding further ventrally

1265 than the anterior side (Fig. 15A, B). There is a slight depression on the lateral side of each
1266 centrum.

1267 The dorsal anterior side of the centrum is expanding a bit further anteriorly beyond the
1268 pedicels of the neural arch, but the dorsal posterior side of the centrum expands
1269 considerably further posteriorly from the neural arch.

1270 The parapophyses are not clearly visible in anterior view, however, they are visible in lateral
1271 and ventral view as rugose oval protrusions on the rugose lateral sides of the cprls.

1272 In anterior view, the neural canal is clearly visible in this specimen. It is oval and
1273 dorsoventrally much more elongated than in the previous vertebrae (Fig. 15A). It is
1274 transversely narrow, and slightly above the midpoint is constricted, so that the neural canal
1275 looks like a figure 8-shape. The neural canal is not clearly visible in posterior view; however,
1276 the neural arch is excavated in a triangular shape around the neural canal (Figure 15D). It is
1277 surrounded by stout centropostzygapophyseal laminae. Dorsal to this depression, the stpol
1278 supports the rhomboid hyposphene from below (see description of postzygapophyses).

1279 The neural arch itself is ventrally restricted transversely. The pedicels of the neural arch are
1280 equally dorsoventrally elongated and transversely narrow. The anterior side of the neural
1281 arch is characterised by a dorsoventrally oriented, long stprl, dividing two mirrored, shallow,
1282 oval to bean-shaped cprf. The lateral sides of the neural arch tilt towards the midline in
1283 posterior view, giving the neural arch a constricted look towards its dorsal end. On the
1284 lateral side of the neural arch, the centrodiaepophyseal fossa (or more foramen in this
1285 vertebra) is visible as a dorsoventrally elongated oval, opening slightly posterior to the
1286 midpoint of the neural arch.

1287 The diapophyses project laterally in a near perpendicular angle from the neural arch (Fig.
1288 15A, D). They are ventrally excavated, with the prdl running concavely from the lateral side
1289 of the prezygapophyses to the diapophyses. In dorsal view, the diapophyses are seen to
1290 bend slightly posteriorly as well as laterally. The tips point sharply to the posterior side. The

1291 diapophyseal articular surfaces are triangular, with a rounded posterior rim, in lateral view.
1292 The dorsal distal ends of the diapophyses have a small triangular protrusion, projecting
1293 dorsally, in anterior view. The diapophyses show round excavations on the posterior side of
1294 their distal ends. The ventral side of the diapophyses is also concavely curved with a
1295 concave paradiapophyseal lamina (ppdl) running parallel to the prdl. The pcdl curve
1296 concavely from the diapophyses down to the ventralmost side of the neural arch. These
1297 sustain a thin sheet of bone that holds the diapophyses on each lateral side in posterior
1298 view.

1299 The prezygapophyses are transversely shorter than in previous dorsals, and are stout;
1300 almost as thick dorsoventrally as transversely (Fig. 15A, B, C). They tilt at an oblique angle
1301 anteriorly and dorsally from this narrow arch. The prezygapophyseal articular surfaces are
1302 horizontally aligned in the axial plane, and are near perpendicular to the neural spine. In
1303 dorsal view, prezygapophyses are directed mostly anteriorly, and there is a deep U-shaped
1304 recess between them. On the lateral side of the prezygapophyses, running from the lateral
1305 ends of the cdf, the cprl are characterized by laterally flaring, rugose, rugged bony flanges,
1306 that spread anteriorly as well as laterally. In anterior and lateral view, prdl and the ppdl run
1307 parallel in a convex arch at the ventral end of the neural spine. They are equally thin and
1308 dorsoventrally flattened.

1309 The postzygapophyses are triangular in shape, and are positioned slightly more dorsally on
1310 the neural arch than the prezygapophyses (Fig. 15D). The postzygapophyses are flat to
1311 slightly convex on articular surface, seen from lateral and ventral view. The stpol tapers
1312 dorsally and posteriorly in an oblique angle from the rhomboid hyposphene to the neural
1313 arch. The postzygapophyses are not visible in lateral view as they are obscured by the
1314 diapophyses. The postzygapophyses connect with the diapophyses through a strongly
1315 bending podl, which is often mistaken for a spinodiapophyseal lamina (spdl; Wilson, 2011a,
1316 Carballido and Sander, 2014).

1317 In this dorsal, the prdl and the podl are seen to support wide, but thin plates of bone
1318 between the prezyga- dia- and postzygapophyses.

1319 The neural spine is roughly cone-shaped, and is constricted toward the summit both
1320 anteriorly and posteriorly. In anterior view, the sprl flare out towards the ventral contact of
1321 the prezygapophyses. The sprls are seen as sharply protruding thin laminae. The sprdfs,
1322 bordered by the sprls, are visible as deep triangular depressions in dorsal view. The neural
1323 spine shows a triangular excavated prezygospinodiapophyseal fossa (prsdff) on each lateral
1324 side, which have clear posterior rims.

1325 Similar to the sprls, in posterior view, the spol are seen to flare out towards the ventral side
1326 of the neural spine. In this dorsal, the spol has divided into a lateral spol and medial spol (l.
1327 spol and m. spol), visible as running from the ventral one-third of the neural spine to the
1328 postzygapophyses. On the midline between these laminae, a deep but transversely narrow
1329 rudimentary spof is present. The lateral spols flare out on the lateral sides, giving the spine a
1330 'rocket-shape' in posterior view. A slight transverse thickening of this stout lateral spol is
1331 visible at about two-thirds of the spinal dorsoventral length.

1332 On the dorsoventral midline of the spine, in posterior view, a rough scar is visible, which
1333 could be a very rudimentary postspinal (posl) lamina.

1334 The spine itself tilts very slightly posteriorly, especially the most distal one-third part. This
1335 distal end is solid, and cone-shaped, with a rounded summit. The spine summit has a slight
1336 bulge on each lateral side, which might be a rudimentary aliform process (see Carballido and
1337 Sander, 2014), and the summit is more rounded than flattened. The summit of the neural
1338 spine in dorsal view is rounded, but has a constricted anterior end, where it points towards
1339 the sprls. The posterior end projects more posteriorly and is round, though with a slightly
1340 pointed end at the posterior midline.

1341

1342 *Dorsal PVL 4170 (14)*: Posterior dorsal with preserved neural arch, spine and centrum.
1343 Because of its fragile state, a ventral image could not be obtained. Parts of the diapophyses
1344 and neural arch are damaged.
1345 In anterior view, the anterior articular surface of the centrum is oval, and dorsoventrally
1346 flattened, so that the transverse width is greater than the dorsoventral height (Fig. 16D). The
1347 dorsal end is slightly heart-shaped. The anterior articular surface of the centrum is
1348 dorsoventrally longer than the posterior side. The posterior dorsal rim of the articular
1349 surface of the centrum extends further posteriorly than the ventral side. The extension is
1350 rounded and is visible on both lateral sides of this dorsal vertebra (Fig. 16A, B). The width of
1351 the centrum extends beyond the width of the pedicels of the neural arch. In posterior view,
1352 the centrum is dorsoventrally flattened and expands a little transversely on the midline
1353 (Fig. 16C). The dorsal end of the posterior articular surface is slightly excavated dorsally, as
1354 are posterior surfaces of the pedicels surrounding the neural canal, embedding the neural
1355 canal. In lateral view, the centrum is ventrally concave. It is slightly reconstructed however,
1356 so there might not be more original curvature preserved. There are shallow, elliptical
1357 depressions visible on each lateral side of the centrum.
1358 The anterior side of the neural canal is oval and dorsoventrally elongated, and narrows in
1359 the upper one-third towards its dorsal end (Fig. 16D). The posterior side is more triangular in
1360 shape, but overall roughly similar to the anterior side (Fig. 16C). The medial sides of the
1361 pedicels of the neural arch are excavated, forming an oval excavation around the neural
1362 canal.
1363 The anterior central part of the neural arch is damaged, thereby revealing the pneumatic
1364 centrodiapophyseal fenestra, which connects to each lateral side of the neural arch below
1365 the diapophyses (Fig. 16A, B). These openings perforate the neural arch to the posterior
1366 side, indicating there must have been only a thin sheet of bone covering them. The neural
1367 arch tapers towards the midpoint on both the anterior and posterior sides in lateral view,

1368 however, the anterior end expands towards the posterior side again together with the
1369 parapophysis and the base of the prezygapophysis (Fig. 16A, B). The neural arch constricts
1370 around the central part of the vertebra in posterior view. On the right lateral neural arch, a
1371 neurocentral suture is present. Posteriorly, the hyposphene is visible as a clear triangular
1372 protrusion below the postzygapophyses. The hyposphene is smaller than in the previous
1373 dorsals (Fig. 16C).

1374 The left lateral side of this dorsal is missing the diapophyses, however, this does give a good
1375 view of the proximal bases of the diapophyseal laminae; the prdl is a relatively delicate and
1376 short lamina that runs obliquely to the ventral anterior base of the prezygapophysis; the
1377 podl lies on the same oblique sagittal plane and projects dorsally and posteriorly towards
1378 the postzygapophysis (Fig. 16B). The right lateral side in lateral view shows the partial right
1379 diapophysis, of which the distal end is broken, revealing two laminae, the distal side of the
1380 prdl and the distal side of the pcdl (Fig. 16A). Also, a thin short lamina runs from the
1381 posterior end of the diapophysis to the postzygapophyses; this lamina connects also to the
1382 lateral spol, therefore is the podl+lspol complex. On both lateral sides, ventral to the
1383 diapophyseal base, the centrodiaophyseal fenestra is clearly visible and perforates the
1384 neural arch completely; however, there would probably have been a thin septum separating
1385 them.

1386 The right diapophysis is partially preserved; it is shorter than in the previous dorsals, and
1387 stout. It projects laterally, slightly dorsally and posteriorly, unlike the diapophyses of the
1388 previous dorsals (Fig. 16A, B, C, D). The diapophysis is wing-shaped in posterior view; the
1389 pcdl encircles a wide sheet of bone on its posterior side. The prezygodiaophyseal lamina is
1390 visible in anterior view, as it curves convexly to the lateral distal end of the diapophysis. The
1391 ventral lateral side of the transverse process is marked by the prcdf.

1392 The only prezygapophysis present is reconstructed. On the right lateral side, a rugose
1393 parapophysis is supported by an anterior centroparapophyseal lamina (cpri), which runs

1394 along a ragged lateral rim of bone from the prezygapophyses to the ventral end of the
1395 pedicel of the neural arch, which is similar to those in PVL 4170 (13), see Fig. 16A. The actual
1396 prezygapophyses are missing or reconstructed, therefore there is no information known
1397 about these in this particular dorsal.

1398 Because most zygapophyseal structures are either broken or reconstructed, not much can
1399 be said about the shape of these in dorsal view, however, the wide sheet of bone between
1400 the prdl and the pcdl is clearly visible in dorsal view (Fig. 16F). The left pedicel of the neural
1401 arch is partially visible. It is positioned slightly posterior to the anterior rim.

1402 The postzygapophyses are ventrally convex, and dorsally stand out from the neural spine,
1403 making the spols protrude from the spine in an equal fashion. The podl + lspol complex is
1404 seen curving sharply convexely from the lateral end of the right postzygapophysis to the
1405 distal end of the diapophysis (Fig. 16C).

1406 The neural spine in anterior view is straight and square in the upper one-third of its
1407 dorsoventral height, however, the anterior side tapers to a V-shaped point towards its
1408 ventral end (Fig. 16D). The 'V' is rugose. On each lateral side, slightly dorsal to this point, the
1409 spinoprezygapophyseal laminae widen the lowermost one-third of the neural spine. The
1410 summit of the neural spine is rugose and shows a small oval protrusion on its anterior
1411 midline (Fig 16F). The lower half of the neural spine shows a clear division between the
1412 lateral and medial spols, between which are evenly sized, slit-like fossae. The spof
1413 completely perforates the area between the postzygapophyses in an elliptical shape (Fig.
1414 16C). The top of the neural spine is cone-shaped and rugose. There is no trace of a
1415 postspinal scar, as in more anterior dorsals. The neural spine in lateral view is excavated by
1416 the prsdf, which is triangular and relatively deep (Fig. 16A, B). The lspol is thick in the ventral
1417 half of the neural spine, however, at the lateral sides of the dorsal half of the neural spine it
1418 is only a thin edge that protrudes posteriorly from the spine. The lateral spols form a bell-
1419 shaped sheet around the lower half of the neural spine in posterior view, whereas the upper

1420 half has the base of the lateral spool only visible as a thin lateral ridge (Fig. 16C). As in the
1421 previous dorsals, the distal end of the neural spine is massive, and cone-shaped. In this
1422 posterior dorsal, however, the lower half of the spine is bending anteriorly, the upper half of
1423 the spine is bending posteriorly (Fig. 16A, B). At the base of the upper half, a ridge is seen
1424 curving from the anterior lateral side to the posterior lateral side. In dorsal view, the summit
1425 of the neural spine is transversely wider posteriorly than anteriorly, giving it a trapezoidal
1426 shape (Fig. 16 E). The surface is rugose.

1427

1428

1429 *Dorsal PVL 4170 (15)*: This dorsal vertebra only has its centrum preserved (Fig. 17; 15). In
1430 anterior view, the anterior articular surface of the centrum is almost trapezoidal in shape,
1431 with lateral protrusions on the midline. The anterior articular surface is equally as high as it
1432 is wide. The posterior articular surface in lateral view is broken and not clearly visible. In
1433 lateral view, the centrum shows a concave ventral side, and a slightly more convex than flat
1434 anterior articular surface. Towards the dorsal middle part of the centrum, in lateral view, a
1435 shallow elliptical fossa is visible. The ventral floor of the neural canal is visible, and the
1436 lowermost lateral walls, indicating an elongated elliptical shape of the neural canal, as in the
1437 other posterior dorsals. In dorsal view, the neural canal is seen to cut deeply into the
1438 centrum, and shows a widening transversely towards the posterior opening. In dorsal view,
1439 the neurocentral sutures are either broken or unfused; the former is the more likely option,
1440 as the sutures are fused in the other dorsals of PVL 4170.

1441

1442 *Dorsal PVL 4170 (16)*: This dorsal, though well-preserved, and only partially reconstructed, is
1443 unfortunately stuck behind a low bar on the ceiling of the Instituto Miguel Lillo, in the
1444 hallway where the holotype is mounted. As a result, only the right lateral side and some
1445 oblique views of the anterior side could be obtained (Fig. 17; 16).

1446 The centrum is partially reconstructed; however, the dorsal end is original and is heart-
1447 shaped. In right lateral view, the centrum is almost quadrangular in shape. The dorsoventral
1448 height is slightly greater than the anteroposterior length. The posterior dorsal side of the
1449 centrum flares slightly laterally and posteriorly, and the neural canal creates a little 'gutter'
1450 on the dorsal surface of the centrum. On the lateral side of the centrum, dorsal to the axial
1451 midpoint, is an oval fossa, which is axially longer than dorsoventrally high. This fossa is
1452 dorsoventrally higher than in the previous dorsals, making it appear more round than
1453 elliptical.

1454 The neural arch is supported by lateral pedicels, which rest more on the anterior side of the
1455 centrum than on the posterior. The pedicels of the neural arch in anterior view are of
1456 irregular shape, and show an almost anastomosing structure. The posterior part of the
1457 pedicels rests a few centimeters medial to the dorsal posterior rim of the posterior articular
1458 surface. From there, the posterior part of the pedicel inclines towards the medial side in
1459 lateral view. The dorsal end of the pedicels is axially constricted. The right lateral pedicel is
1460 broken off laterally. The anterior medial area, between the prezygapophyses, is excavated;
1461 this is probably due to a thin sheet of bone having been broken away, revealing the internal
1462 pneumatic structure.

1463 The diapophysis is not very clearly visible in anterior view. The diapophyses are located
1464 slightly posterior to the midline of the neural arch. In lateral view, the articular surface is a
1465 thin, semi-lunate dorsoventrally elongated ridge.

1466 The prezygapophyses are supported below by stout columns that project obliquely anteriorly
1467 and dorsally; these are also convex anteriorly.

1468 The prezygapophyses have a flat axial articular surface, and are supported from below by
1469 stout convex columns.

1470 The postzygapophyses are situated at around the same elevation as the prezygapophyses.

1471 The articular surface of the postzygapophyses is slightly inclined ventrally. The hyposphene

1472 extends further posteriorly than the postzygapophyses, and has a ragged outline in lateral
1473 view; this could however be caused by damage to the bone.

1474 The neural spine is slightly inclined towards the posterior side in its lower half, the upper
1475 half is more or less erect in the dorsoventral plane. It is slightly wider at its base, however
1476 the upper 2/3rd is of an equal axial width. The summit is rod-shaped. The accessory lamina
1477 seen in the previous two dorsals is seen around halfway to the summit, running in a
1478 semicircular line from anterior dorsal to posterior ventral.

1479

1480 *Dorsal PVL 4170 (17)*: The posteriormost dorsal is only partially preserved, and therefore is
1481 partially reconstructed (Fig. 17; 17). It is also not possible to unmount this dorsal, therefore
1482 the view is limited to the anterior side and the (partial) lateral side. The centrum shows deep
1483 lateral depressions, and is more oval than round, as in the previous dorsals. The neural arch
1484 is similar in morphology to the previous posterior dorsals, with stout prpls and a deep
1485 depression between each lateral side of the neural arch. The prezygapophyses are inclined
1486 medially, rather than being horizontally aligned with the sagittal plane. The neural spine has
1487 very sharp outstanding sprls and spols between which the spine has deep depressions on
1488 anterior and lateral sides, which are oriented dorsoventrally. The spine summit is a massive
1489 block of bone, and has a square shape. Two rudimentary but clearly visible aliform processes
1490 are positioned slightly ventral to the dorsal spine summit on each lateral side.

1491

1492 *Sacrals PVL 4170 (18)*: The complete sacrum is well-preserved (see Bonaparte 1986b, Fig. 43
1493 and 44, and this manuscript, Fig. 18, lower row, A-D). Unfortunately, because the holotype
1494 specimen is mounted, it is difficult to access. Most recent pictures can only show the neural
1495 arches and the spines, as the rest of the view is blocked by the ilium laterally (Fig. 18C), by
1496 the dorsal vertebrae anteriorly, and by the caudal vertebrae posteriorly, although the caudal
1497 vertebrae can be unmounted. Bonaparte's 1986 *Patagosaurus* description shows a detailed

1498 illustration, however; see Bonaparte (1986b), and Fig. 18D. The sacrum consists of five sacral
1499 vertebrae, of which all centra are fused. This is in contrast to *Vulcanodon*, *Barapasaurus*,
1500 *Shunosaurus* and *Spinophorosaurus*, who are reported to have had four sacral centra (Remes
1501 et al. 2009; Bandyopadhyay et al. 2010; Carballido et al. 2017b). *Ferganasaurus* and *Jobaria*
1502 *tiguidensis* had five sacral centra (Alivanov and Averianov 2003; Carballido et al. 2017b).
1503 *Haplocanthosaurus*, *Camarasaurus* and diplodocids had five (Although some have been
1504 reported to have had six, Tschopp et al. 2015; Carballido et al. 2017b). In PVL 4170 (18), the
1505 second, and third of the neural spines are fused together by their anterior and posterior
1506 sides. This is similar to *Barapasaurus* (Bandyopadhyay et al. 2010), but different from
1507 *Ferganasaurus* and neosauropods; e.g. *Ferganasaurus verzilini* Alifanov & Averianov, 2003
1508 and diplodocids fuse the sacral neural spines 2-4, whereas *Camarasaurus* Cope, 1877 and
1509 *Haplocanthosaurus* fuse sacral neural spines 1-3 (Alivanov and Averianov 2003; Upchurch
1510 2004). All neural spines are rugosely striated (Fig. 18B). They all possess *spri* and *spol*, which
1511 are roughly similar to the morphology of the posteriormost dorsal vertebrae. No *spdi* is
1512 present. The dorsal rim of the ilium terminates at about the diapophyseal height of the
1513 sacrum (Fig. 18C). The neural spines extend dorsally beyond the upper rim of the ilium for
1514 about 30 cm. In mamenchisaurids, as well as in *Camarasaurus* and basal titanosauriforms,
1515 the neural spines of the sacrum are much shorter (not as dorsoventrally high as the neural
1516 arch and centrum combined), and more robust (Ouyang and Ye 2002; Taylor 2009). In
1517 neosauropods such as *Apatosaurus*, *Diplodocus* and *Haplocanthosaurus*, however, the
1518 neural spines do extend further beyond the ilium. In *Haplocanthosaurus*, the neural spine is
1519 and are as dorsoventrally high as the neural arch and centrum together, like in
1520 *Patagosaurus*; however, some diplodocids have higher sacral neural spines. (Gilmore 1936;
1521 Hatcher 1901, 1903). The sacral ribs do not project over the ilium, as they do in
1522 neosauropods (Carballido et al. 2017b).

1523 The first sacral PVL 4170 18.1 is, as in most sauropods, relatively similar to the posteriormost
1524 dorsal (Upchurch 2004). The centrum is oval, and dorsoventrally elongated (Fig. 18D). The
1525 neural canal is oval and also dorsoventrally elongated, as in the posterior dorsals. The sacral
1526 rib is unattached to the diapophysis in this sacral vertebra. It is a lateral dorsoventrally
1527 elongated extension, as in most sauropods, a C-shaped plate that extends laterally towards
1528 the medial side of the ilium (Upchurch et al. 2004). The prezygapophyses are anteriorly
1529 elongated, and flat dorsally, and have a deep U-shaped recess between them, as in the
1530 posterior dorsals (Fig. 18A). They connect to the neural spine via the spinoprezygapophyseal
1531 laminae, which project as sharp ridges off the lateral sides of the anterior side of the neural
1532 spine. Lateral and anterior to the postzygapophysis, the *podl* runs to the transverse process
1533 of the first sacral. As in the posterior dorsals, dorsal to the postzygapophyses, a rudimentary
1534 aliform process is present. From here, the lateral *spol* flares out laterally and dorsally before
1535 it joins the postzygapophysis. The *spri* encases a deep triangular depression, which is visible
1536 on the lateral side of the neural spine, which could be the sacral equivalent of the *spdf* in
1537 *Patagosaurus* (see Wilson et al. 2011).

1538 The neural spine inclines slightly anteriorly, as in the posteriormost dorsals. The anterior
1539 surface of the neural spine shows rugosities for ligament attachments. On the lateral side of
1540 the neural spine, a triangular depression runs over about 2/3rds of the dorsoventral length
1541 (Fig. 18A, D), with a sharp dorsal semicircular rim. Dorsal to this rim, the spine becomes
1542 solid. The spine summit is rounded laterally and has a crest-like shape in anterior view.

1543 The second and third sacral neural spines PVL 4170 18.2 and 18.3 are fused (Fig. 18A, C, D).

1544 Both the second and third sacral vertebrae have large C-shaped sacral ribs that connect to
1545 the medial side of the ilium. These sacral ribs project laterally and slightly posteriorly from
1546 the neural arch above the centra. Between these sacral ribs, dorsoventrally elongated and
1547 axially short intervertebral foramina (*ivf*; Wilson et al. 2011) are visible as slit-like apertures,

1548 which in this sacrum are fenestrae that connect to large internal pneumatic chambers inside
1549 the sacral centra.

1550 The second sacral neural spine is projecting mainly dorsally, and only slightly anteriorly (Fig.
1551 18A, C, D). At the base of the spine, the sprl and spol and the dorsal side of the sacral
1552 transverse process border a triangular sdf, as in the first sacral. This fossa is more oval-to-
1553 triangular, which is different from the first sacral. This fossa is also present on the third
1554 sacral and is more pronounced there; being axially wider and more triangular. Between both
1555 neural spines, a thin plate of bone was probably present, as there is a small slit, which does
1556 not appear natural. The neural spines are dorsally connected by rugose bone tissue. In
1557 lateral view, this connection has a U-shaped concavity between both neural spine summits.

1558 The fourth sacral vertebra PVL 4170 18.4 inclines slightly more posteriorly than the previous
1559 sacrals (Fig. 18A, C, D). The sacral rib of this sacral is a C- or heartshaped laterally projecting
1560 bony plate. Between this sacral rib and the sacral rib of the third sacral, a large
1561 dorsoventrally elongated slitlike opening is seen to connect to the internal pneumatic
1562 chamber of the sacrum.

1563 The prezygapophyses are not visible; the postzygapophyses are rhomboid, laterally
1564 projecting protrusions. The hyosphene is equally rhomboid.

1565 In anterior view, the neural spine is transversely shorter than the previous sacrals, however,
1566 axially it is equally wide, giving the spine summit a rhomboidal shape. At the anterior side of
1567 the base of the spine, a triangular protrusion is visible, which appears broken, therefore this
1568 sacral might have been connected to the third sacral by a bony protrusion at the bases of
1569 the neural spines. On the lateral side of the spine, a deep groove is seen to run concavely
1570 from the dorsal anterior lateral side to the ventral posterior lateral side, as in some anterior
1571 caudals (see caudals later). The dorsal lateral side of the neural spine shows a weakly
1572 developed aliform process. In posterior view, the lateral spinopostzygapophyseal laminae

1573 are seen to protrude dorsally from the neural spine, which is very rugosely dorsoventrally
1574 striated.

1575 The fifth sacral PVL 4170 18.5 is slightly different in morphology from the previous four, in
1576 that it is slightly posteriorly offset from the others (Fig. 18A, B). The posterior articular
1577 surface of the centrum is clearly visible in this last sacrum, and is flat to slightly
1578 amphicoelous. It is oval in shape, and slightly dorsoventrally elongated, and slightly
1579 transversely flattened. The neural canal is a dorsoventrally elongated oval shape. Directly
1580 dorsal to the neural canal, a small triangular and posteriorly projected protrusion is visible,
1581 which resembles the small anteriorly projected protrusions above the neural canal of some
1582 of the dorsal vertebrae. The lamina that projects laterally towards the sacral rib has a
1583 dorsolaterally directed bulge, so that the rib projects laterally in two stages (Fig. 18B). The
1584 main body of the sacral ribs of this last sacral are directed laterally, but also bend anteriorly
1585 towards the other sacrals. The postzygapophyses are diamond-shaped, as is the
1586 hyosphene. The spoli in posterior view are slightly offset from the spine, and at about half
1587 of the dorsoventral height of the spine, protrude in a rounded triangular shape. This might
1588 have been a ligament attachment site. The spine itself is rugosely striated and resembles the
1589 fourth sacral in morphology.

1590

1591 *Caudals:* The holotype PVL 4170 has a few anterior, mid, and mid-posterior caudals
1592 preserved. The caudal numbering is rather discontinuous, indicating that the caudal series
1593 was already incomplete when it was found. Two caudals are without collection reference
1594 numbers, but will be described here for completeness, and positioned in the caudal series
1595 relative to their size and morphology. Two caudals are repeated, as one is a cast of the
1596 other.

1597 Anterior- to anterior-mid caudals (PVL 4170 19-20-21) have dorsoventrally high and axially
1598 short centra (Fig. 19), as seen in *Cetiosaurus*, *Tazoudasaurus* and *Chebsaurus*. They display

1599 rounded triangular-to-heart-shaped anterior vertebral articular surfaces, and slightly more
1600 heart-shaped posterior vertebral articular surfaces, the most acute tip being the ventral
1601 side. The centrum in lateral view is concavely curved on the ventral side, with the slope on
1602 the anterior half less acute than on the posterior half. A faint raised ridge of bone is seen in
1603 some caudals on the lateral centrum, ventral to the diapophyses. This is also seen in
1604 *Cetiosaurus*, and could be a rudimentary lateral ridge as seen in neosauropods (Tschopp et
1605 al. 2015). The posterior dorsal rim of the centrum shows an inlet for the neural canal, as in
1606 the cervicals and dorsals, and stretches slightly beyond the posterior end of the base of the
1607 neural spine.

1608 In ventral view, two parallel axially positioned struts are visible, between which is a 'gully';
1609 an axially running depression. This feature is seen in other basal eusauropods (*Cetiosaurus*
1610 *oxoniensis* and the Rutland *Cetiosaurus*; (Upchurch and Martin 2002, 2003) as well as an
1611 unnamed specimen from Skye, UK (Liston 2004), though is not as prominently developed in
1612 *Patagosaurus* as in the latter taxa. This feature is named the 'ventral hollow' in
1613 neosauropods, and is also found in derived non-neosauropodan eusauropods (Mocho et al.,
1614 2016), as well as in a possible neosauropodan caudal centrum from the Callovian of the UK
1615 (Holwerda et al. 2019). Pronounced chevron facets are present, as in all sauropods (e.g.
1616 *Cetiosaurus oxoniensis*, *Lapparentosaurus*, '*Bothriospondylus madagascariensis*' Bonaparte,
1617 1986b, *Chebsaurus* and in caudals from unnamed taxa from the Late Jurassic of Portugal
1618 (Upchurch & Martin 2003; Läng and Mahammed 2010; Mannion 2010; Mocho *et al.* 2016))
1619 but not as prominent as in *Vulcanodon* (Raath 1972; Cooper 1984) or *Cetiosaurus*.

1620 The transverse processes are short and blunt, and project slightly posteriorly as well as
1621 laterally. Below them, rounded shallow depressions are visible, which are a vestigial caudal
1622 remnant of the pleurocoels. These depressions are both in anterior and middle caudals
1623 bordered by slight rugosities protruding laterally from the centrum, which could be very
1624 rudimentary lateral and ventrolateral ridges, but this is unsure, and not recorded in non-

1625 neosauropodan eusauropods (Mocho et al. 2016). The neural arch is both dorsoventrally as
1626 well as axially shortened compared to the dorsals and sacrals. Lamination is rudimentarily
1627 present; in particular the *sp_{rl}*, *sp_{ol}*, *st_{pol}* and *tp_{rl}* are visible anteriorly and posteriorly. Small,
1628 blunt pre- and postzygapophyses are also present. The prezygapophyses rest on short, stout
1629 stalks that project anteriorly and dorsally. The postzygapophyses are considerably smaller
1630 than the prezygapophyses, and project only posteriorly as small triangular protrusions.
1631 These are, however, still prominent in anterior caudals; more so than in *Spinophorosaurus*
1632 (Remes *et al.* 2009). Prezygapophyses and postzygapophyses are strongly diminished in the
1633 anterior caudals and continue to do so towards the posterior caudals. Prezygapophyses are
1634 expressed as small oval protrusions, in anterior caudals still projecting from stalks, in middle
1635 and posterior simply projecting from the neural arch. The postzygapophyses are even
1636 further diminished, are only seen as small triangular protrusions from the base of the neural
1637 spine, and disappear completely in posterior caudals. The hypophsene remains visible,
1638 however, as a straight rectangular structure projecting at 90° with the horizontal. The neural
1639 spine is dorsoventrally high, and projects dorsally and posteriorly.

1640 The most distinctive features of this set of vertebrae, however, are the elongated neural
1641 spines. These taper posteriorly, and dorsally, in a gradual gentle curve, which becomes more
1642 straightened towards the dorsal end. Towards the tip of the neural spine, the lateral surface
1643 expands axially. The spine summit displays the same characteristic saddle shape as in the
1644 posterior dorsals, in that in lateral view both anterior and posterior dorsal ends bulge
1645 slightly, with a slight depression on the midline between these bulges. In lateral view, as well
1646 as posterior view, the posterior side of the spine shows long coarse rugose dorsoventrally
1647 running striations, probably for ligament attachments. In particular, one or two grooves of
1648 approximately 1 cm wide are seen aligned in the dorsoventral plane, a few centimeters from
1649 the posterior rim in lateral view. These run from the midline of the spine, a few centimeters
1650 below the spine summit, to the posterior rim of the spine, just above the hyposphene.

1651 Middle caudals (PVL 4170 22-25) are more elongated axially, with the axial length slightly
1652 higher than the height or width of the centrum (Fig. 20). However, the centrum height and
1653 width are still similar to the anterior-mid caudals (see Table 2). The centrum in lateral view
1654 shows a concave surface between two slightly raised ridges, as seen in *Cetiosaurus*. The
1655 ventral side of the centra is concavely and symmetrically curved, as opposed to the more
1656 anterior caudals. The base of the spine is axially wider than in the anterior caudals, and
1657 together with the base of the prezygapophyses, forming the simplified neural arch, rest
1658 more on the anterior half of the centrum, a feature commonly seen in non-neosauropodan
1659 eusauropods as well as in neosauropods (Tschopp et al. 2015). The posterior dorsal side of
1660 the centrum inclines slightly dorsally. The diapophyses are reduced to small rounded stumps
1661 that protrude laterally and slightly dorsally. They are positioned on the ventral and posterior
1662 side of the neural spine bases. Below the transverse processes a very shallow depression can
1663 be seen, unlike in *Tazoudasaurus* where well-defined round fossae are still present on the
1664 middle caudals (To1-288, Allain and Aquesbi 2008). Most prezygapophyses are broken; their
1665 bases are visible as broad stout bulges. The base of the neural spine bulges out laterally, and
1666 is extended axially to the base of the prezygapophyses, creating a broad stout pillar in lateral
1667 view. The spine is inclined posteriorly, and shows a gentle sinusoidal curvature on the
1668 posterior rim. The neural arch and spine shift towards the anterior side of the centrum in
1669 middle and posterior caudals.

1670 Posterior-mid caudals (PVL 4170 (26) – (30) increase in axial centrum length and decrease in
1671 centrum height, giving the centrum a dorsoventrally flattened oval shape. The posterior
1672 articular surfaces of the centra have a small inlet on their dorsal rim, rendering them heart-
1673 shaped. From PVL 4170 (26) the transverse processes diminish into slight bulges underneath
1674 which a small shallow elliptical depression is visible. The postzygapophyses are present as
1675 stunted, slightly square ventral protrusions on the neural spine; the prezygapophyses are
1676 more developed and protrude as short stout struts anteriorly and dorsally from just above

1677 the base of the neural spine. The neural spine inclines heavily posteriorly, and becomes
1678 rectangular; losing the sinusoidal curvature.
1679 The last preserved, posteriormost caudals of the holotype (note that these are not the
1680 posterior-most caudals of the skeleton, PVL 4170 (31) – (34) display an elongated centrum,
1681 further decreased centrum height and a symmetrically curved concave ventral side. Most
1682 neural spines are broken off or damaged; only PVL 4170 (32) has a neural spine that curves
1683 posteriorly and aligns with the axial plane. The diapophyses are further reduced as small
1684 rugose stumps, and the elliptical depression below these is barely discernible. The
1685 prezygapophyses are short stunted protrusions on the anterior end of the spine, nearly
1686 equal in height with the spine. The articular surfaces are round rather than heart-shaped.

1687

1688 *PVL 4170 (19):*

1689 The first caudal that is preserved is an anterior- to mid- caudal. The centrum is
1690 dorsoventrally higher than transversely wide, and is axially short, as in the posterior dorsals
1691 and sacrals (Fig. 21 A, B).
1692 In anterior view, the anterior articular surface of the centrum is oval, and dorsoventrally
1693 higher than transversely wide (Fig. 21D). However, the upper 1/3rd of the anterior articular
1694 surface is transversely broader than the transverse width of the midpoint, and towards the
1695 lower 1/3rd this width decreases further. The ventral side of the articular surface is slightly
1696 V-shaped (Fig. 21E). The dorsal section of the articular surface shows a protruding sharp 'lip-
1697 like' rim. 'Lips' on the dorsal rim of the articular surface of the caudals are an autapomorphy
1698 in *Cetiosaurus* (Upchurch and Martin 2003). However, *Patagosaurus* has less distinctive 'lips'
1699 than *Cetiosaurus*, potentially hinting at a shared feature for Cetiosaurids. The articular
1700 surface is concave, with the deepest point slightly dorsal to the midpoint. In posterior view,
1701 the articular surface of the centrum is heart-shaped, due to two parallel elevations of the
1702 dorsal rim between which a gully for the neural canal exists (Fig. 21C). The articular surface

1703 is less concave than its anterior counterpart, and also less extensive; the outer rim stretches
1704 towards the centre of the articular surface, which is flattened, and only the area slightly
1705 dorsal to the midpoint is slightly concave. In lateral view, the centrum is ventrally mildly
1706 concave, and the rims of both posterior and anterior articular surfaces show thick circular
1707 striations, seen in weight-bearing bones of sauropods, e.g. *Cetiosaurus*, *Giraffatitan*,
1708 *Tornieria* (H. Mallison pers. comm.; see Fig. 21A, B). The centrum is dorsoventrally much
1709 higher than it is axially long, however; this length has decreased with respect to the sacrals
1710 and the posterior dorsals. The neural canal is triangular to rounded in shape, both in anterior
1711 and posterior views.

1712 The diapophyses project laterally and dorsally in anterior view, and in dorsal view, they are
1713 also seen to project slightly posteriorly (Fig. 21D, F). Their shape is triangular with a stunted
1714 distal tip; the dorsal angle made with the centrum is less acute than the ventral one.

1715 Between the diapophyses and the neural arch, a raised ridge of bone is present, similar to
1716 that of anterior caudals of *Cetiosaurus* (Upchurch and Martin 2003). Whether this is a
1717 rudimentary lateral ridge, seen in neosauropods (Tschopp et al. 2015) is unsure.

1718 The neural arch is formed of a square elevated platform upon which the prezygapophysis
1719 and the neural spine rest (Fig. 21A, B, F). The prezygapophysis projects anteriorly and
1720 dorsally from the neural arch, at an angle of $\pm 100^\circ$ with the horizontal. The base of the
1721 prezygapophyses is stout, after which it tapers towards the distal end. The medial articular
1722 surface of the prezygapophysis is round with an internal rounded depression. In posterior
1723 and lateral view, the hyposphene is visible as a squared protrusion at the posterior base of
1724 the neural spine. It makes an angle of 90° with respect to the axial and dorsoventral planes.

1725 The postzygapophyses are only visible as raised oval facades, dorsal to the hyposphene. The
1726 postzygapophyses are formed as triangular lateral protrusions, which project from the base
1727 of the neural spine, between which is an oval depression, likely a rudimentary caudal spof.

1728 The neural spine is diverted to the left lateral side in anterior view; this is probably a
1729 taphonomic alteration (Fig. 21D). It has roughly the same morphology as in the dorsals; a
1730 constricted base and a widened summit, with gently curving lateral sides. The spine is
1731 heavily striated on the surface of the upper 2/3rds of the dorsoventral height. The neural
1732 spine in lateral view gently curves convexly posteriorly and concavely anteriorly. The summit
1733 has a distinct saddle shape in lateral view. The spine summit is elevated in the centre and
1734 has two anterior and posterior rims, which are at a lower elevation than the middle part, as
1735 is seen in the neural spine summits of the dorsal vertebrae. The neural spine is rugosely
1736 striated in the dorsoventral plane in posterior view, and is offset to the right (Figure 21C).
1737 Two spots are clearly visible.

1738

1739 *PVL 4170 (20)*: This anterior caudal resembles PVL 4170 (19). In anterior view, the anterior
1740 articular surface is asymmetrically oval, with a slightly flattened dorsal rim, and a slightly
1741 triangular ventral one (Figure 22D). It is also transversely broadest slightly dorsal to the
1742 midline. The dorsal edge shows lateral elevations, between which a slight rounded
1743 indentation exists on the midline. In posterior view, the articular surface of the centrum is
1744 more heart-shaped than oval (Fig. 22C). It has a thick rim, showing circular striation marks,
1745 which is not as concave as the inner part of the articular surface. This concave surface,
1746 however, is less concave than the anterior articular surface. The posterior dorsal rim of the
1747 centrum does not extend posteriorly, but it faces ventrally in an oblique angle towards the
1748 axial plane, as in PVL 4170 (19), however, the posterior dorsal rim of the centrum extends
1749 further ventrally in PVL 4170 (20). In lateral view, the centrum is axially short and
1750 dorsoventrally elongated as in the posterior dorsals and the sacrals. The ventral side of the
1751 centrum, however, is symmetrically concavely curved, with posterior and anterior rims
1752 bulging out concavely towards the ventral side.

1753 The neural canal is visible as a semi-circular indentation in the neural arch. It is much
1754 broader ventrally than in PVL 4170 (19), see Fig. 22C, D.

1755 In ventral view, the anterior chevron facets are broken off Fig. 22F). The centrum is concave
1756 on both lateral sides, and shows a slight depression beneath the diapophysis. Right at the
1757 base of the diapophysis however, it shows a slight convexity.

1758 The centrum is anteriorly slightly convex, and posteriorly slightly convex, in dorsal view.

1759 The left diapophysis is preserved, and this projects laterally in anterior view, with an angle of
1760 90° with respect to the dorsoventral plane (Fig.22C, D). The diapophysis in dorsal view
1761 projects posteriorly and slightly dorsally. The diapophysis is flat and rectangular in dorsal
1762 view, with the anterior edge being convex and the posterior one concave.

1763 The prezygapophyses are visible above the neural canal as short rounded triangular stubs,
1764 which project dorsally and slightly laterally (Fig. 22A, B, D). In dorsal view, the
1765 prezygapophyses are rounded-triangular protrusions that fork from the base of the neural
1766 arch, and which bend slightly medially, towards each other. The postzygapophyses are
1767 broken off, although the bases are present, showing a dorsoventrally elongated, dorsally
1768 triangular and ventrally oval shape (Fig. 22C).

1769 The neural spine is stout and cone-shaped in anterior view, and displays paired sprl (Fig.
1770 22D). The base of the neural spine is axially constricted; the neural spine broadens axially
1771 towards its dorsal end. The spine shows rugose longitudinal striations on its lateral sides (Fig.
1772 22A, B). Though possibly broken and damaged, it shows a similar curve as in PVL 4170 (19),
1773 in that the posterior side curves convexly and the anterior concavely, allowing the neural
1774 spine to curve gently in a sort of L-shape. The tip of the neural spine is not as saddle-shaped
1775 as in PVL 4170 (19), however, there is still a slight curvature of the neural spine summit
1776 visible on its posterior side (Fig. 22A, B). The spine summit is similar in shape to those of the
1777 posterior dorsals of PVL 4170 (19), in that the sides of the summit are tapering slightly

1778 ventrally from a 'platform' that is the dorsalmost part. The summit is a rhomboid-shaped
1779 knob, which is transversely broader anteriorly than posteriorly (Fig. 22E).

1780

1781 *PVL 4170 (21)*: This anterior - mid caudal has a much more heart-shaped anterior articular
1782 surface than *PVL 4170 (19-20)*, however, the lower half of the articular surface is
1783 reconstructed, therefore it is not certain that the original form persists (Fig. 23D). The
1784 deepest concavity is not at the midpoint but slightly above it, about 1/3rd of the
1785 dorsoventral length of the articular surface down from its dorsal rim. The dorsal rim has a
1786 slight 'lip'; an anteriorly protruding part of the rim that cups the articular surface. The
1787 midpart of this lip is bent ventrally with two lateral bulges, giving it a heart-shape, as in *PVL*
1788 *4170 (19-20)*, see Fig. 23C. In posterior view, the articular surface of the centrum is
1789 rounded-to-triangular in shape. The posterior articular surface is less concave than the
1790 anterior articular surface. In lateral view the centrum is more elongated than in *PVL 4170*
1791 *(19-20)*. In ventral view, the posterior edge of the centrum shows slightly developed chevron
1792 facets (Fig. 23E). The lateral sides of the centrum are strongly concave, the axial centrum
1793 length is increased in this caudal vertebra, compared to *PVL 4170 (19-20)*.

1794 The neural canal is near semi-circular with the horizontal axis on the ventral side. In dorsal
1795 view, the posterior dorsal rim of the centrum retreats towards the neural arch in a U-shaped
1796 recess, posterior to the neural canal opening (Fig. 23C).

1797 The left diapophysis is preserved; the right is broken off (Fig. 23C, D). The left diapophysis is
1798 a stout straight element in anterior view, and is slightly tilted towards the anterior and
1799 dorsal side. The extremity is roughly triangular in outline (Fig. 23B). In dorsal view, the
1800 diapophysis is seen to bend posteriorly as in *PVL 4170 (19-20)*. The prezygapophyses are
1801 flattened in dorsal view, and slightly spatulate. The diapophysis is seen to deflect slightly
1802 posteriorly Fig. 23F).

1803 The prezygapophyses are stout dorsoventrally broad struts (Fig. 23A, B, D). They are
1804 triangular in shape, with dorsoventrally elongated struts, and are directed dorsally. The
1805 neural arch is tilted, probably due to taphonomical alteration. The postzygapophyses are
1806 small rounded triangular bosses posterior to a large bulge on the neural spine (Fig. 23A, B,
1807 C). This bulge is set right ventral to an axial constriction of the neural spine, after which it
1808 constricts slightly again.

1809 The spine summit is similar to PVL 4170 (19) - (20). It constricts transversely at about 1/3rd
1810 of the dorsoventral length towards the summit, after which it slightly transversely widens
1811 towards the summit; the sprl follow a similar pattern (Fig. 23A, B, F). Dorsal to the
1812 postzygapophyses, the spine also bends more posteriorly after this bulge, similar to PVL
1813 4170 (20). The top 1/3rd of the spine shows ligament attachment sites in lateral view. The
1814 neural spine expands slightly towards the summit in a rhomboid shape, with dorsoventrally
1815 deep striations for ligament attachments. The summit is 'saddle shaped', as in the other
1816 anterior caudals PVL 4170 (19-20), see Fig. 23F.

1817

1818 *PVL 4170 (22)*: This anterior middle caudal has a partially broken neural spine and partially
1819 broken right prezygapophysis (Fig. 24A, B). In anterior view, the articular surface of the
1820 centrum is oval, with the dorsal edge similar to PVL 4170 (19) – (21), see Fig. 24D. In
1821 posterior view, the articular surface is oval to round, with the long axis on the dorsoventral
1822 plane (Fig. 24C). The rim that cups the articular surface is thinner than in PVL 4170 (19) –
1823 (21). In lateral view, the ventral side of the centrum is concave, and in ventral view the
1824 anterior rim showing chevron facets (Fig. 24A, E). Because the ventral side of the centrum
1825 slopes down, the posterior end lies lower than the anterior end (Fig. 24A). In ventral view,
1826 the centrum is symmetrically concave transversely. The axial midline is smooth, with no keel
1827 or struts, however, anteriorly two large, rugose semi-circular chevron facets are visible, and
1828 posteriorly two smaller semi-circular ones (Fig. 24E).

1829 The neural canal is triangular to semi-circular. In posterior view, the neural canal is semi-oval
1830 (Fig. 24C, D).

1831 The prezygapophyses are less triangular than in PVL 4170 (21), rather they are blunted
1832 triangular to rounded (Fig. 24A, D). The prezygapophyses are stout struts that protrude
1833 anteriorly and dorsally from the neural arch. They have a rounded tip at their extremities. In
1834 dorsal view, the prezygapophyses show stout beams and stout sprl. Posteriorly, the same U-
1835 shaped recess is visible as in PVL 4170 (19) – (21), ventral to the hyposphene and
1836 postzygapophyses, which together have the same morphology as the previous caudals PVL
1837 4170 (19) – (21) and the posterior dorsals PVL 4170 (16) - (17), see Fig. 24A, C.

1838 The diapophyses bend towards the posterior side (Fig. 24B). The centrum is broadened
1839 transversely around the diapophyses.

1840 The neural spine is inclined posteriorly, directly dorsally from an axial thickening of the
1841 neural spine (Fig. 24A). This part however, is broken off.

1842

1843 *PVL 4170 (23)*: In anterior view, this middle caudal has a round articular surface (Fig. 25C).
1844 The articular surface is concave, with the deepest point in the center. The same thick rim is
1845 present as in PVL 4170 (19) –(22), however it is less rugose in this caudal. In posterior view,
1846 the articular surface is round (Fig. 25D). The rim surrounding the articular surface shows
1847 rounded striations as in the previous caudals. In ventral view, the centrum is of a similar
1848 morphology to in PVL 4170 (22), see Fig. 25E. It has two well-developed chevron facets on
1849 the anterior ventral rim of the anterior articular surface. These chevron facets are connected
1850 medially by a rugose elevated ridge of bone. On the posterior rim two small semi-circular
1851 chevron facets are discernible.

1852 The neural canal is rounded to triangular in shape, with the horizontal plane on the ventral
1853 side (Fig. 25C, D).

1854 The prezygapophyses are directed more dorsally than anteriorly (Figure 25A, C). In dorsal
1855 view, the prezygapophyses are bent towards their medial side, as in PVL 4170 (22), see Fig.
1856 25B. In lateral view, the neural arch is of similar morphology as in PVL 4170 (22), however,
1857 the prezygapophyses are directed more dorsally than ventrally and the diapophyses are
1858 shorter in length (Fig. 25A).

1859 The diapophyses are thickened axially compared to previous caudals, and remain closer to
1860 the central body, where the centrum is thickened transversely (Fig. 25B). Both the
1861 diapophyses and postzygapophyses are reduced in size compared to previous caudals. The
1862 postzygapophyses are present as small triangular bosses (Fig. 25A, D).

1863 The neural spine is of equal transverse width, unlike the previous caudals (Figure 25A). The
1864 neural spine is still elongated as in previous caudals; however, it is straighter and does not
1865 bend dorsally more than $1/3^{\text{rd}}$ of its dorsoventral length onwards. The axial thickening
1866 however, is still visible as in the previous caudals. The spine summit is slightly saddle shaped
1867 as in the previous anterior caudals (Fig. 25B). The neural spine summit does still show the
1868 elevated rhomboid morphology as in the previous anterior caudals and in the posterior
1869 dorsals of PVL 4170.

1870

1871 *PVL 4170 (24)*: In anterior view, this caudal has a more oval than round articular surface,
1872 with the long axis in the dorsoventral plane (Fig. 26D). This is different to the other caudals;
1873 however, it and its surrounding thick rim are also partially damaged on the anterior surface.
1874 In posterior view, the articular surface of the centrum is oval, with the long axis in the
1875 transverse axis, giving the articular surface a more flattened appearance (Fig. 26C). In lateral
1876 view, the centrum shows an elliptical fossa ventral to the diapophyses (Fig. 26A, B). In
1877 ventral view, the centrum is smooth, without a keel or rugosities, with only a faint ventral
1878 groove, and is transversely concave (Fig. 26F). The anterior chevron facets are similar to
1879 those in PVL 4170 (23), however they are less developed (Fig. 26F).

1880 The neural canal is more semi-circular than triangular (Fig. 26C, D). The neural arch
1881 supporting the posterior neural canal opening is triangular in shape, and the neural canal
1882 itself is oval with an elongation on the dorsoventral plane (Fig. 26C).

1883 The right prezygapophysis is slightly damaged; the left is complete (Fig. 26A, B, E). Its
1884 articular surface bends towards the lateral side, unlike in the previous caudals. The
1885 prezygapophyses are more elongated, and the postzygapophyses (Fig. 26C) are more
1886 pronounced in this caudal, unlike PVL 4170 (23), which might mean that this caudal should
1887 be switched with the former caudal, in terms of vertebral order.

1888 The neural spine is straight and rectangular in shape in anterior, posterior and lateral view,
1889 showing a more basal morphology than the previous caudals (Fig. 26A, B, E). The spine
1890 summit has a faint saddle shape, however not as pronounced as in previous anterior
1891 caudals; the summit shows a flatter surface, with only a slight posterior elevation (Fig. A, B,
1892 E).

1893

1894 *PVL 4170 (25)*: In anterior view, the dorsal rim of the anterior articular surface is well
1895 developed, and shows a slight indentation below the neural canal, giving it a small
1896 heartshape as in the more anterior caudals (Fig. 27D). In posterior view, the articular surface
1897 of the centrum is round, and shows pronounced round striations on the rim (Fig. 27E). In
1898 lateral view, the centrum displays a larger anterior articular surface than posteriorly
1899 (Fig. 27A, B), as in other middle caudals of eusauropods (Upchurch 2004). The anterior rim is
1900 also more rugose than the posterior one. In ventral view, the centrum shows two large
1901 chevron facets on the anterior side, and two smaller ones on the posterior side (Fig. 27C).

1902 The neural canal is similar in morphology to that of PVL 4170 (23) – (24), see Fig. 27D, E.

1903

1904 The prezygapophyses are connected medially by a ridge of bone, which is different from the
1905 previous caudal vertebrae, where a deep U-shaped gap between the prezygapophyses exists

1906 (Fig. 27A, B, D, F). The prezygapophyses themselves are damaged. In dorsal view, the
1907 prezygapophyses and spinoprezygapophyseal laminae are clearly visible as stout beams, as
1908 in PVL 4170 (22). The posterior dorsal rim of the centrum shows a sharp U-shaped recess
1909 towards the postzygapophyses, which are positioned in an angle at almost 90° to the
1910 horizontal, Fig. 27A, B, E). The postzygapophyses are visible as lateral triangular protrusions
1911 ventral to the neural spine.

1912 The diapophyses in this caudal are reduced to small protrusions on the more dorsal side of
1913 the centrum, indicating the transition from the middle caudals to a more posterior caudal
1914 morphology (Fig. 27E, F). They are shaped as round bosses on the lateral sides of the
1915 centrum, in dorsal view.

1916 The neural spine is straight, and increases in axial width towards the summit (Fig.27A, B, F).
1917 It is more inclined posteriorly than dorsally, confirming its middle-posterior caudal position.
1918 On the lateral side, rugose dorsoventrally positioned striations are visible. The spine summit
1919 is not straight, but shows a faint saddle shape (Fig. 27A, B).

1920

1921

1922 *PVL 4170 (26)*: In anterior view, the articular surface of the centrum is oval and
1923 dorsoventrally flattened as in PVL 4170 (25), see Fig. 28B. In posterior view, the articular
1924 surface is oval and elongated in the dorsoventral axis (Fig. 28A). It has rough circular
1925 striations as in the other caudals. In lateral view, the centrum is axially elongated, suggesting
1926 a possibly more posterior position than the numbering might indicate (Fig. 28C, D). In dorsal
1927 view, the axial elongation of the centrum is apparent, again indicating this caudal might be
1928 more posterior than middle (Fig. 28F). This could also imply that some caudals that originally
1929 existed between PVL 4170 (25) and (26) are missing here. The outline of the centrum is
1930 symmetrical in dorsal view; the flaring of the extremities and the constriction of the centrum
1931 in the middle (Fig. 28F). In ventral view, the centrum is smooth and concave, and the
1932 chevron facets are not pronounced (Fig. 28E).

1933 The same indentation as in most caudals, ventral to the neural canal, is visible, however, this
1934 part is also partially broken. The anterior neural canal is large and triangular to oval in shape
1935 (Fig. 28B). It occupies most of the anterior surface of the neural arch. The posterior neural
1936 canal is oval and also dorsoventrally elongated (Fig. 28A).

1937 The prezygapophyses are still protruding anteriorly, however as in PVL 4170 (25), the recess
1938 between them is not pronounced (Fig. 28B, C, D). The prezygapophyses are inclined dorsally
1939 and medially, and make an angle of about 45 degrees with respect to the centrum, with the
1940 triangular articular surface on the medial side. The postzygapophyses are reduced to
1941 triangular bosses, ventral to the neural spine (Fig. 28A, C, D).

1942 The diapophyses are reduced to bulges on the lateral side of the centrum, beneath which a
1943 slight depression still remains (Figure 28C, D, F).

1944 The neural spine is partially broken off at the base. Dorsal to the postzygapophyses, the
1945 neural spine displays rough dorsoventrally elongated striations (Fig. 28C, D). The neural
1946 spine is projecting dorsally and posteriorly, being parallel to the centrum. In dorsal view, all
1947 extremities are symmetrical, giving the caudal the outline of a cross in dorsal view (Fig. 28F).

1948

1949 *PVL 4170 (27)*: The centrum of this middle-posterior caudal amphicoelus and symmetrically
1950 shaped. In anterior view, the articular surface is oval and dorsoventrally flattened as in PVL
1951 4170 (25) – (26), see Fig. 29F. Similarly, the dorsal rim of the articular surface is heart-
1952 shaped. In lateral view, the anterior articular surface is slightly longer dorsoventrally than
1953 the posterior one (Fig. 29C, D). The anterior also shows the chevron facets clearly as ventral
1954 rugose protrusions. The centrum on the ventral side is concave, and on the lateral axial
1955 surface the centrum seems to be slightly transversely flattened (Fig. 28B). In posterior view,
1956 the articular surface is oval, with the elongation in the dorsoventral plane (Fig. 28E). It is also
1957 flattened transversely. In ventral view, no chevron facets are visible, however, the centrum
1958 shows a flattening in the axial midline, which is slightly concave (Fig. 29B).

1959 On the lateral sides of the centrum, the diapophyses are visible as rudimentary, rugose
1960 rounded bulges (Fig. 29C, D). The prezygapophyses are damaged, however, this renders the
1961 neural canal clearly visible as a semi-circular/triangular structure (Fig. 29E, F).
1962 The neural spine is broken; however, it is straight and directed posteriorly and dorsally, it
1963 being more flattened towards the centrum than in previous caudals, indicating again a more
1964 posterior caudal morphology (Fig. 29C, D). In dorsal view, the spine is clearly flattened
1965 towards the centrum (Fig. 29A).

1966

1967 *PVL 4170 (30 / 31 / 32)*: The last preserved caudals are middle/posterior caudals. They are
1968 dorsoventrally and transversely smaller than previous caudals, and show an even more
1969 simplified morphology than middle caudals. The anterior articular surface is oval with the
1970 elongation axis on the dorsoventral plane, see Fig. 30A. The posterior articular surface is
1971 smaller in size and more rounded than oval (Fig. 30B). These caudals do not have the
1972 prezygapophyses, postzygapophyses or neural spines preserved (Fig. 30), except for PVL
1973 4170 (32). In lateral view, PVL 4170 (32) has prezygapophyses present as small rounded
1974 protrusions that project anteriorly. The postzygapophyses are no longer visible. PVL 4170
1975 (32) has a short, robust spine. It is inclined posteriorly and ventrally, back towards the
1976 centrum, indicating a posterior caudal position.

1977

1978 **APPENDICULAR SKELETON**

1979

1980 *Ilium PVL 4170 (34)*: According to the Cerro C6ndor Norte quarry map (Fig 1), two ilia were
1981 recovered in the original excavations. However, the whereabouts of the second ilium are
1982 unknown. Even though the MACN in Buenos Aires hosts several ilia, which can be attributed
1983 to *Patagosaurus*, none of these are large enough to match the holotype ilium in the
1984 collections of the Instituto Miguel Lillo in Tucuman.

1985 The right ilium is axially longer than dorsoventrally high (Fig. 31C). The dorsal rim is convex
1986 as in most sauropods, however, the curvature resembles the high dorsal rim of basal
1987 neosauropods/derived eusauropods (e.g. *Apatosaurus*, *Haplocanthosaurus*, *Diplodocus*,
1988 *Cetiosaurus*) more than those of more basal forms, which tend to be less convex, as seen in
1989 *Tazoudasaurus* (Allain et al. 2004; Allain and Acquesbi 2008). The iliac body is not entirely
1990 straight; it is offset from the axial plane to the lateral side at the anterior lobe, whereas the
1991 midsection is axially aligned, and the posterior end is slightly offset to the medial side. The
1992 ilium of the eusauropod *Lapparentosaurus* also follows this curvature. *Cetiosaurus*
1993 *oxoniensis* shows a more or less straight anterior half of the iliac body, though the posterior
1994 half is also slightly offset medially.

1995 The preacetabular process in lateral view is hook-shaped (Fig. 31C); a common feature
1996 among sauropods, and found in the eusauropods *Cetiosaurus*, *Barapasaurus*, *Omeisaurus*
1997 *junghsiensis*, and *Shunosaurus lii* (Tang et al. 2001; Upchurch and Martin 2003;
1998 Bandyopadhyay et al. 2010), although not in *Tazoudasaurus* (Allain and Aquesbi 2008). The
1999 anteriormost part of the process has a thickened rugose dorsal side, which is much thicker
2000 than the dorsal edge of the more posterior part of the ilium, and is slightly constricted
2001 dorsoventrally. However, the posteriormost dorsal rim of the iliac blade shows another
2002 thickened ridge. Ventrally the preacetabular process slopes down gently, not in a sharp
2003 curve, towards the pubic peduncle of the ilium.

2004 The preacetabular process in anterior view (Fig. 31A) is dorsally rugose and pitted for muscle
2005 and cartilage attachment. It is slightly bent towards the lateral side, thus not entirely aligned
2006 in the axial plane. The pubic peduncle in anterior view is a stout element, which flares out
2007 distally and is less wide at its proximal base. The articular surface of the distal end of the
2008 pubic peduncle is not symmetrical, but slightly triangular in shape. The dorsal part of the
2009 preacetabular lobe is similar to *Haplocanthosaurus* in that it has a similar thickening rugosity
2010 of the anteriormost hook-shaped process, but differs from *Haplocanthosaurus* in that it

2011 constricts slightly behind this process, whereas in *Haplocanthosaurus* the dorsal rugosity
2012 behind the anterior process continues smoothly (Hatcher 1903; Upchurch et al. 2004). The
2013 constriction does seem to be natural and not due to damage.

2014 The pubic peduncle is a slender rod-shaped element, which widens towards the distal end,
2015 both anteriorly and posteriorly, in lateral view (Fig. 31C). The anterior distal side of this
2016 peduncle bulges slightly convexly. The posterior side of the pubic peduncle (or the anterior
2017 edge of the acetabulum) is concave. The extremity of the peduncle is convex anteriorly and
2018 flat posteriorly, and the surface is rugose.

2019 The acetabulum is relatively wide as in *Barapasaurus*, *Haplocanthosaurus*, and diplodocids
2020 (Hatcher 1903; Upchurch et al. 2004; Bandyopadhyay 2010), but differs in width from
2021 *Cetiosaurus*, *Tazoudasaurus* and titanosauriforms (Upchurch and Martin 2003; Allain and
2022 Aquesbi 2008; Díez Díaz et al. 2013; Poropat et al. 2015), see Figure 31C. Its dorsal rim is
2023 transversely acute towards the medial side. The rim itself is concave.

2024 The ischial lobe is clearly visible as the ventral half of the heart-shaped posterior end of the
2025 iliac blade (Fig. 31B, C). In lateral view it is a semi-round structure. The surface of the ischial
2026 peduncle bulges out laterally, giving it a slight offset from the iliac blade to the lateral and
2027 ventral side. It is also offset ventrally and posteriorly from the acetabulum (Fig. 31B). The
2028 articular surface for the ischium is oval in shape and rugosely pitted and striated. The ischial
2029 peduncle of the ilium in lateral view is a semi-round, non-prominent lobe.

2030

2031 *Pubis PVL 4170 (35)*: The right pubis is almost complete. In lateral view, the pubic shaft
2032 shows a slightly convex dorsal side and a slightly concave ventral side of the shaft, providing
2033 the shaft with a slight curvature in lateral view (Fig. 32A). The shaft is gracile, taking up
2034 approximately 2/3rds of the entire pubic length. The shaft is more compressed
2035 lateromedially than that of *Cetiosaurus oxoniensis* (Upchurch and Martin, 2003)
2036 *Mamenchisaurus youngi* (Pi et al. 1996), or *Bothriospondylus madagascariensis* (Mannion

2037 2010). Moreover, the length of the pubis is more or less similar to that of the ischium. In this
2038 way it more resembles that of *Haplocanthosaurus* than other sauropods (Hatcher 1903). The
2039 shaft and proximal part are aligned (Fig. 32A); in that there is no torsion of the pubis as in
2040 more derived sauropods (Upchurch and Martin 2003; Upchurch et al. 2004). Interestingly,
2041 the African and Malagasi basal eusauropods *Spinophorosaurus* and '*Bothriospondylus*' have
2042 a much more 'robust' pubis than *Patagosaurus* (Remes et al. 2009; Läng 2010). The pubis of
2043 *Tazoudasaurus* appears to be of the more robust type as well, however this is not entirely
2044 clear, as it belongs to a juvenile (Allain et al. 2008). The elongated and slender shaft is also
2045 seen in *Vulcanodon* (Cooper 1984), however in this taxon the pubic apron is smaller. Also, in
2046 *Vulcanodon*, the pubis is much shorter than the ischium, as in most sauropods (Cooper 1984;
2047 Upchurch et al. 2004).

2048 The distal expansion of the pubis in lateral view flares more dorsally than ventrally, and
2049 tapers acutely to a point (Fig. 32B, D). This distal shape is similar to that of *Barapasaurus*
2050 (Bandhyopadhyay 2010) is more flared than *Haplocanthosaurus* (Hatcher 1903). The distal
2051 end of the pubis in distal view is suboval in shape (Fig. 32B, D).

2052 The pubic apron is slightly convex ventrally in lateral view, with the ischial peduncle tapering
2053 obliquely (Fig. 32A). The pubic peduncle of the pubis projects medially and slightly ventrally.
2054 Even though the mirroring pubis is not present, the pubic basin can be estimated to be wider
2055 than that of *Barapasaurus*, in which the pubic basin is narrow.

2056 The pubic foramen is 'pear-shaped' in lateral view; a dorsoventrally elongated oval that is
2057 constricted slightly dorsal to the middle (Fig. 32A).

2058 The pubic rim of the acetabulum is a steeply sloping surface from the iliac peduncle to the
2059 ischial peduncle in lateral view. This rim tapers ventrally and posteriorly towards the
2060 acetabulum.

2061 The ischial peduncle has a roughly triradiate, transversely narrow and dorsoventrally
2062 elongated articulation surface, with the narrowest point on the ventral side. The length of

2063 the ischial peduncle of the pubis is less than 33% of the length of the entire pubis; further
2064 reinforcing the elongation of this pubis. In *Haplocanthosaurus* the length of the ischial
2065 peduncle is also less than 33%, in *Cetiosaurus* as well (Hatcher 1903; Upchurch and Martin
2066 2003). The iliac peduncle is dorsally elevated from the pubic apron and the shaft, as in
2067 *Cetiosaurus*. The iliac articulation surface is rugose, and curves slightly medially and
2068 posteriorly. There is no 'hook'-shaped ambiens process present as in *Lapparentosaurus*,
2069 *Bothriospondylus* or derived sauropods (Mannion 2010). The pubic symphysis projects
2070 medially and ventrally, as in most sauropods (Upchurch et al. 2004)

2071

2072 *Ischia PVL 4170 (36)*: The fused distal parts of both ischia are preserved, with fusion
2073 occurring at around 2/3 of the shaft length (Fig. 33). The proximal parts are recreated in
2074 plaster; therefore, these will not be described. However, part of the shaft of the right
2075 ischium is preserved (Fig. 33C). In lateral view, the ventral side is concave, and the shaft
2076 expands both dorsally and ventrally towards the limit of the distal end (as far as it is
2077 preserved).

2078 There is a peculiar oval depression on the lateral side of the right ischium, approximately at
2079 the height of the fusion with the left ischium (Fig. 33A). This could be a pathology, however,
2080 seeing as the femur originally was overlaying the ischium in situ during excavations (see Fig.
2081 1), this depression is most probably taphonomic in nature. The extremities of the fused
2082 ischia flare out distally towards the sagittal plane. In posterior view, the distal ends are
2083 directed laterodorsally and medioventrally (Fig. 33B). The fusion forms a wide V-shape with
2084 an angle of 110° with the horizontal; an intermediate stage between the coplanar
2085 *Camarasaurus* ischial fusion state and that of diplodocoids, *Cetiosaurus*, '*Bothriospondylus*
2086 *madagascariensis*' and *Vulcanodon* (Janensch 1961; Cooper 1984; Upchurch and Martin
2087 2003; Mannion 2010; Tschopp et al. 2015). In dorsal view, the shaft of the right ischium
2088 bends and bulges slightly towards the lateral side at 2/3rd of shaft length, but this is probably

2089 due to the taphonomic/pathological damage, as the left ischial shaft is concave laterally in
2090 dorsal view. The surfaces of the ischial extremities are convex and rugose (Fig. 33B).

2091

2092 *Femur PVL 4170 (37)*: The right femur is well-preserved (Figure 34). It is a stout element,
2093 transversely nearly three times wider than axially long. This makes it anteroposteriorly
2094 shorter than transversely, as in most sauropods other than Titanosauriformes. The stoutness
2095 already distinguishes it from *Lapparentosaurus* (MNHN-MAA 67), has a more slender femur,
2096 albeit this taxon is only known from juveniles. The shaft has an elliptical cross-section. There
2097 is no lateral bulge present as in Titanosauriformes (Upchurch et al. 2004). The fourth
2098 trochanter is positioned slightly medial to the dorsoventral midpoint of the shaft; therefore,
2099 it is not entirely medially positioned. This is also seen in *Tazoudasaurus*, *Cetiosaurus*,
2100 *Volkheimeria*, and neosauropods like *Tornieria* (Bonaparte 1986a; Upchurch and Martin
2101 2003; Allain and Aquesbi 2008; Remes 2009).

2102 In anterior view, on the proximal side of the femur, a distinct groove is present, which runs
2103 along the midline from the proximal end to about 3/5th of the femoral length (Fig. 34). This
2104 groove ends in a square-shaped depression, which has a rugose surface on its lateral side.

2105 The lateral side of the femur is slightly convex, and the medial side slightly concave, giving
2106 the femur a curved appearance. It is not entirely certain whether this is due to taphonomy,
2107 or if it is the actual natural curvature. In the latter case, this could have implications for the
2108 stance and gait of *Patagosaurus*, (Wilson and Carrano 1999), as the pubic basin might be
2109 wide compared to other sauropods. This cannot be proven, however, without the other
2110 pubis present, which was never recovered from the Cerro Cóndor Norte locality.

2111 The distal end of the anterior side of the femur shows a slight sub-quadrangular depression
2112 between the lateral and medial condyles, which forms a triangular shape more dorsally, as is
2113 common in basal sauropods. The lateral condyle is slightly offset, but this could be due to
2114 the taphonomic deformation slightly dorsal to it.

2115 In posterior view, the curvature of the femur is still visible (Fig. 34). A deep longitudinal
2116 muscle attachment scar is visible at around the midpart of the shaft. The greater trochanter
2117 is clearly visible in posterior view, as a small rounded protrusion, projecting dorsally from
2118 the proximolateral end of the femur. Directly medial to this, the proximal end of the femur
2119 shows a slight depression, before the medial onset of the femoral head. Distally, in posterior
2120 view, the tibial condyle is slightly damaged. It expands strongly medially, and
2121 medioposteriorly; this is also seen in *Cetiosaurus* (Upchurch and Martin 2003). Between the
2122 tibial and fibular condyles, the distal end of the posterior part of the femur shows a deep
2123 depression, also seen in *Cetiosaurus*, and possibly *Lapparentosaurus* (MNHN-MAA 64). The
2124 fibular condyle is offset to the lateral side, and clearly protrudes posteriorly as a teardrop-
2125 shaped solid structure. The distal lateral condyle flares to the lateral side.

2126 In dorsal view, the proximal end of the femur is strongly rugose and pitted, for cartilage and
2127 muscle attachments. Medial to the greater trochanter, the proximal end is axially
2128 constricted, after which the femoral head widens again. Unfortunately, the femoral head is
2129 not very clearly visible due to the mounting of the specimen, however, it is rounded,
2130 standing out medially at about 20 cm. The medial end of the femoral head is not completely
2131 rounded, but a little pointed, though not as abruptly as in *Cetiosaurus*.

2132

2133 **DISCUSSION**

2134

2135 **COMPARATIVE MORPHOLOGICAL CHARACTERS OF *PATAGOSAURUS FARIASI***

2136

2137 *Cervicals*: the number of cervicals of *Patagosaurus* is possibly closer to that of *Cetiosaurus*
2138 and *Spinophorosaurus*, and possibly slightly lower than that of the Rutland *Cetiosaurus*. It is
2139 most likely also lower than in neosauropods, placing it within known derived non-
2140 neosauropodan eusauropods (Mannion et al. 2019).

2141 One feature that differentiates *Patagosaurus* from other sauropods is the wide angle
2142 between the postzygodiapophyseal laminae and the posterior centrodiapophyseal lamina.
2143 This angle is as wide as 55° to the horizontal (contra McPhee et al. (2016) who measured
2144 41°) and is not found in any basal non-neosauropodan eusauropod (all have an angle
2145 between the podl and pcdl of between 30 and 40°). In basal sauropods and
2146 sauropodomorphs, this angle is much lower, and even in many and even in many
2147 eusauropods the angle is less wide (McPhee et al 2015). Thus, this elevation seems to mark
2148 the transition from sauropodomorphs to sauropods. *Shunosaurus* and *Kotasaurus* (Tang et
2149 al. 2001; Yadagiri 2001), have a high projection of the podl, but not a lower projection of the
2150 pcdl, therefore still not equating the high angle of *Patagosaurus*. Potentially in *Jobaria*
2151 (Wilson 2012), and certainly in neosauropods, such as *Haplocanthosaurus* and *Diplodocus*
2152 (Hatcher 1901; 1903), higher angles are reached with higher projections of the podl
2153 (Upchurch et al 2004). In general, high posterior cervical neural arches are achieved by
2154 mamenchisaurids and titanosauriforms (Mannion et al. 2019).
2155 The cervicals of *Patagosaurus* are different from most other Early and Middle Jurassic non-
2156 neosauropodan eusauropods in that they are rather stout and short but high dorsoventrally.
2157 The aEI is on average lower than most other eusauropods (*Cetiosaurus*, *Spinophorosaurus*,
2158 *Lapparentosaurus*, *Amygdalodon*, see Table 1). However, as the cervical series is not
2159 complete, some cervicals that are missing might have had a higher aEI. The aEI is possibly
2160 similar to that of *Tazoudasaurus*, however, the morphology of the cervicals between these
2161 two taxa is different, and also *Tazoudasaurus* does also not have a complete cervical series
2162 (Allain and Aquesbi 2008).
2163 The anterior condyle of the cervicals is most comparable to those of *Cetiosaurus*, especially
2164 as there is a rugose rim that cups the condyle, and as there is a protrusion on the condyle.
2165 The condylar rim of *Cetiosaurus*, however, is more rugose than in *Patagosaurus* (Upchurch
2166 and Martin, 2002; 2003). The cervicals of *Cetiosaurus* used in this study belong to the

2167 Rutland *Cetiosaurus*, which itself might be a slightly more derived, separate taxon than the
2168 holotype of *Cetiosaurus oxoniensis* (Läng 2008; P. Upchurch & M. Evans pers.comm.).
2169 The other cervical features, such as a pronounced ventral keel and posteriorly extending
2170 ventral end of the posterior cotyle, are more plesiomorphic features shared with
2171 *Lapparentosaurus*, *Amygdalodon*, *Tazoudasaurus*, and *Spinophorosaurus*. *Cetiosaurus*
2172 *oxoniensis* (Upchurch and Martin 2003; 2002) does not seem to have a ventral keel on its
2173 anterior cervicals. *Lapparentosaurus* shows a posterior V-shaped forking of the keel, which is
2174 not seen in *Patagosaurus*. Moreover, some more derived sauropods possess ventral keels,
2175 such as the titanosaurs *Opisthocoelicaudia* and *Diamantinasaurus* (Poropat et al. 2015).
2176 The next outstanding cervical feature is the non-juncture of the intrapostzygapophyseal
2177 laminae. This is a feature that distinguishes *Patagosaurus* from *Cetiosaurus*, and unites it
2178 with *Tazoudasaurus*, therefore a connection between this non-juncture and the elevation of
2179 the neural spine can be ruled out. Whether or not this is a feature shared between
2180 Gondwanan sauropods is uncertain. The single intraprezygapophyseal lamina is a feature
2181 shared with *Cetiosaurus* and *Tazoudasaurus*. The centrodiapophyseal fossa, as seen in
2182 *Patagosaurus*, is not shared with *Tazoudasaurus*, rather, it is shared with *Mamenchisaurus*.
2183 The centroprezygapophyseal fossa is shared with *Tazoudasaurus* (To1-354, contra Wilson
2184 2011).

2185

2186 *Dorsals:*

2187 The slightly rectangular shape of anterior and middle dorsal centra is shared with non-
2188 neosauropodan sauropods, and differs from neosauropods (Mannion et al. 2019). The
2189 slightly more mediolaterally wide posterior dorsal centra are not as wide as in
2190 titanosauriforms (Mannion et al. 2019). The inconspicuous small round depressions on the
2191 posterior side of some of the more well preserved posterior dorsals is a feature thus far not
2192 seen in any other sauropod, and could be an autapomorphy. However, as it is a small

2193 feature, it might have been missed in osteological descriptions of contemporaneous
2194 sauropods to *Patagosaurus*. Most (eu)sauropods do have a rectangular fossa or depression
2195 at the posterior side of the transverse process of (posterior) dorsals, bordered by the pcdl,
2196 and the podl, which is named the pocdf, or postzygocentrodiaepophyseal fossa (Wilson
2197 2011). Whether this has compartmentalized in *Patagosaurus* is not clear, as the pocdf is
2198 rather prominently present, however, in *Patagosaurus* this fossa is more expressed towards
2199 the neural arch than towards the distal end of the diapophysis, as is the case in
2200 *Spinophorosaurus* and *Cetiosaurus* (Rutland *Cetiosaurus* as well as *C. oxoniensis*; Upchurch
2201 and Martin 2002, 2003; Remes et al. 2009). One observation is that these latter taxa have
2202 more dorsally projecting diapophyses, at an angle of about 45° to the horizontal, compared
2203 to a more horizontal and lateral projection in *Patagosaurus*. Whether or not the extra fossa
2204 in *Patagosaurus* is correlated to the projection of the diapophyses (e.g. as extra ligament
2205 attachment site for additional support) remains an unanswered question. In *Barapasaurus*,
2206 no such fossa is seen, whilst the diapophyses of that taxon also project laterally as in
2207 *Patagosaurus*.

2208 The rudimentary aliform process in the neural spines of dorsal vertebrae is seen in high
2209 ontogenetic stages of development in *Europasaurus holgeri* Sander et al., 2006, where it
2210 projects as a triangular protrusion dorsal to the spinal onset of the sprl in anterior view, and
2211 dorsal to the lateral spdl + spol complex in posterior view (Carballido and Sander 2014). In
2212 *Patagosaurus*, this feature is seen dorsal to the lspol+podl complex. This feature could be a
2213 convergence of a laterally projecting triangular process for ligament attachment, found in
2214 basal eusauropods in the configuration as in *Patagosaurus*, and in neosauropods in the
2215 configuration of *Europasaurus*. Note also that this feature develops more in mature
2216 specimens of *Europasaurus* and that the holotype of *Patagosaurus* PVL 4170 is a (sub)adult
2217 and still growing (as evidenced by fused but visible neurocentral sutures), and in
2218 *Patagosaurus* the feature is only seen in posteriormost dorsals as a very rudimentary form.

2219 Posterior dorsal neural arches with rudimentary aliform processes are now known for
2220 *Patagosaurus*, and are also seen in more distinct form in basal macronarians such as
2221 *Europasaurus*, and also in *Bellusaurus sui* Mo, 2913 and *Haplocanthosaurus* (Hatcher 1903;
2222 Upchurch 1998; Mo 2013; Carballido and Sander 2014; Foster and Wedel 2014).
2223
2224 The absence of a spinodiapophyseal lamina on dorsal vertebrae is another characteristic
2225 dorsal feature in *Patagosaurus*. This lamina is seen in dorsals of basal sauropods such as
2226 *Tazoudasaurus* and *Barapasaurus*, then disappears in *Patagosaurus*, *C. oxoniensis* and the
2227 Rutland *Cetiosaurus*, then reappears in neosauropods such as *Apatosaurus*, *Diplodocus*,
2228 *Haplocanthosaurus*, *Camarasaurus*, *Dicraeosaurus* and *Amargasaurus* (Wilson 1999). It's
2229 absence is therefore interpreted as an apomorphic character uniting the cetiosaurids
2230 (Holwerda and Pol 2018). In *Patagosaurus*, the diapophyses are supported solely by the acdl,
2231 pcdl from the ventral and lateral sides, and prdl and podl from the lateral and dorsal sides. In
2232 posterior dorsals, the diapophysis is additionally supported by the lspol+podl complex,
2233 which is sometimes mistaken for the spdl (Allain et al. 2008). This podl+lspol complex is also
2234 seen in the Rutland *Cetiosaurus*. This complex could possibly be the 'replacement' of the
2235 spdl found in basal sauropods and neosauropods. In any case, the absence of the spdl in
2236 *Patagosaurus* and *Cetiosaurus* cannot be connected with either neural spine elongation, as
2237 neosauropods (and especially diplodocids) display similar spine elongation. Neither can the
2238 spdl be correlated with neural spine bifurcation, as the spdl is found in basal non-
2239 neosauropodan sauropods.
2240
2241 Whereas anterior dorsals and middle dorsals of *Patagosaurus* resemble other non-
2242 neosauropodan eusauropods, particularly *Cetiosaurus*, *Tazoudasaurus* and
2243 *Lapparentosaurus*, the posterior dorsals display non-neosauropodan eusauropod features
2244 such as unbifurcated neural spines, simple hyposphene/hypantrum complexes (hyposphene

2245 rhomboid and small, hypanthrum a rugose scar) and unexcavated parapophyses. The neural
2246 spine summit, however, resembles more those of the non-neosauropodan eusauropod
2247 *Lapparentosaurus* and also of the basal neosauropod *Haplocanthosaurus*. The phylogenetic
2248 position of *Lapparentosaurus* is not completely resolved, as the type specimen is a juvenile,
2249 and has been retrieved as either a brachiosaurid by Bonaparte (1986a), as a titanosauriform
2250 (Upchurch 1998), and as non-neosauropodan eusauropod (Läng 2008; Mannion et al. 2013),
2251 therefore it is not possible to draw any conclusions from this.

2252 The lamination of the anterior dorsals is largely similar to that of *Cetiosaurus* and
2253 *Tazoudasaurus*, in that the spol flare out laterally and ventrally, broadening the neural spine.
2254 However, the transition from anterior to middle to posterior dorsal vertebrae brings some
2255 changes in lamination. The centroprezygapophyseal laminae extend dorsoventrally as the
2256 neural arch, pedicels and neural canal extend in dorsoventral height. This is seen in several
2257 other sauropods, although not in the same degree as in *Patagosaurus*. The configuration of
2258 the intrapostzygapophyseal laminae shifts from a non-juncture to a juncture, and then these
2259 laminae disappear. Instead, a single intrapostzygapophyseal lamina appears. This seems to
2260 be unique for a select group of eusauropods (see Allain and Aquesbi 2008; Carballido and
2261 Sander 2014). The posterior dorsals also display a split in the spol, into a medial and a lateral
2262 running lamina. This is described for *Europasaurus* (Carballido 2012), a basal macronarian.
2263 However, this pattern is also observed in the Rutland *Cetiosaurus*. It is therefore possibly a
2264 more widespread configuration than for solely (basal) macronarians, and also existed in non-
2265 neosauropodan eusauropods. Throughout the dorsal vertebral column, the cpol becomes a
2266 rather secondary lamina to the tpols and stpol. In *Europasaurus*, this feature coincides with
2267 a division of the cpol into a lateral and medial one, however, in *Patagosaurus*, only one cpol
2268 exists, which matches the description of the medial cpol of *Europasaurus*.

2269 Posterior dorsals show the dorsoventrally elongated neural spine seen in *Cetiosaurus*, and
2270 also in *Haplocanthosaurus* and flagellicaudatans (Hatcher 1901; 1903). The posterior

2271 inclination of the neural spines of posterior dorsals is also seen in *Klamelisaurus sui* Zhao,
2272 1993, *Mamenchisaurus* and *Omeisaurus* (Xijing 1993; Tang et al. 2001; Ouyang and Ye 2002;
2273 Moore et al. 2017). The deep excavations of the fossae on the posterior dorsal neural spines,
2274 especially on the lateral sides, noted by Bonaparte (1986a), is also seen in *Cetiosaurus*,
2275 mamenchisaurids and neosauropods, suggesting a widespread character (Upchurch and
2276 Martin 2002, 2003; Upchurch et al. 2004).

2277 The presence of a single intraprezygapophyseal and single intrapostzygapophyseal lamina is
2278 a relatively newly named feature for sauropods, as this was named a median strut or single
2279 lamina below the hypantrum/hyposphene (Upchurch et al. 2004; Wilson 1999) before
2280 Carballido and Sander (2014) named it the stprl. These laminae are noted only for
2281 *Camarasaurus* and the titanosauriform *Tehuelchesaurus beneteezii* Rich et al., 1999
2282 (Carballido et al. 2011; Carballido and Sander 2014); however, they appear to also be
2283 present in *Patagosaurus*. The presence of a small stprl accompanied by a large oval cprf on
2284 either lateral side, is shared with many other eusauropods, showing this to be a
2285 plesiomorphic character common in the cetiosaurids, and reappearing in Macronaria and
2286 basal titanosauriforms.

2287

2288 *Sacrum*: One possible source of bias in the comparison of the sacrum of *Patagosaurus* with
2289 other sauropods is that not many sacra of basal sauropods or non-neosauropodan
2290 eusauropods are preserved. Sacral elements are known from *Lapparentosaurus* and
2291 *Tazoudasaurus*, but mostly from juvenile individuals. Neither show the neural spine
2292 elongation of PVL 4170 (18). The sacral count of *Patagosaurus* shows one more sacral
2293 vertebra than the basal eusauropods *Barapasaurus*, *Spinophorosaurus* and *Shunosaurus*,
2294 and resembles that of derived non/neosauropodan eusauropods such as *Ferganasaurus* and
2295 *Jobaria*, as well as basal neosauropods such as *Haplocanthosaurus* (Lang and Mohammed
2296 2010, Tschopp et al. 2015, Carballido et al. 2017b). The fusion of sacral neural spines

2297 number 2-3, however, shows a more basal non-neosauropodan state. The morphology of
2298 the neural spines resembles that of *Haplocanthosaurus* in particular (Hatcher 1903). The
2299 neural spine elongation of PVL 4170 (18) is at an intermediate stage between *Shunosaurus*,
2300 *Camarasaurus*, *Haplocanthosaurus* and diplodocids, but without the sacral ribs extending
2301 beyond the ilium, the sacral neural spines of *Patagosaurus* do not resemble those of
2302 neosauropods.

2303

2304 *Caudals*: The anterior caudal vertebrae of *Patagosaurus* strongly resemble those of
2305 *Spinophorosaurus* and *Cetiosauriscus* (P. Upchurch pers. comm., Charig 1993; Heathcote and
2306 Upchurch 2003, Noè et al. 2010). *Cetiosauriscus* is currently under revision, and its
2307 phylogenetic position is debated. According to [Heathcote and Upchurch \(2003\)](#); [Rauhut](#)
2308 [et al. \(2005\)](#); and [Tschopp et al. \(2015\)](#), it is a non-neosauropodan eusauropod, although in
2309 the last analysis, it is also recovered as a basal diplodocoid as well. Holwerda et al. (2019)
2310 recover it as a diplodocimorph in some analyses. A formal redescription is ongoing
2311 (P.Upchurch pers. comm.). The middle and posterior caudals of *Patagosaurus* are more
2312 resembling those of the holotype of *Cetiosaurus*.

2313 The elongated neural spines of PVL 4170, which are not straight but curve convexly
2314 posteriorly at 2/3rd of the height of the spine, are possibly a diagnostic feature that is not
2315 seen in other sauropods, even though anterior neural spine elongation is seen in
2316 *Cetiosauriscus*, and diplodocids (Charig 1980; Upchurch et al. 2004; Noè et al. 2010).

2317

2318 *Appendicular elements*: The round dorsal rim and hook-shaped anterior lobe of the ilium,
2319 together with the elongated pubic peduncle are diagnostic features for the ilium of
2320 *Patagosaurus*. Whereas *Cetiosaurus oxoniensis* displays a more flattened dorsal rim
2321 (Upchurch and Martin 2002), and *Chebsaurus* possibly as well (Läng and Mahammed 2010),
2322 *Barapasaurus* does share a rounded ilium (Bandyopadyay 2010), but not as highly dorsally

2323 projecting as in *Patagosaurus*. The morphology of PVL 4170 is more similar to
2324 *Haplocanthosaurus*, and with diplodocids (Hatcher 1903, Wedel and Taylor 2013; Tschopp et
2325 al. 2015).

2326 Together with the sacrum, which is similar to (basal) neosauropods (*Haplocanthosaurus*,
2327 *Diplodocus* and *Apatosaurus*), the sacricostal complex of *Patagosaurus* is more of a
2328 neosauropod build, supporting a phylogenetic position as a derived eusauropod (Holwerda
2329 and Pol 2018). Similarly, the 110° angle with the horizontal of the fused distal ischia, shows
2330 an intermediate stage between neosauropods and basal eusauropods. Finally, the
2331 intermediate morphology of the pubis, showing a torsion similar to that seen in
2332 neosauropods like *Tornieria* (Remes 2009), but showing a kidney-shaped pubic foramen as in
2333 *Cetiosaurus oxoniensis*, adds to the pelvic complex of *Patagosaurus* resembling a derived
2334 non-neosauropodan eusauropod, or basal neosauropod.

2335 The femur of the holotype of *Patagosaurus* is a stout element, which does not resemble the
2336 elongated femora of neosauropods, but rather that of *Cetiosaurus*, *Tazoudasaurus* and
2337 *Barapasaurus*. The slightly convex femur towards the lateral side shows a possible gait
2338 modification that is diagnostic for *Patagosaurus* and that has not been found in the other
2339 aforementioned Jurassic sauropods. While the femoral morphology of *Cetiosaurus* is similar
2340 to that of *Patagosaurus*, the femur of the former is straighter. A wide-gauge, which might be
2341 inferred from the femoral morphology of *Patagosaurus*, is more common in titanosaurs
2342 (Henderson 2006) and Titanosauriformes (Wilson and Carrano 1999). There are, however,
2343 earlier ichnological indications of a possible wide-gauge: a footprint site from the early
2344 Middle Jurassic from the UK shows the presence of both a narrow-, as well as wide-gait
2345 sauropod track (Day et al. 2004), and also footprints from the Late Jurassic of Morocco show
2346 a wide-gauge (Marty et al. 2010). The trackmaker from these sites unfortunately cannot be
2347 identified.

2348

2349 **PNEUMATICITY IN BASAL EUSAUROPODS**

2350 The cervicals of *Patagosaurus* show anteriorly deep pleurocoels with a gradual shallowing
2351 towards the posterior end, and with clearly defined anterior, dorsal and ventral rims, but no
2352 clearly defined posterior rim. The anteriorly deep part of the pleurocoel is visible as a
2353 circular concavity. Damage in some cervicals show that only a thin plate of bone divided
2354 mirroring pleurocoels (e.g PVL 4170 6). Bonaparte (1979, 1986a, 1999) already noted the
2355 presence of a pleurocoel. Note that the pleurocoel is present, but is shallower in the dorsals,
2356 as is also noted by Bonaparte (1986a). The pleurocoel is defined for sauropods either as a
2357 pneumatopore or as a pneumatic structure (Wilson 2002; Wedel 2003, 2005, 2013;
2358 Upchurch et al. 2004), however, Carballido and Sander (2014) defined the structure using
2359 *Patagosaurus* as an example, as a lateral excavation on the centrum, with clear anterior,
2360 dorsal and ventral margins, and a posterior margin that could be either well-defined or more
2361 gradually merging with the lateral body of the centrum (Carballido & Sander 2014). As
2362 already remarked on by Bonaparte (1986a, 1999) and Carballido and Sander (2014),
2363 *Patagosaurus* does not show the internal pneumatic structure that neosauropods display.
2364 This type of pleurocoel outline is seen in other Jurassic non-neosauropodan eusauropods,
2365 such as the Rutland *Cetiosaurus*, *Barapasaurus*, *Tazoudasaurus*, *Spinophorosaurus*,
2366 *Lapparentosaurus* (Bonaparte 1986c; Upchurch and Martin 2003; Allain and Aquesbi 2008;
2367 Remes et al 2009). The lack of a clear posterior margin of the pleurocoel is also common,
2368 except in the Rutland *Cetiosaurus* (Upchurch and Martin 2003). The anterior depth of the
2369 pleurocoel in *Patagosaurus*, however, is probably unique to this taxon. In *Spinophorosaurus*
2370 (Remes et al., 2009), as well as *Lapparentosaurus* (MNHN-MAA 13), the pleurocoel is shallow
2371 at its anterior margin, and even shows a shallowing at its anterior ventral margin. In
2372 *Barapasaurus* (Bandyopadhyay 2010), the entire pleurocoel is shallow. In *Shunosaurus*, the
2373 pleurocoel is anteriorly deep, but the concavity is more elongated and elliptic in shape, while
2374 in *Patagosaurus* this is circular and restricted to the anterior-most part of the pleurocoel. In

2375 *Klamelisaurus* (Zhao 1993) the pleurocoel is entirely shallow, and in the mamenchisaurids
2376 *Mamenchisaurus youngi* (Ouyang and Ye 2002), *Zigongosaurus* (Hou et al. 1976),
2377 *Tonganosaurus* Liu et al., 2010, and *Qijianglong* Xing et al., 2015 the pleurocoel is
2378 compartmentalized by one or more accessory laminae into small deep pockets over the
2379 length of the centrum. Only in the Rutland *Cetiosaurus* (Upchurch and Martin 2003), the
2380 pleurocoel is anteriorly deep as well. In some cervicals, an oblique accessory lamina, which
2381 divides the pleurocoel into a deeper anterior section and a shallower posterior section, is
2382 faintly present. This feature is also seen in the Rutland *Cetiosaurus*, in mamenchisaurids, and
2383 in neosauropods like *Apatosaurus* (Upchurch and Martin 2003; Xing et al. 2015; Taylor and
2384 Wedel 2017). The poor development of this oblique accessory lamina, however, and the
2385 irregularity of its presence are probably not enough to make it a character. Note that in the
2386 roughly contemporaneous Rutland *Cetiosaurus* (Upchurch and Martin 2003) this lamina is
2387 more consistently present.

2388

2389 *Dorsals*: The pneumatic structure on dorsal neural arches, appearing first in the middle
2390 dorsal neural arches and expanding in the posterior dorsal neural arches, is the key feature
2391 that Bonaparte mentioned for *Patagosaurus*, also using it to distinguish it from
2392 *Volkheimeria*, the other sauropod described from Cerro Cóndor (Bonaparte 1979, 1986b,
2393 1999). This feature is still the main autapomorphy for *Patagosaurus*, and marks new
2394 pneumatic features for basal eusauropods that were previously unknown. Pneumaticity in
2395 sauropods is well-known for neosauropods (Wedel 2003; Wedel et al. 2005; Schwarz and
2396 Fritsch 2006; Schwarz et al. 2007; Fanti et al. 2013; Taylor and Wedel 2013). It is not well
2397 understood for basal non-neosauropod eusauropods, and *Patagosaurus* is the first taxon to
2398 give conclusive evidence for this structure. However, other basal sauropods may have this
2399 structure (e.g. *Cetiosaurus*, *Barapasaurus*, *Tazoudasaurus*, see Figure 35B). The
2400 centrodiaiphyseal fenestrae, which extend ventrally in a pneumatic chamber separated

2401 from the neural canal, is a feature possibly shared with *Cetiosaurus* and *Barapasaurus*
2402 (Bandyopadhyay et al. (2010); this feature often pairing these taxa with *Patagosaurus* as
2403 sister-taxa in phylogenetic analyses, e.g. Remes et al. (2009a)); however, it is not clearly
2404 shown whether these latter taxa possess the same ventral pneumatic chamber as in
2405 *Patagosaurus*. This feature has however been shown to be present in the basal neosauropod
2406 *Haplocanthosaurus* (Foster and Wedel 2014).
2407 A preliminary phylogenetic analysis using the holotype PVL 4170 by Holwerda & Pol (2018)
2408 and implementing the dorsal neural spine pneumaticity shows a close affinity of
2409 *Patagosaurus* with the Rutland *Cetiosaurus*, and *Patagosaurus* being nested within
2410 specimens referred to *Cetiosaurus*. It is furthermore more derived than *Barapasaurus*, and
2411 more basal to mamenchisaurids, and neosauropods (see Figure 35A).

2412

2413

2414 **CONCLUSIONS**

2415 To summarize and conclude, the holotype of the Middle Jurassic sauropod *Patagosaurus*
2416 *fariasi* shows a set of morphological features that are typically broadly non-neosauropodan
2417 eusauropod and are shared with other non-neosauropodan eusauropods. This includes
2418 features in the cervical vertebrae, such as unbifurcated neural spines, presence of a ventral
2419 keel, unexcavated parapophyses and the absence of neosauropodan laminae. In the dorsal
2420 vertebrae, these features include amphicoelus middle and posterior dorsal centra, the
2421 absence of the spdl and unbifurcated neural spines. In caudal vertebrae, this includes simple
2422 lamination, and small transverse processes. In the pelvis and femur, these include V-shaped
2423 fusion of distal ischia, and a stout femur. However, some elements seem to be slightly more
2424 derived, and are found in derived eusauropods and/or (non)-neosauropods. These include
2425 deep excavations in cervical and dorsal vertebrae, elongated neural spines in dorsal, sacral
2426 and anterior caudal vertebrae, and convex femur. The dorsal vertebral pneumaticity

2427 patterns found in *Patagosaurus* may unite it with other derived non-neosauropodan
2428 eusauropods such as *Cetiosaurus*. Finally, the main diagnostic characters for *Patagosaurus*
2429 *fariasi* are low (a)EI for cervical vertebrae, high neural spines in dorsal, sacral and anterior
2430 caudal vertebrae, cervical and dorsal vertebral pneumaticity, and convex femur.

2431

2432 ACKNOWLEDGEMENTS

2433 The authors would like to dedicate this manuscript to the memory of Jaime Powell, curator
2434 of vertebrate palaeontology at the Instituto Miguel Lillo (PVL), Tucuman, Argentina, and also
2435 to the memory of José Bonaparte, director of vertebrate palaeontology both at PVL and the
2436 Museo Argentino de Ciencias Naturales Bernardino Rivadavia (MACN).

2437 Furthermore, the authors are indebted to editor Emmanuel Côté, and to the critical and
2438 thorough reviews of Phil Mannion and Verónica Díez Díaz, whose comments improved this
2439 paper. This research was funded by DFG grant RA 1012/13-1 to OR.

2440

2441

2442 **REFERENCES**

2443

- 2444 ALIFANOV V.R. & AVERIANOV A.O. 2003. — Ferganasaurus verzilini, gen. et sp. nov., a new
2445 neosauropod (Dinosauria, Saurischia, Sauropoda) from the Middle Jurassic of
2446 Fergana Valley, Kirghizia. *Journal of Vertebrate Paleontology* 23 (2): 358–372
- 2447 ALLAIN R. & AQUESBI N. 2008. — Anatomy and phylogenetic relationships of *Tazoudasaurus*
2448 *naimi* (Dinosauria, Sauropoda) from the late Early Jurassic of Morocco. *Geodiversitas*
2449 30 (2): 345–424
- 2450 ALLAIN R., AQUESBI N., DEJAX J., MEYER C., MONBARON M., MONTENAT C., RICHIR P., ROCHDY M.,
2451 RUSSELL D. & TAQUET P. 2004. — A basal sauropod dinosaur from the Early Jurassic of
2452 Morocco. *Comptes Rendus Palevol* 3 (3): 199–208
- 2453 BANDYOPADHYAY S., GILLETTE D.D., RAY S. & SENGUPTA D.P. 2010. — Osteology of *Barapasaurus*
2454 *tagorei* (Dinosauria: Sauropoda) from the Early Jurassic of India. *Palaeontology* 53
2455 (3): 533–569
- 2456 BARRETT P.M. & UPCHURCH P. 2007. — The evolution of herbivory in sauropodomorph
2457 dinosaurs. *Special Papers in Palaeontology* 77: 91–112
- 2458 BARRETT P.M. 2006. — A sauropod dinosaur tooth from the Middle Jurassic of Skye, Scotland.
2459 *Earth and Environmental Science Transactions of the Royal Society of Edinburgh* 97
2460 (01): 25–29. <https://doi.org/10.1017/S0263593300001383>
- 2461 BARRETT P.M. & UPCHURCH P. 2005. — Sauropodomorph diversity through time, *The*
2462 *Sauropods: evolution and paleobiology*. p. 125–156.
- 2463 BECERRA M.G., GOMEZ K.L. & POL D. 2017. — A sauropodomorph tooth increases the diversity
2464 of dental morphotypes in the Cañadón Asfalto Formation (Early–Middle Jurassic) of
2465 Patagonia. *Comptes Rendus Palevol* 16 (8): 832–840
- 2466 BONAPARTE J.F. 1999. — Evolución de las vértebras presacras en Sauropodomorpha.
2467 *Ameghiniana* 36 (2): 115–187
- 2468 BONAPARTE J.F. 1996. — *Dinosaurios de America del Sur*. Museo Argentino de Ciencias
2469 Naturales. 174 pp.
- 2470 BONAPARTE J.F. 1986. — The dinosaurs (Carnosaurs, Allosaurids, Sauropods, Cetiosaurids) of
2471 the Middle Jurassic of Cerro Cóndor (Chubut, Argentina) ., Masson, Paris. *Annales de*
2472 *Paléontologie (Vert.-Invert.)* 72 (3): 325–386.
- 2473 BONAPARTE J.F. 1986. — Les dinosaures (Carnosaures, Allosauridés, Sauropodes,
2474 Cétoosauridés) du Jurassique Moyen de Cerro Cóndor (Chubut, Argentina)., Masson,
2475 Paris. *Annales de Paléontologie (Vert.-Invert.)* 72 (3): 247–289
- 2476 BONAPARTE J.F. 1986. — The early radiation and phylogenetic relationships of the Jurassic
2477 sauropod dinosaurs, based on vertebral anatomy, in PADIAN K. (ed.), *The Beginning of*
2478 *the Age of Dinosaurs*. Cambridge, Cambridge University Press. p. 247–258.
- 2479 BONAPARTE J.F. 1979. — Dinosaurs: A Jurassic Assemblage from Patagonia. *Science* 205
2480 (4413): 1377–1379. <https://doi.org/10.1126/science.205.4413.1377>
- 2481 BRUSATTE S.L., CHALLANDS T.J., ROSS D.A. & WILKINSON M. 2015. — Sauropod dinosaur trackways
2482 in a Middle Jurassic lagoon on the Isle of Skye, Scotland. *Scottish Journal of Geology*
2483 5:1-9
- 2484 BUFFETAUT E., SUTEETHORN V., LE LOEUFF J., CUNY G., TONG H. & KHANSUBHA S. 2002. — The first
2485 giant dinosaurs: a large sauropod from the Late Triassic of Thailand. *Comptes Rendus*
2486 *Palevol* 1 (2): 103–109
- 2487 CABALERI N., VOLKHEIMER W., SILVA NIETO D., ARMELLA C., CAGNONI M., HAUSER N., MATTEINI M. &
2488 PIMENTEL M.M. 2010. — U-Pb ages in zircons from las Chacritas and Puesto Almada
2489 members of the Jurassic Cañadón Asfalto Formation, Chubut province, Argentina *In*:
2490 p. 190–193.

- 2491 CABALERI N., ARMELLA C., 2005. — Influence of a biohermal belt on the lacustrine
2492 sedimentation of the Cañadón Asfalto Formation (Upper Jurassic, Chubut province,
2493 Southern Argentina). *Geologica Acta* 3:205-214.
- 2494 CABALERI N., ARMELLA C., NIETO, D.G.S., 2005. — Saline paleolake of the Cañadón Asfalto
2495 Formation (Middle-Upper Jurassic), Cerro Cóndor, Chubut province (Patagonia),
2496 Argentina. *Facies* 51: 350–364.
- 2497 CABRERA, A., 1947. — Un saurópodo nuevo del Jurásico de Patagonia. *Notas del Museo de La*
2498 *Plata, Paleontología* 95:1–17.
- 2499 CARBALLIDO J.L., POL D., CERDA I. & SALGADO L. 2011. — The osteology of Chubutisaurus insignis
2500 del Corro, 1975 (Dinosauria: Neosauropoda) from the ‘middle’ Cretaceous of central
2501 Patagonia, Argentina. *Journal of Vertebrate Paleontology* 31 (1): 93–110
- 2502 CARBALLIDO J.L., HOLWERDA F.M., POL D. & RAUHUT O.W. 2017. — An Early Jurassic sauropod
2503 tooth from Patagonia (Cañadón Asfalto Formation): implications for sauropod
2504 diversity. *Publicación Electrónica de la Asociación Paleontológica Argentina* 17 (2):
2505 50–57
- 2506 CARBALLIDO J.L., POL D., OTERO A., CERDA I.A., SALGADO L., GARRIDO A.C., RAMEZANI J., CÚNEO N.R. &
2507 KRAUSE J.M. 2017. — A new giant titanosaur sheds light on body mass evolution
2508 among sauropod dinosaurs. *Proceedings of the Royal Society B* 284 (1860):
2509 20171219. <https://doi.org/10.1098/rspb.2017.1219>
- 2510 CARBALLIDO J.L. & SANDER P.M. 2014. — Postcranial axial skeleton of *Europasaurus holgeri*
2511 (Dinosauria, Sauropoda) from the Upper Jurassic of Germany: implications for
2512 sauropod ontogeny and phylogenetic relationships of basal Macronaria. *Journal of*
2513 *Systematic Palaeontology* 12 (3): 335–387.
2514 <https://doi.org/10.1080/14772019.2013.764935>
- 2515 CARBALLIDO J.L., SALGADO L., POL D., CANUDO J.I. & GARRIDO A. 2012. — A new basal
2516 rebbachisaurid (Sauropoda, Diplodocoidea) from the Early Cretaceous of the
2517 Neuquén Basin; evolution and biogeography of the group. *Historical Biology* 24 (6):
2518 631–654. <https://doi.org/10.1080/08912963.2012.672416>
- 2519 CASAMIQUELA R.M. 1963. — CONSIDERACIONES ACERCA DE AMYGDALODON CABRERA
2520 (SAUHOPODA, CETIOSAURIDAE) DEL JURASICO MEDIO DE LA PATAGONIA.
2521 *Ameghiniana* 3 (3): 79–95
- 2522 CHARIG A.J. 1993. — Case 1876. *Cetiosauriscus* von Huene, 1927 (Reptilia,
2523 Sauropodomorpha): proposed designation of *C. stewarti* Charig, 1980 as the type
2524 species. *Bulletin of Zoological Nomenclature* 50: 282–283
- 2525 CHARIG A.J. 1980. — A diplodocid sauropod from the Lower Cretaceous of England, in JACOBS
2526 L.L. (ed.), *Aspects of Vertebrate History. Essays in Honor of Edwin Harris Colbert*.
2527 Flagstaff, Museum of Northern Arizona Press. p. 231–244.
- 2528 CHATTERJEE S. & ZHENG Z. 2002. — Cranial anatomy of Shunosaurus, a basal sauropod dinosaur
2529 from the Middle Jurassic of China. *Zoological Journal of the Linnean Society* 136 (1):
2530 145–169
- 2531 CHURE D., BRITT B., WHITLOCK J. & WILSON J. 2010. — First complete sauropod dinosaur skull
2532 from the Cretaceous of the Americas and the evolution of sauropod dentition.
2533 *Naturwissenschaften* 97 (4): 379–391. <https://doi.org/10.1007/s00114-010-0650-6>
- 2534 COOPER M.R. 1984. — A reassessment of *Vulcanodon karibaensis* Raath (Dinosauria:
2535 Saurischia) and the origin of the Sauropoda. *Palaeontologia africana* 25: 203–231
- 2536 COPE E.D. 1877. — On a gigantic saurian from the Dakota epoch of Colorado. *Paleontological*
2537 *Bulletin* 25: 5–10
- 2538 CÚNEO R., RAMEZANI J., SCASSO R., POL D., ESCAPA I., ZAVATTIERI A.M. & BOWRING S.A. 2013. —
2539 High-precision U–Pb geochronology and a new chronostratigraphy for the Cañadón
2540 Asfalto Basin, Chubut, central Patagonia: Implications for terrestrial faunal and floral

- 2541 evolution in Jurassic. *Gondwana Research* 24 (3): 1267–1275.
 2542 <https://doi.org/10.1016/j.gr.2013.01.010>
- 2543 DAY J.J., NORMAN D.B., GALE A.S., UPCHURCH P. & POWELL H.P. 2004. — A Middle Jurassic
 2544 dinosaur trackway site from Oxfordshire, UK. *Palaeontology* 47 (2): 319–348
- 2545 DÍEZ DÍAZ V., TORTOSA T. & LE LOEUFF J. 2013. — Sauropod diversity in the Late Cretaceous of
 2546 southwestern Europe: The lessons of odontology. *Annales de Paléontologie* 99 (2):
 2547 119–129. <https://doi.org/10.1016/j.annpal.2012.12.002>
- 2548 DONG Z. & TANG Z. 1984. — Note on a new mid-Jurassic sauropod (*Datousaurus bashanensis*
 2549 gen. et sp. nov.) from Sichuan Basin, China. *Vertebrata Palasiatica* 22 (1): 69–75
- 2550 DONG Z., ZHOU S.W. & ZHANG Y. 1983. — Dinosaurs from the Jurassic of Sichuan.
 2551 *Palaeontologica Sinica, New Series C* 162 (23): 1–136
- 2552 FIGARI E.G., SCASSO R.A., CÚNEO R.N. & ESCAPA I. 2015. — Estratigrafía y evolución geológica de
 2553 la Cuenca de Cañadón Asfalto, provincia del Chubut, Argentina. *Latin American*
 2554 *journal of sedimentology and basin analysis* 22 (2): 135–169
- 2555 FOSTER J. 2014. — Haplocanthosaurus (Saurischia: Sauropoda) from the lower Morrison
 2556 Formation (Upper Jurassic) near Snowmass, Colorado. *Volumina Jurassica* (Vol. 12,
 2557 2): 197–210. <https://doi.org/10.5604/17313708.1130144>
- 2558 FRENGUELLI J. 1949. — Los estratos con “Estheria” en el Chubut (Patagonia). *Revista de la*
 2559 *Asociación Geológica Argentina* 4 (1): 1–4
- 2560 GALTON P.M. 2005. — Bones of large dinosaurs (Prosauropoda and Stegosauria) from the
 2561 Thaetic Bone Bed (Upper Triassic of Aust Cliff, southwest England. *Revue de*
 2562 *Paléobiologie* 24 (1): 51
- 2563 HARRIS J.D. 2006. — The axial skeleton of the dinosaur *Suuwassea emilieae* (Sauropoda:
 2564 Flagellicaudata) from the Upper Jurassic Morrison Formation of Montana, USA.
 2565 *Palaeontology* 49 (5): 1091–1121
- 2566 HATCHER J.B. 1903. — Osteology of *Haplocanthosaurus*, with description of a new species and
 2567 remarks on the probable habits of the Sauropoda and the age and origin of the
 2568 *Atlantosaurus* beds: Additional remarks on *Diplodocus*. *Memoirs of the Carnegie*
 2569 *Museum* 2: 1–72
- 2570 HATCHER J.B. 1901. — *Diplodocus* (Marsh): its osteology, taxonomy, and probable habits, with
 2571 a restoration of the skeleton. *Memoirs of the Carnegie Museum* 1: 1–63
- 2572 HAUSER N., CABALERI N.G., GALLEGO O.F., MONFERRAN M.D., NIETO D.S., ARMELLA C., MATTEINI M.,
 2573 GONZÁLEZ P.A., PIMENTEL M.M., VOLKHEIMER W. & OTHERS 2017. — U-Pb and Lu-Hf
 2574 zircon geochronology of the Cañadón Asfalto Basin, Chubut, Argentina: Implications
 2575 for the magmatic evolution in central Patagonia. *Journal of South American Earth*
 2576 *Sciences* 78: 190–212
- 2577 HE X., LI K. & CAI K. 1988. — *The Middle Jurassic dinosaur fauna from Dashanpu, Zigong,*
 2578 *Sichuan. Vol. IV. Sauropod Dinosaurs (2)* Omeisaurus tianfuensis. Chengdu, China,
 2579 Sichuan Publishing House of Science and Technology. 143 p.
- 2580 HE X., LI K., CAI K. & GAO Y. 1984. — *Omeisaurus tianfuensis*—a new species of *Omeisaurus*
 2581 from Dashanpu, Zigong, Sichuan. *Journal of Chengdu College Geology, Supplement* 2:
 2582 13–32
- 2583 HEATHCOTE J. & UPCHURCH P. 2003. — The relationships of *Cetiosauriscus stewarti* (Dinosauria;
 2584 Sauropoda): implications for sauropod phylogeny. *Journal of Vertebrate*
 2585 *Paleontology* 23 (Suppl. 3): 60A
- 2586 HENDERSON D.M. 2006. — Burly gaits: centers of mass, stability, and the trackways of
 2587 sauropod dinosaurs. *Journal of Vertebrate Paleontology* 26 (4): 907–921
- 2588 HOLWERDA F.M., EVANS M. & LISTON J.J. 2019. — Additional sauropod dinosaur material from
 2589 the Callovian Oxford Clay Formation, Peterborough, UK: evidence for higher
 2590 sauropod diversity. *PeerJ* 7: e6404

- 2591 HOLWERDA F.M. & POL D. 2018. — Phylogenetic analysis of Gondwanan basal eusauropods
2592 from the Early-Middle Jurassic of Patagonia, Argentina. *Spanish Journal of*
2593 *Palaeontology* 33(2):298-298
- 2594 HOLWERDA F.M., POL D. & RAUHUT O.W.M. 2015. — Using dental enamel wrinkling to define
2595 sauropod tooth morphotypes from the Cañadón Asfalto Formation, Patagonia,
2596 Argentina. *PLOS ONE* 10 (2): e0118100.
2597 <https://doi.org/10.1371/journal.pone.0118100>
- 2598 HOU L., ZHOU S. & CAO Y. 1976. — New discovery of sauropod dinosaurs from Sichuan.
2599 *Vertebrata Palasiatica* 14 (3): 160–165
- 2600 VON HUENE. 1927. — Sichtung der Grundlagen der jetzigen Kenntnis der Sauropoden. *Eclogae*
2601 *Geologica Helvetiae* 20:444–470.
- 2602 IRMIS R.B. 2010. — Evaluating hypotheses for the early diversification of dinosaurs. *Earth and*
2603 *Environmental Science Transactions of the Royal Society of Edinburgh* 101 (3–4):
2604 397–426
- 2605 JAIN S.L., KUTTY T.S., ROY-CHOWDHURY T. & CHATTERJEE S. 1975. — The sauropod dinosaur from
2606 the Lower Jurassic Kota formation of India. *Proceedings of the Royal Society of*
2607 *London B: Biological Sciences* 188 (1091): 221–228
- 2608 JANENSCH W. 1961. — Die Gliedmassen und Gliedmassengürtel der Sauropoden der
2609 Tendaguru-Schichten. *Palaeontographica-Supplementbände* 4: 177–235
- 2610 LÄNG É. 2008. — Les cétiosaures (Dinosauria, Sauropoda) et les sauropodes du Jurassique
2611 moyen: révision systématique, nouvelles découvertes et implications
2612 phylogénétiques Ph. D. dissertation. Paris, France, *Centre de recherche sur la*
2613 *paléobiodiversité et les paléoenvironnements*. 639 p.
- 2614 LÄNG E. & MAHAMMED F. 2010. — New anatomical data and phylogenetic relationships of
2615 *Chebsaurus algeriensis* (Dinosauria, Sauropoda) from the Middle Jurassic of Algeria.
2616 *Historical Biology* 22 (1–3): 142–164. <https://doi.org/10.1080/08912960903515570>
- 2617 LAOJUMPON C., SUTEETHORN V., CHANTHASIT P., LAUPRASERT K. & SUTEETHORN S. 2017. — New
2618 evidence of sauropod dinosaurs from the Early Jurassic period of Thailand. *Acta*
2619 *Geologica Sinica-English Edition* 91 (4): 1169–1178
- 2620 LISTON J.J. 2004. — A re-examination of a Middle Jurassic sauropod limb bone from the
2621 Bathonian of the Isle of Skye. *Scottish Journal of Geology* 40 (2): 119–122
- 2622 LIU L.K.Y.C.-Y. & ZHENG-XIN J.W. 2010. — A NEW SAUROPOD FROM THE LOWER JURASSIC OF
2623 HUILI, SICHUAN, CHINA. *Vertebrata Palasiatica* 3:185-202.
- 2624 LONGMAN H.A. 1927. — *The giant dinosaur: Rhoetosaurus brownei*. Queensland Museum 8
2625 (3): 183-194
- 2626 MAHAMMED F., LÄNG É., MAMI L., MEKAHLI L., BENHAMOU M., BOUTERFA B., KACEMI A., CHÉRIEF S.-A.,
2627 CHAOUATI H. & TAQUET P. 2005. — The 'Giant of Ksour', a Middle Jurassic sauropod
2628 dinosaur from Algeria. *Comptes Rendus Palevol* 4 (8): 707–714
- 2629 MANNION P.D. 2010. — A revision of the sauropod dinosaur genus '*Bothriospondylus*' with a
2630 redescription of the type material of the Middle Jurassic form '*B. madagascariensis*'.
2631 *Palaeontology* 53 (2): 277–296. <https://doi.org/10.1111/j.1475-4983.2009.00919.x>
- 2632 MANNION P.D. & UPCHURCH P. 2010. — Completeness metrics and the quality of the
2633 sauropodomorph fossil record through geological and historical time. *Paleobiology*
2634 36 (2): 283–302
- 2635 MANNION P.D., UPCHURCH P., BARNES R.N. & MATEUS O. 2013. — Osteology of the Late Jurassic
2636 Portuguese sauropod dinosaur *Lusotitan atalaiensis* (Macronaria) and the
2637 evolutionary history of basal titanosauriforms. *Zoological Journal of the Linnean*
2638 *Society* 168 (1): 98–206. <https://doi.org/10.1111/zoj.12029>
- 2639 MANNION P.D., UPCHURCH P., SCHWARZ D. & WINGS O. 2019. — Taxonomic affinities of the
2640 putative titanosaurs from the Late Jurassic Tendaguru Formation of Tanzania:
2641 phylogenetic and biogeographic implications for eusauropod dinosaur evolution.

- 2642 *Zoological Journal of the Linnean Society* 185 (3): 784–909.
2643 <https://doi.org/10.1093/zoolinnea/zly068>
- 2644 MARSH O.C. 1890. — Description of new dinosaurian reptiles. *American Journal of Science*
2645 (*series 3*) 39: 81–86
- 2646 MARSH O.C. 1878. — Principal characters of American Jurassic dinosaurs, Part I. *American*
2647 *Journal of Science (series 3)* 16 (95): 411–416. [https://doi.org/10.2475/ajs.s3-](https://doi.org/10.2475/ajs.s3-16.95.411)
2648 16.95.411
- 2649 MARSH O.C. 1877. — Notice of some new dinosaurian reptiles from the Jurassic Formation.
2650 *American Journal of Science (series 3)* 14: 514–516
- 2651 MARTY D., BELVEDERE M., MEYER C.A., MIETTO P., PARATTE G., LOVIS C., & Thüring B. 2010. —
2652 Comparative analysis of Late Jurassic sauropod trackways from the Jura Mountains
2653 (NW Switzerland) and the central High Atlas Mountains (Morocco): implications for
2654 sauropod ichnotaxonomy. *Historical Biology: An International Journal of*
2655 *Paleobiology* 22:1-3, 109-133
- 2656 MATTINSON J.M. 2005. — Zircon U–Pb chemical abrasion (“CA-TIMS”) method: combined
2657 annealing and multi-step partial dissolution analysis for improved precision and
2658 accuracy of zircon ages. *Chemical Geology* 220 (1): 47–66
- 2659 MCPHEE B.W., BONNAN M.F., YATES A.M., NEVELING J. & CHOINIÈRE J.N. 2015. — A new basal
2660 sauropod from the pre-Toarcian Jurassic of South Africa: evidence of niche-
2661 partitioning at the sauropodomorph–sauropod boundary? *Scientific Reports* 5:
2662 13224. <https://doi.org/10.1038/srep13224>
- 2663 MCPHEE B.W., UPCHURCH P., MANNION P.D., SULLIVAN C., BUTLER R.J. & BARRETT P.M. 2016. — A
2664 revision of *Sanpasaurus yaoi* Young, 1944 from the Early Jurassic of China, and its
2665 relevance to the early evolution of Sauropoda (Dinosauria). *PeerJ* 4: e2578
- 2666 MCPHEE B.W., YATES A.M., CHOINIÈRE J.N. & ABDALA F. 2014. — The complete anatomy and
2667 phylogenetic relationships of *Antetonitrus ingenipes* (Sauropodiformes, Dinosauria):
2668 implications for the origins of Sauropoda. *Zoological Journal of the Linnean Society*
2669 171 (1): 151–205. <https://doi.org/10.1111/zoj.12127>
- 2670 MO J. 2013. — *Topics in Chinese Dinosaur Paleontology-Bellusaurus sui*, in XU X. (ed.).
2671 Zhengzhou, China, Henan Science and Technology Press. 231 p.
- 2672 MOORE A., XU X. & CLARK J. 2017. — Anatomy and systematics of *Klamelisaurus gobiensis*, a
2673 mamenchisaurid sauropod from the Middle-Late Jurassic Shishugou Formation of
2674 China. In: 77th annual meeting of the SVP, Calgary, Canada. Taylor & Francis. p. 165A.
- 2675 NAIR J.P. & SALISBURY S.W. 2012. — New anatomical information on *Rhoetosaurus brownei*
2676 Longman, 1926, a gravisaurian sauropodomorph dinosaur from the Middle Jurassic
2677 of Queensland, Australia. *Journal of Vertebrate Paleontology* 32 (2): 369–394.
2678 <https://doi.org/10.1080/02724634.2012.622324>
- 2679 NICHOLL C.S., MANNION P.D. & BARRETT P.M. 2018. — Sauropod dinosaur remains from a new
2680 Early Jurassic locality in the Central High Atlas of Morocco. *Acta Palaeontologica*
2681 *Polonica* 63 (1): 147–157.
- 2682 NOÈ L.F., LISTON J.J. & CHAPMAN S.D. 2010. — ‘Old bones, dry subject’: the dinosaurs and
2683 pterosaur collected by Alfred Nicholson Leeds of Peterborough, England. *Geological*
2684 *Society, London, Special Publications* 343 (1): 49–77
- 2685 NULLO F.E. 1983. — *Descripción geológica de la Hoja 45 c, Pampa de Agnia, provincia del*
2686 *Chubut: carta geológico-económica de la República Argentina, escala 1: 200.000.*
2687 *Servicio Geológico Nacional* 199:1-94.
- 2688 OLIVERA D.E., ZAVATTIERI A.M. & QUATTROCCHIO M.E. 2015. — The palynology of the Cañadón
2689 Asfalto Formation (Jurassic), Cerro Cóndor depocentre, Cañadón Asfalto Basin,
2690 Patagonia, Argentina: palaeoecology and palaeoclimate based on ecogroup analysis.
2691 *Palynology* 39 (3): 362–386

- 2692 OUYANG H. & YE Y. 2002. — *The first mamenchisaurian skeleton with complete skull,*
2693 *Mamenchisaurus youngi.* Chengdu, China, Sichuan Publishing House of Science and
2694 Technology. 138 p.
- 2695 PENG Z., YE Y., GAO Y., SHU C.K. & JIANG S. 2005. — *Jurassic Dinosaur Faunas in Zigong.*
2696 Chengdu, China, Sichuan Peoples Publishing House. 69–98 p.
- 2697 PHILLIPS J. 1871. — *Geology of Oxford and the Valley of the Thames.* Clarendon Press. Oxford,
2698 390p.
- 2699 PI L., OU Y. & YE Y. 1996. — A new species of sauropod from Zigong, Sichuan,
2700 *Mamenchisaurus youngi.* In: Papers on Geosciences Contributed to the 30th
2701 International Geological Congress. 87–91p.
- 2702 PIATNITZKY C. 1936. — Informe preliminar sobre el estudio geológico de la región situada al
2703 norte de los lagos Colhué Huapi y Musters. *Boletín Informaciones Petroleras,*
2704 *Yacimientos Petrolíferos Fiscales* 137: 2–15
- 2705 POL D., RAUHUT O.W.M. & CARBALLIDO J.L. 2009. — Skull anatomy of a new basal eusauropod
2706 from the Cañadon Asfalto Formation (Middle Jurassic) of Central Patagonia. *Journal*
2707 *of Vertebrate Paleontology* 29 (Suppl. to 3): 100A.
- 2708 POROPAT S.F., UPCHURCH P., MANNION P.D., HOCKNULL S.A., KEAR B.P., SLOAN T., SINAPIUS G.H.K. &
2709 ELLIOTT D.A. 2015. — Revision of the sauropod dinosaur *Diamantinasaurus matildae*
2710 Hocknull et al. 2009 from the mid-Cretaceous of Australia: Implications for
2711 Gondwanan titanosauriform dispersal. *Gondwana Research* 27 (3): 995–1033.
2712 <https://doi.org/10.1016/j.gr.2014.03.014>
- 2713 RAATH M.A. 1972. — Fossil vertebrate studies in Rhodesia: a new dinosaur (Reptilia:
2714 Saurischia) from near the Trias-Jurassic boundary. *Arnoldia (Rhodesia)* 7: 1–7
- 2715 RAUHUT O.W.M. 2002. — Dinosaur evolution in the Jurassic: a South American perspective/In:
2716 62nd Society of Vertebrate Paleontology annual meeting, Norman, Oklahoma, USA.
2717 22.
- 2718 RAUHUT O.W.M. 2003. — A dentary of *Patagosaurus* (Sauropoda) from the Middle Jurassic of
2719 Patagonia. *Ameghiniana* 40 (3): 425–432
- 2720 RAUHUT O.W.M. 2003. — Revision of *Amygdalodon patagonicus* Cabrera, 1947 (Dinosauria,
2721 Sauropoda). *Fossil Record* 6 (1): 173–181
- 2722 RAUHUT O.W. 2004. — Braincase structure of the Middle Jurassic theropod dinosaur
2723 *Piatnitzkysaurus.* *Canadian Journal of Earth Sciences* 41 (9): 1109–1122.
2724 <https://doi.org/10.1139/e04-053>
- 2725 RAUHUT O.W.M., REMES K., FECHNER R., CLADERA G. & PUERTA P. 2005. — Discovery of a short-
2726 necked sauropod dinosaur from the Late Jurassic period of Patagonia. *Nature* 435
2727 (7042): 670–672
- 2728 REMES K. 2009. — Taxonomy of Late Jurassic diplodocid sauropods from Tendaguru
2729 (Tanzania). *Fossil Record* 12 (1): 23–46
- 2730 REMES K., ORTEGA F., FIERRO I., JOGER U., KOSMA R., FERRER J.M.M., IDE O.A. & MAGA A. 2009. — A
2731 new basal sauropod dinosaur from the Middle Jurassic of Niger and the early
2732 evolution of Sauropoda. *PLoS One* 4 (9): e6924.
2733 <https://doi.org/10.1371/journal.pone.0006924>
- 2734 RICH T.H., VICKERSRICH P., GIMENEZ O., CUNEO R., PUERTA P. & VACCA R. 1999. — A new sauropod
2735 dinosaur from Chubut Province, Argentina. *National Science Museum Monographs*
2736 15: 61–84
- 2737 RUSSELL D.A. & ZHENG Z. 1993. — A large mamenchisaurid from the Junggar Basin, Xinjiang,
2738 People's Republic of China. *Canadian Journal of Earth Sciences* 30 (10): 2082–2095
- 2739 SANDER P.M., MATEUS O., LAVEN T. & KNÖTSCHKE N. 2006. — Bone histology indicates insular
2740 dwarfism in a new Late Jurassic sauropod dinosaur. *Nature* 441 (7094): 739–741.
2741 <https://doi.org/10.1038/nature04633>

- 2742 SERENO P.C., BECK A.L., DUTHEIL D.B., LARSSON H.C.E., LYON G.H., MOUSSA B., SADLEIR R.W., SIDOR
2743 C.A., VARRICCHIO D.J. & WILSON G.P. 1999. — Cretaceous sauropods from the Sahara
2744 and the uneven rate of skeletal evolution among dinosaurs. *Science* 286 (5443):
2745 1342–1347
- 2746 SILVA NIETO D.G., CABALERI N.G., SALANI F.M. & COLUCCIA A. 2002. — Cañadón Asfalto, una
2747 cuenca tipo “pull apart” en el área de cerro Cóndor, provincia del Chubut *In*: p. 238–
2748 244.
- 2749 STIPANIC P.N., RODRIGO F., BAULIES O.L. & MARTÍNEZ C.G. 1968. — Las formaciones
2750 presenonianas en el denominado Macizo Nordpatagónico y regiones adyacentes.
2751 *Revista de la Asociación Geológica Argentina* 23 (2): 67–98
- 2752 STUMPF S., ANSORGE J. & KREMPIEN W. 2015. — Gravisaurian sauropod remains from the
2753 marine late Early Jurassic (Lower Toarcian) of North-Eastern Germany. *Geobios* 48
2754 (3): 271–279
- 2755 TANG F., JING X., KANG X. & ZHANG G. 2001. — [*Omeisaurus maoianus*: a complete sauropod
2756 from Jingyuan, Sichuan]. Beijing, China, China Ocean Press. 112 p.
- 2757 TASCH P. & VOLKHEIMER W. 1970. — Jurassic conchostracans from Patagonia. *The University of*
2758 *Kansas Paleontological Contributions* 50:1-23.
- 2759 TAYLOR M.P. 2009. — A re-evaluation of *Brachiosaurus altithorax* Riggs 1903 (Dinosauria,
2760 Sauropoda) and its generic separation from *Giraffatitan brancai* (Janensch 1914).
2761 *Journal of Vertebrate Paleontology* 29 (3): 787–806
- 2762 TODD C.N., ROBERTS E.M., KNUITSEN E.M., ROZEFELDS A.C., HUANG H.-Q. & SPANDLER C. 2019. —
2763 Refined age and geological context of two of Australia’s most important Jurassic
2764 vertebrate taxa (*Rhoetosaurus brownei* and *Siderops kehli*), Queensland. *Gondwana*
2765 *Research* 76: 19–25
- 2766 TSCHOPP E., MATEUS O. & BENSON R.B.J. 2015. — A specimen-level phylogenetic analysis and
2767 taxonomic revision of Diplodocidae (Dinosauria, Sauropoda). *PeerJ* 3: e857.
2768 <https://doi.org/10.7717/peerj.857>
- 2769 UPCHURCH P., BARRETT P.M. & DODSON P. 2004. — Sauropoda, *in* WEISHAMPEL D.B., DODSON P. &
2770 OSMÓLSKA H. (eds.), *The Dinosauria. Second edition*. Berkeley, CA, University of
2771 California Press. p. 259–322.
- 2772 UPCHURCH P. & MARTIN J. 2002. — The Rutland *Cetiosaurus*: the anatomy and relationships of
2773 a Middle Jurassic British sauropod dinosaur. *Palaeontology* 45 (6): 1049–1074
- 2774 UPCHURCH P. & MARTIN J. 2003. — The anatomy and taxonomy of *Cetiosaurus* (Saurischia,
2775 Sauropoda) from the Middle Jurassic of England. *Journal of Vertebrate Paleontology*
2776 23 (1): 208–231
- 2777 VOLKHEIMER W., QUATTROCCHIO M.E., CABALERI N.G., GARCÍA V. 2001. — Palynology and
2778 paleoenvironment of the Jurassic lacustrine Cañadón Asfalto Formation, at Cañadón
2779 Lahuincó locality, Chubut Province, Central Patagonia, Argentina. *Revista Española*
2780 *de Microplaeontología* 40:77-96.
- 2781 VOLKHEIMER W., QUATTROCCHIO M.E., CABALERI N.G., NARVAEZ P.L. & ROSENFELD U. 2015. —
2782 ENVIRONMENTAL AND CLIMATIC PROXIES FOR THE CAÑADÓN ASFALTO AND
2783 NEUQUÉN BASINS (PATAGONIA, ARGENTINA): REVIEW OF MIDDLE TO UPPER
2784 JURASSIC CONTINENTAL AND NEAR COASTAL SEQUENCES. *REVISTA BRASILEIRA DE*
2785 *PALEONTOLOGIA* 18 (1): 71–82
- 2786 VOLKHEIMER W., RAUHUT O.W., QUATTROCCHIO M.E. & MARTINEZ M.A. 2008. — Jurassic
2787 paleoclimates in Argentina, a review. *Revista de la Asociación Geológica Argentina*
2788 63 (4): 549–556
- 2789 WANG J., YE Y., PEI R., TIAN Y., FENG C., ZHENG D. & CHANG S.-C. 2018. — Age of Jurassic basal
2790 sauropods in Sichuan, China: A reappraisal of basal sauropod evolution. *Geological*
2791 *Society of America Bulletin* 130 (9/10): 1493–1500

- 2792 WEDEL M.J. 2003. — Vertebral pneumaticity, air sacs, and the physiology of sauropod
2793 dinosaurs. *Paleobiology* 29 (2): 243
- 2794 WEDEL M.J. 2005. — Postcranial skeletal pneumaticity in sauropods and its implications for
2795 mass estimates, in CURRY ROGERS K. A. & WILSON J.A. (eds.), *The sauropods: evolution*
2796 *and paleobiology*. Berkeley, USA, University of California Press. p. 201–228.
- 2797 WEDEL M.J. & TAYLOR M.P. 2013. — Caudal pneumaticity and pneumatic hiatuses in the
2798 sauropod dinosaurs *Giraffatitan* and *Apatosaurus*. *PLoS ONE* 8 (10): e78213.
2799 <https://doi.org/10.1371/journal.pone.0078213>
- 2800 WILSON J.A. 2002. — Sauropod dinosaur phylogeny: critique and cladistic analysis. *Zoological*
2801 *Journal of the Linnean Society* 136 (2): 215–275
- 2802 WILSON J.A. 1999. — A nomenclature for vertebral laminae in sauropods and other
2803 saurischian dinosaurs. *Journal of Vertebrate Paleontology* 19 (4): 639–653
- 2804 WILSON J.A., D’EMIC M.D., IKEJIRI T., MOACDIEH E.M. & WHITLOCK J.A. 2011. — A nomenclature
2805 for vertebral fossae in sauropods and other saurischian dinosaurs. *PLoS ONE* 6 (2):
2806 e17114
- 2807 WILSON J.A. 2011. — Anatomical terminology for the sacrum of sauropod dinosaurs.
2808 *Contributions from the museum of Paleontology, University of Michigan* 32:59–69.
- 2809 WILSON J.A. & UPCHURCH P. 2009. — Redescription and reassessment of the phylogenetic
2810 affinities of *Euhelopus zdanskyi* (Dinosauria: Sauropoda) from the Early Cretaceous
2811 of China. *Journal of Systematic Palaeontology* 7 (02): 199–239.
2812 <https://doi.org/10.1017/S1477201908002691>
- 2813 WILSON J.A. & CARRANO M.T. 1999. — Titanosaurs and the origin of “wide-gauge” trackways: a
2814 biomechanical and systematic perspective on sauropod locomotion. *Paleobiology* 25
2815 (2): 252–267
- 2816 WILSON J.A. 2011. — Anatomical terminology for the sacrum of sauropod dinosaurs
- 2817 WOODWARD A.S. 1905. — On parts of the skeleton of *Cetiosaurus leedsi*, a sauropodous
2818 dinosaur from the Oxford Clay of Peterborough. *Proceedings of the Zoological*
2819 *Society of London* 1: 232–243
- 2820 XING L., MIYASHITA T., CURRIE P.J., YOU H., ZHANG J. & DONG Z. 2013. — A new basal eusauropod
2821 from the Middle Jurassic of Yunnan, China, and faunal compositions and transitions
2822 of Asian sauropodomorph dinosaurs. *Acta Palaeontologica Polonica* 60 (1): 145–154
- 2823 XING L., MIYASHITA T., ZHANG J., LI D., YE Y., SEKIYA T., WANG F. & CURRIE P.J. 2015. — A new
2824 sauropod dinosaur from the Late Jurassic of China and the diversity, distribution,
2825 and relationships of mamenchisaurids. *Journal of Vertebrate Paleontology* 35 (1):
2826 e889701
- 2827 XU X., UPCHURCH P., MANNION P.D., BARRETT P.M., REGALADO-FERNANDEZ O.R., MO J., MA J. & LIU
2828 H. 2018. — A new Middle Jurassic diplodocoid suggests an earlier dispersal and
2829 diversification of sauropod dinosaurs. *Nature communications* 9 (1): 2700
- 2830 YADAGIRI P. 2001. — The osteology of *Kotasaurus yamanpalliensis*, a sauropod dinosaur from
2831 the Early Jurassic Kota Formation of India. *Journal of Vertebrate Paleontology* 21 (2):
2832 242–252
- 2833 YADAGIRI P. 1988. — A new sauropod *Kotasaurus yamanpalliensis* from Lower Jurassic Kota
2834 Formation of India. *Records of the Geological Survey of India* 11: 102–127
- 2835 YATES A.M. & KITCHING J.W. 2003. — The earliest known sauropod dinosaur and the first steps
2836 towards sauropod locomotion. *Proceedings of the Royal Society of London. Series B:*
2837 *Biological Sciences* 270 (1525): 1753–1758. <https://doi.org/10.1098/rspb.2003.2417>
- 2838 YATES A.M., BONNAN M.F., NEVELING J., CHINSAMY A. & BLACKBEARD M.G. 2010. — A new
2839 transitional sauropodomorph dinosaur from the Early Jurassic of South Africa and
2840 the evolution of sauropod feeding and quadrupedalism. *Proceedings of the Royal*
2841 *Society of London B: Biological Sciences* 277 (1682): 787–794.
2842 <https://doi.org/10.1098/rspb.2009.1440>

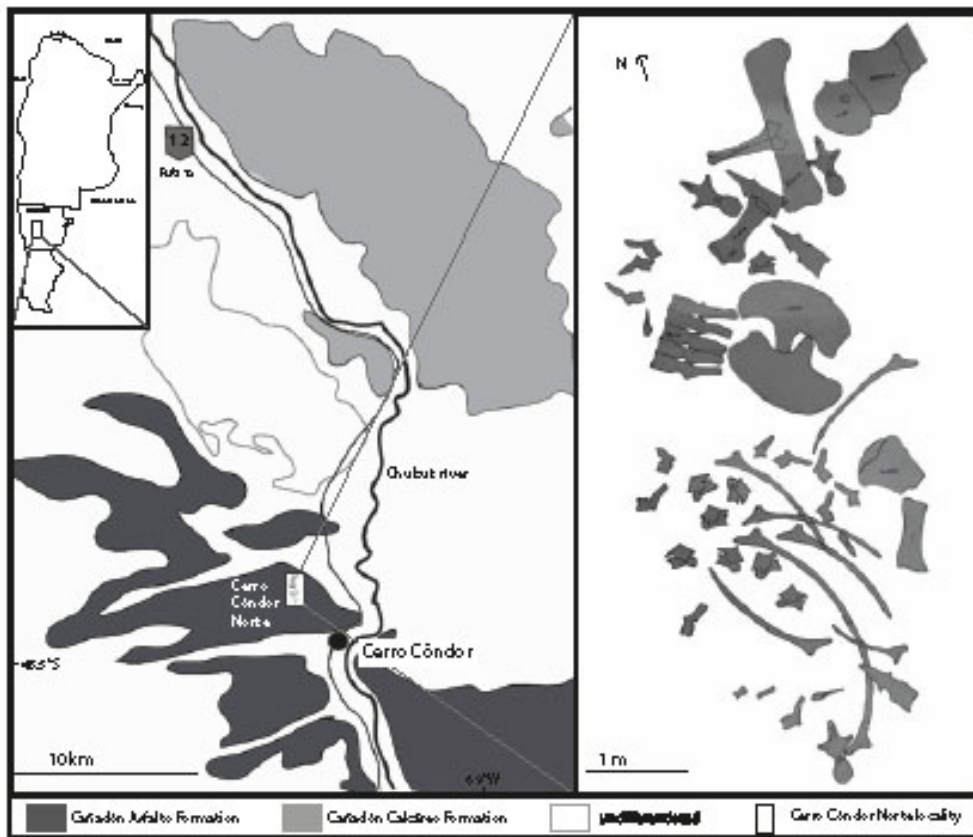
- 2843 YOUNG C.-C. 1939. — On a new sauropoda, with notes on other fragmentary reptiles from
2844 Szechuan. *Bulletin of the Geological Society of China* 19 (3): 279–315.
2845 <https://doi.org/10.1111/j.1755-6724.1939.mp19003005.x>
2846 YOUNG C.-C. & ZHAO X. 1972. — Description of the type material of *Mamenchisaurus*
2847 *hochuanensis*. *Institute of Vertebrate Paleontology and Paleoanthropology*
2848 *Monograph Series* 18: 1–30
2849 ZAVATTIERI A.M., ESCAPA I.H., SCASSO R.A. & OLIVERA D. 2010. — Contribución al conocimiento
2850 palinoestratigráfico de la Formación Cañadón Calcáreo en su localidad tipo,
2851 provincia del Chubut, Argentina *In*:
2852 ZHANG Y. 1988. — *The Middle Jurassic dinosaur fauna from Dashanpu, Zigong, Sichuan, vol.*
2853 *1: sauropod dinosaur (I): Shunosaurus*. Chengdu, China, Sichuan Publishing House of
2854 Science and Technology. 114 p.
2855 ZHANG Y., LI K., ZENG Q. & DOWNS T.B.W. 1998. — A new species of sauropod from the Late
2856 Jurassic of the Sichuan Basin (*Mamenchisaurus jingyanensis* sp. nov.). *Journal of the*
2857 *Chengdu University of Technology* 25 (1)
2858 ZHAO X.J. 1993. — A NEW MID-JURASSIC SAUROPOD (*KLAMELISAURUS GOBIENSIS* GEN. ET
2859 SP. NOV.) FROM XINJIANG, CHINA. *Vertebrata Palasiatica* 2: 007
2860 ZHAO X.J. 1993. — A new mid-Jurassic sauropod (*Klamelisaurus gobiensis* gen. et sp. nov.)
2861 from Xinjiang, China. *Vertebrata Palasiatica* 2: 243-265.
2862
2863
2864

2865

2866 **FIGURE AND TABLE CAPTIONS**

2867

2868 *Figures*

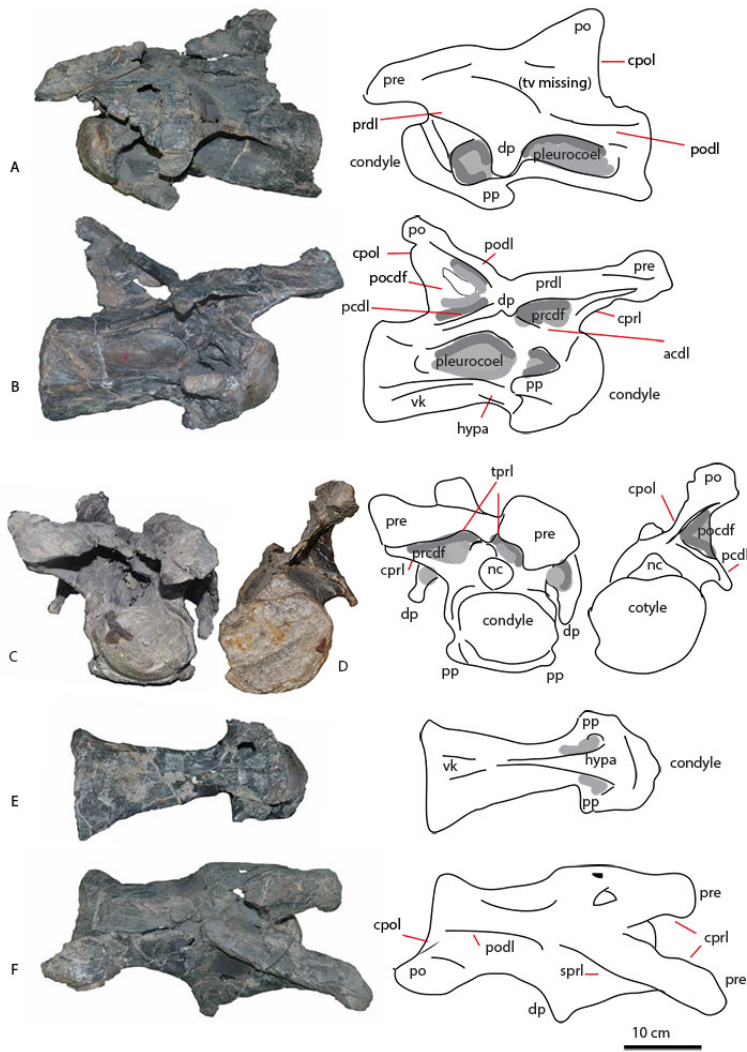


2869

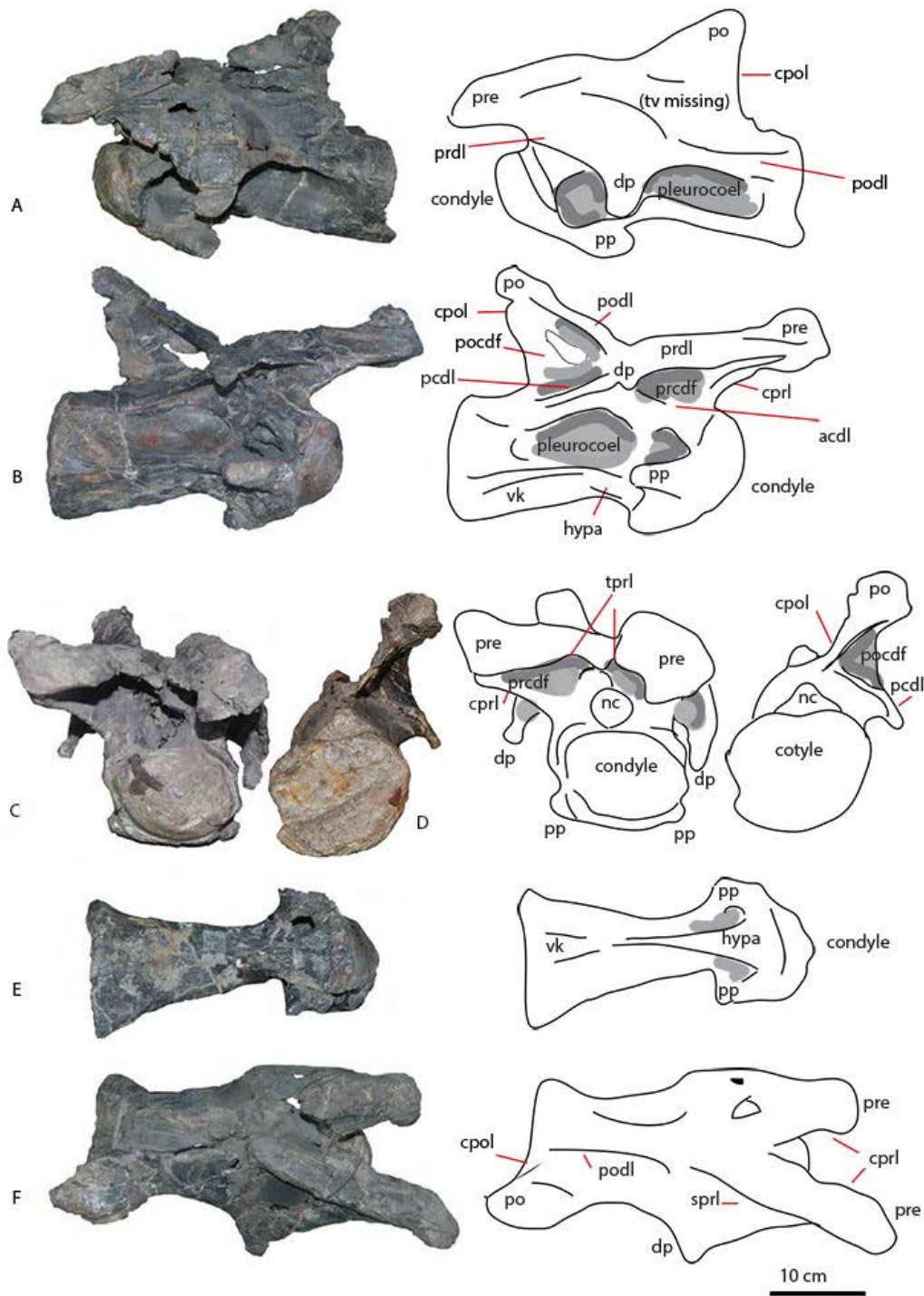
2870

2871

Figure 1: Geological setting of the locality Cerro Cóndor Norte, and bonebed with holotype highlighted

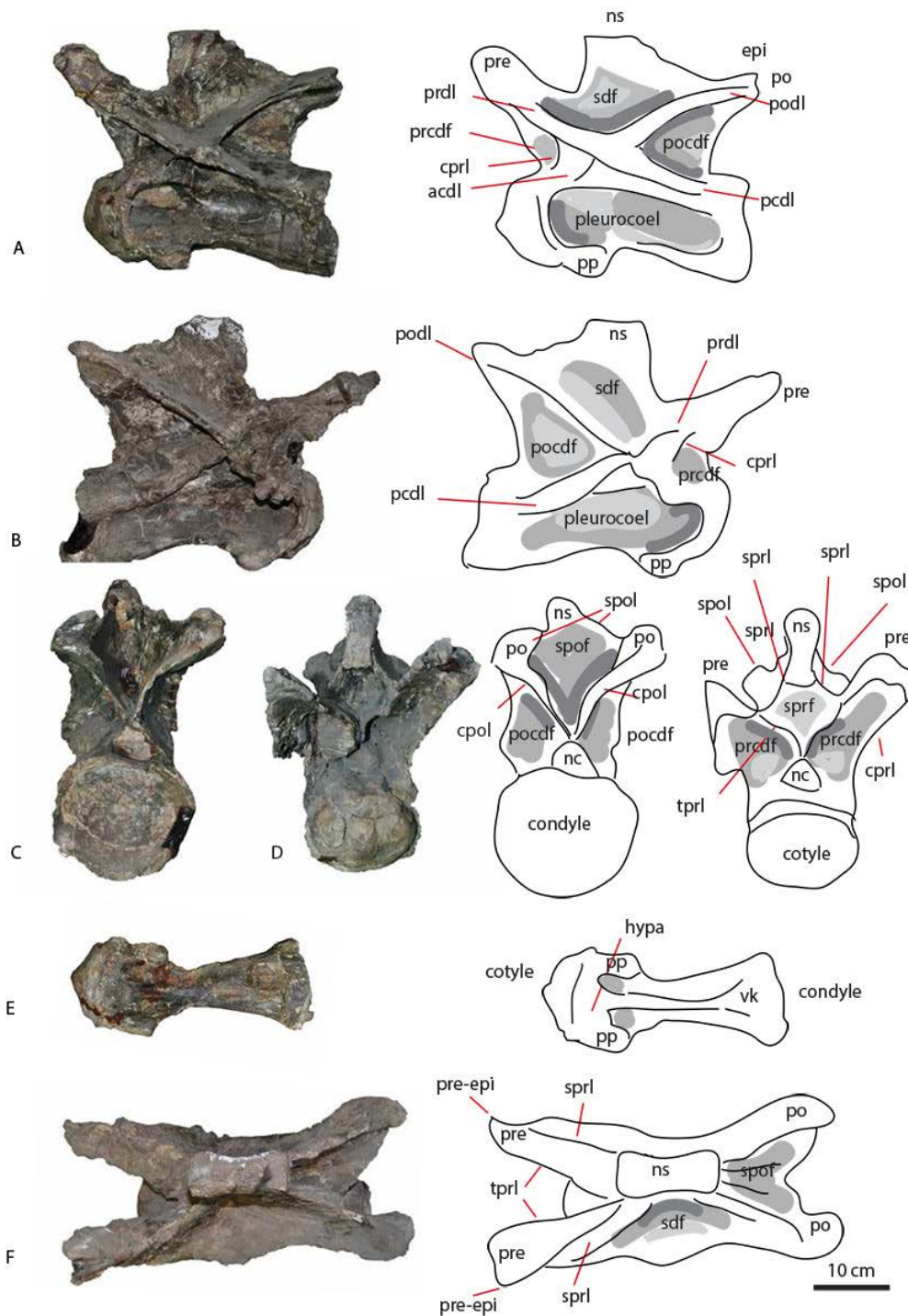


2872
 2873 Figure 2: Cervical PVL 4170 (1) in lateral (A,B), anterior (C), posterior (D), ventral (E) and
 2874 dorsal (F) views. Abbreviations: acdl = anterior centrodiapophyseal lamina, cpri =
 2875 centroprezygapophyseal lamina, cpol = centropostzygapophyseal lamina, dp = diapophysis,
 2876 hypa = hypapophysis, nc = neural canal, ns = neural spine, pcdl = posterior
 2877 centrodiapophyseal lamina, pp = parapophysis, po = postzygapophysis, prcdf =
 2878 prezygapophyseal centrodiapophyseal fossa, pocdf = postzygapophyseal centrodiapophyseal
 2879 fossa, prdl = prezygapophyseal diapophyseal lamina, pre = prezygapophysis, spof =
 2880 spinopostzygapophyseal fossa, spol = spinopostzygapophyseal lamina, sprf =
 2881 spinoprezygapophyseal fossa, sprl = spinoprezygapophyseal lamina, vk = ventral keel.



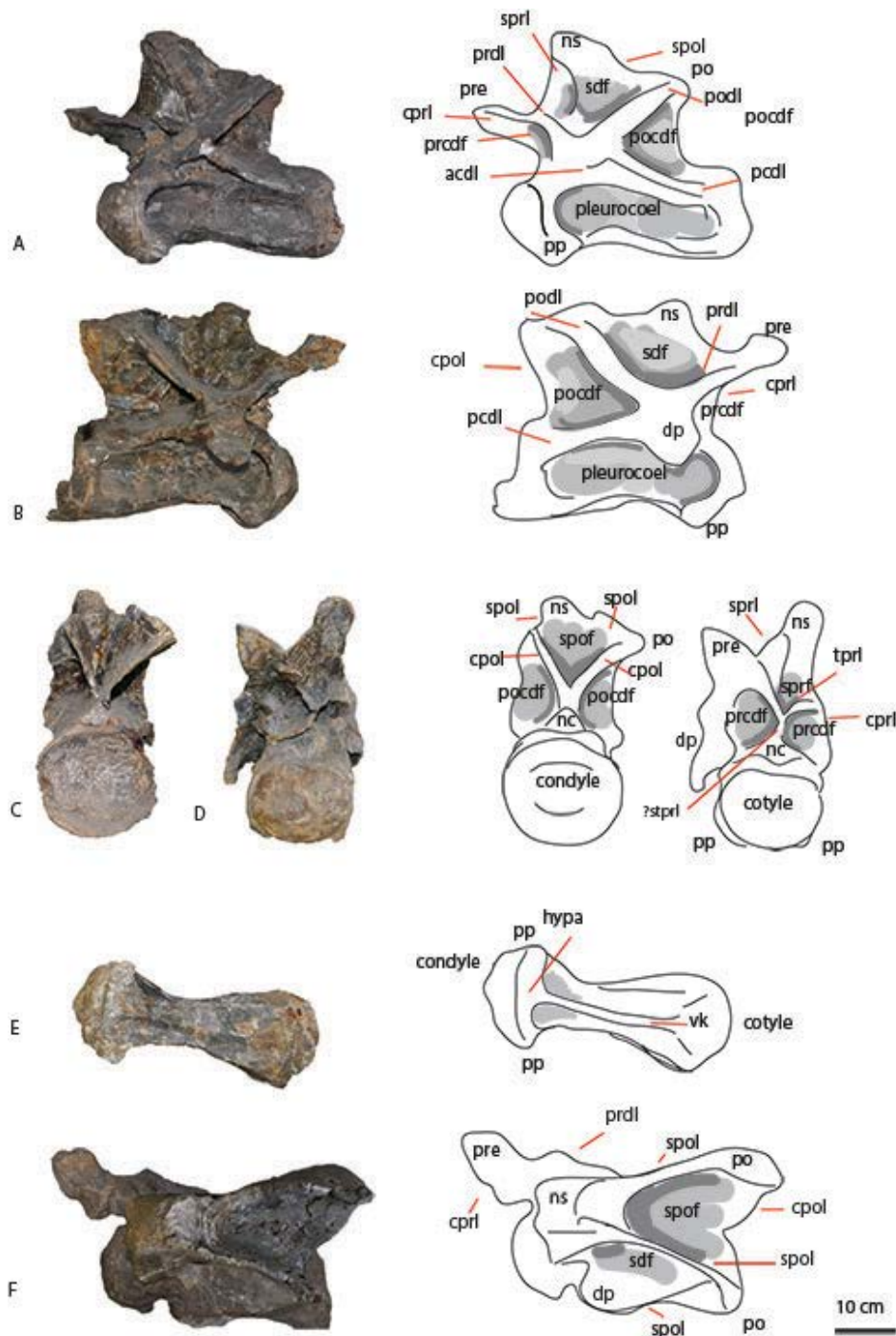
2882
 2883
 2884
 2885
 2886
 2887
 2888
 2889
 2890
 2891
 2892

Figure 3: Cervical PVL 4170 (2) in lateral (A,B), anterior (C), posterior (D), ventral (E) and dorsal (F) views. Abbreviations: acdl = anterior centrodiapophyseal lamina, cpri = centroprezygapophyseal lamina, cpol = centropostzygapophyseal lamina, dp = diapophysis, hypa = hypapophysis, nc = neural canal, ns = neural spine, pcld = posterior centrodiapophyseal lamina, pp = parapophysis, po = postzygapophysis, prcdf = prezygapophyseal centrodiapophyseal fossa, pocdf = postzygapophyseal centrodiapophyseal fossa, prdl = prezygapophyseal diapophyseal lamina, pre = prezygapophysis, spof = spinopostzygapophyseal fossa, spol = spinopostzygapophyseal lamina, sprf = spinoprezygapophyseal fossa, sprl = spinoprezygapophyseal lamina, tprl = intraprezygapophyseal lamina, vk = ventral keel.



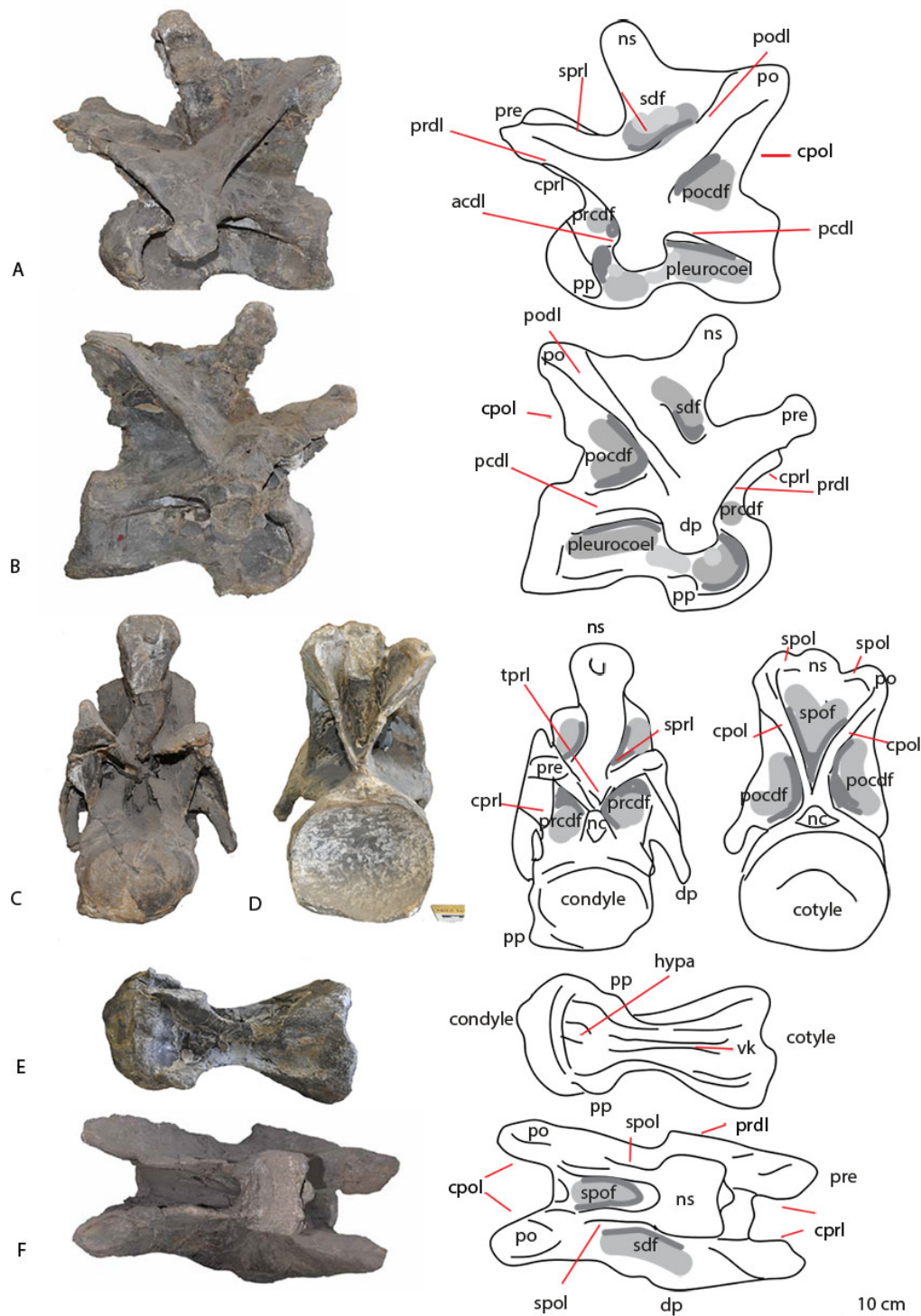
2893
 2894
 2895
 2896
 2897
 2898
 2899
 2900
 2901
 2902
 2903
 2904

Figure 4: Cervical PVL 4170 (3) in lateral (A,B), posterior (C) anterior (D), ventral (E) and dorsal (F) views. Abbreviations: acdl = anterior centrodiapophyseal lamina, cprl = centroprezygapophyseal lamina, cpol = centropostzygapophyseal lamina, dp = diapophysis, hypa = hypapophysis, nc = neural canal, ns = neural spine, pcdl = posterior centrodiapophyseal lamina, pp = parapophysis, po = postzygapophysis, prcdf = prezygapophyseal centrodiapophyseal fossa, pocdf = postzygapophyseal centrodiapophyseal fossa, prdl = prezygapophyseal diapophyseal lamina, pre = prezygapophysis, sdf = spinodiapophysal fossa, spof = spinopostzygapophyseal fossa, spol = spinopostzygapophyseal lamina, sprf = spinoprezygapophyseal fossa, sprl = spinoprezygapophyseal lamina, tprl = intraprezygapophyseal lamina, vk = ventral keel.



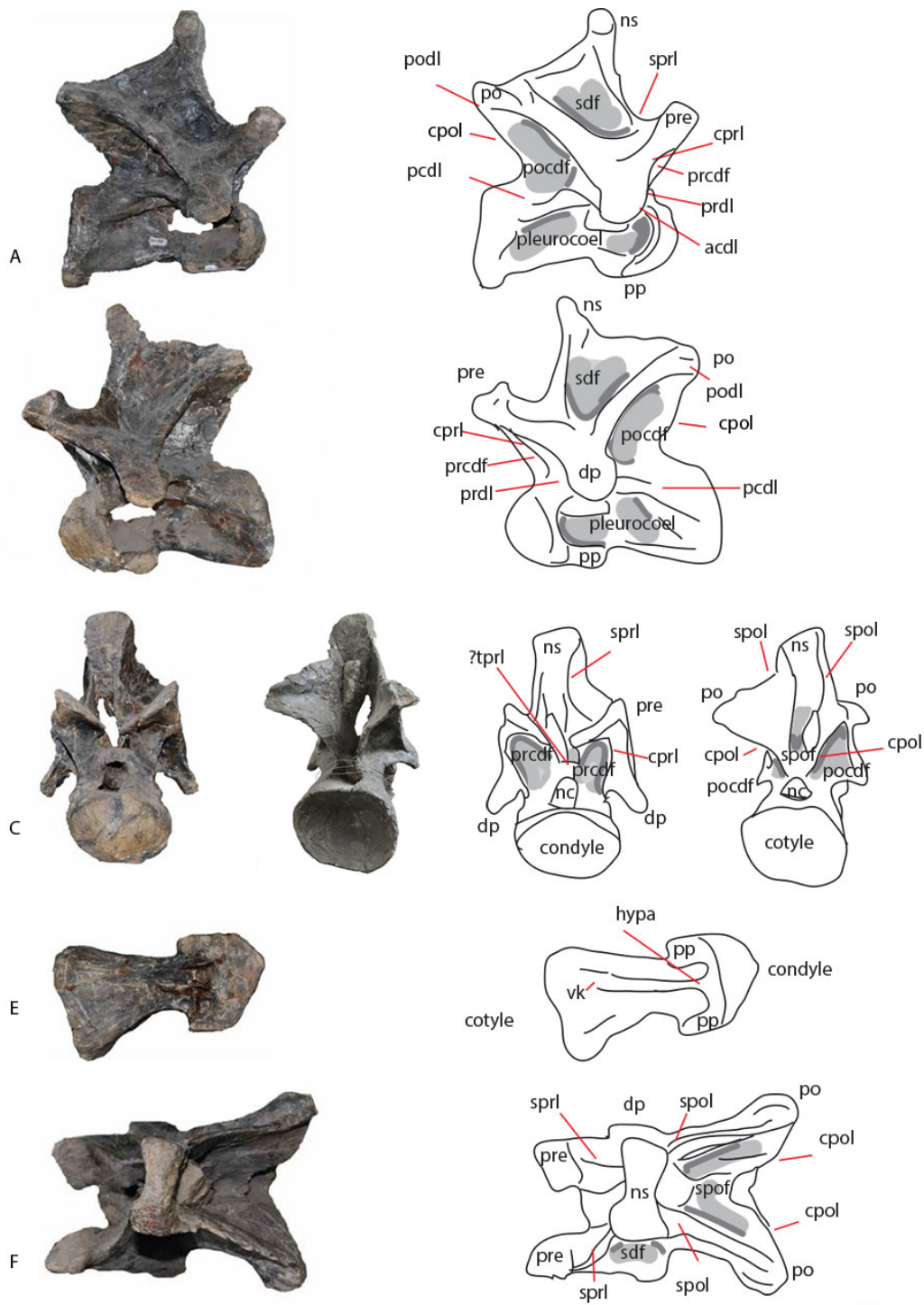
2905
 2906
 2907
 2908
 2909
 2910
 2911
 2912
 2913
 2914
 2915
 2916

Figure 5: Cervical PVL 4170 (4) in lateral (A,B), posterior (C), anterior (D), ventral (E) and dorsal (F) views. Abbreviations: acdl = anterior centrodiapophyseal lamina, cprl = centroprezygapophyseal lamina, cpol = centropostzygapophyseal lamina, dp = diapophysis, hypa = hypapophysis, nc = neural canal, ns = neural spine, pcdl = posterior centrodiapophyseal lamina, pp = parapophysis, po = postzygapophysis, prcdf = prezygapophyseal centrodiapophyseal fossa, pocdf = postzygapophyseal centrodiapophyseal fossa, prdl = prezygapophyseal diapophyseal lamina, pre = prezygapophysis, sdf = spinodiapophysal fossa, spof = spinopostzygapophyseal fossa, spol = spinopostzygapophyseal lamina, sprf = spinoprezygapophyseal fossa, sprl = spinoprezygapophyseal lamina, tprl = intraprezygapophyseal lamina, vk = ventral keel.



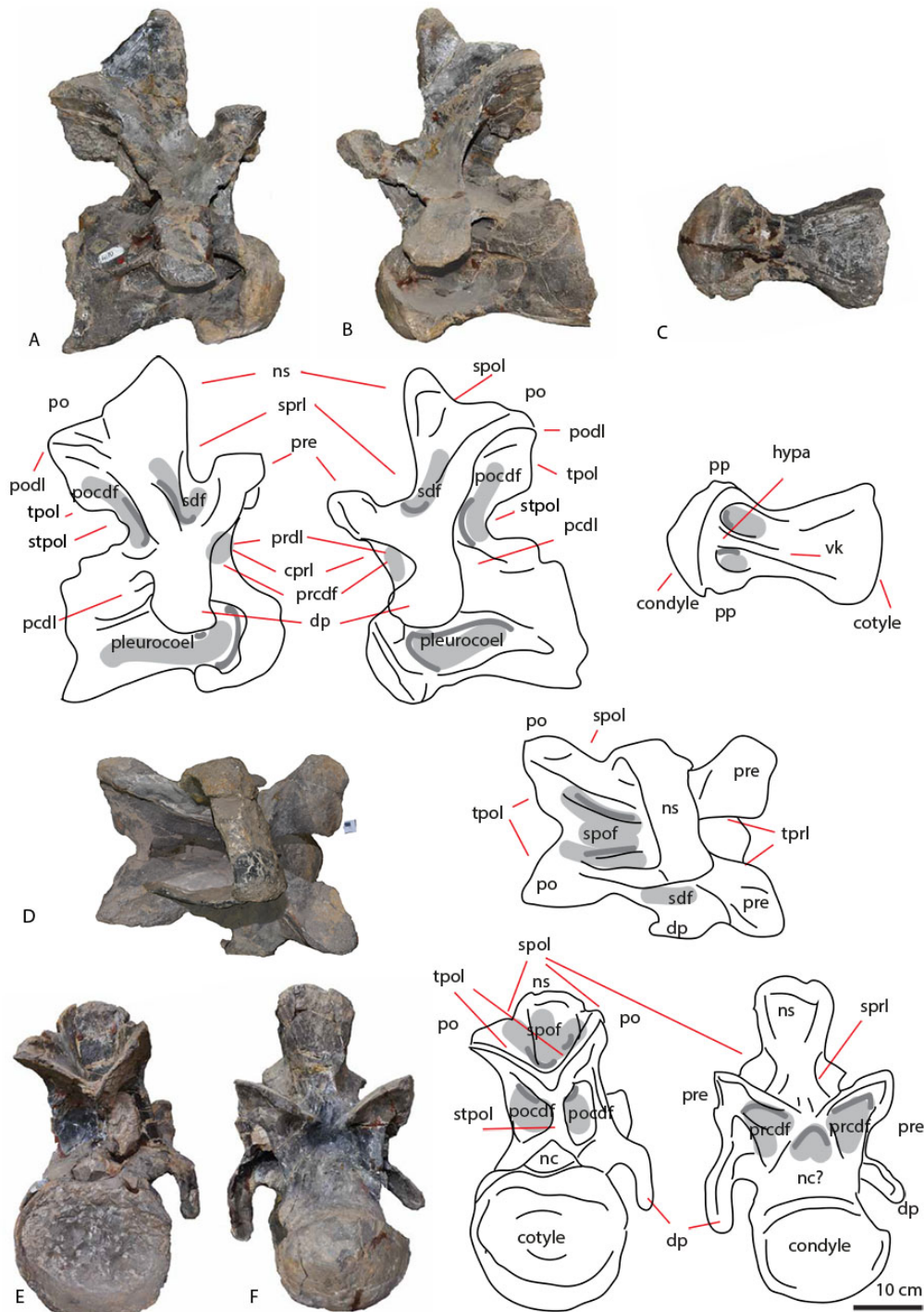
2917
 2918
 2919
 2920
 2921
 2922
 2923
 2924
 2925
 2926
 2927

Figure 6: Cervical PVL 4170 in lateral (A,B), anterior (C), posterior (D), ventral (E) and dorsal (F) views. Abbreviations: acdl = anterior centrodiapophyseal lamina, cpri = centroprezygapophyseal lamina, cpol = centropostzygapophyseal lamina, dp = diapophysis, hypa = hypapophysis, nc = neural canal, ns = neural spine, pcdl = posterior centrodiapophyseal lamina, pp = parapophysis, po = postzygapophysis, prcdf = prezygapophyseal centrodiapophyseal fossa, pocdf = postzygapophyseal centrodiapophyseal fossa, prdl = prezygapophyseal diapophyseal lamina, pre = prezygapophysis, sdf = spinodiapophysal fossa, spof = spinopostzygapophyseal fossa, spol = spinopostzygapophyseal lamina, sprl = spinoprezygapophyseal lamina, tprl = intraprezygapophyseal lamina, vk = ventral keel.



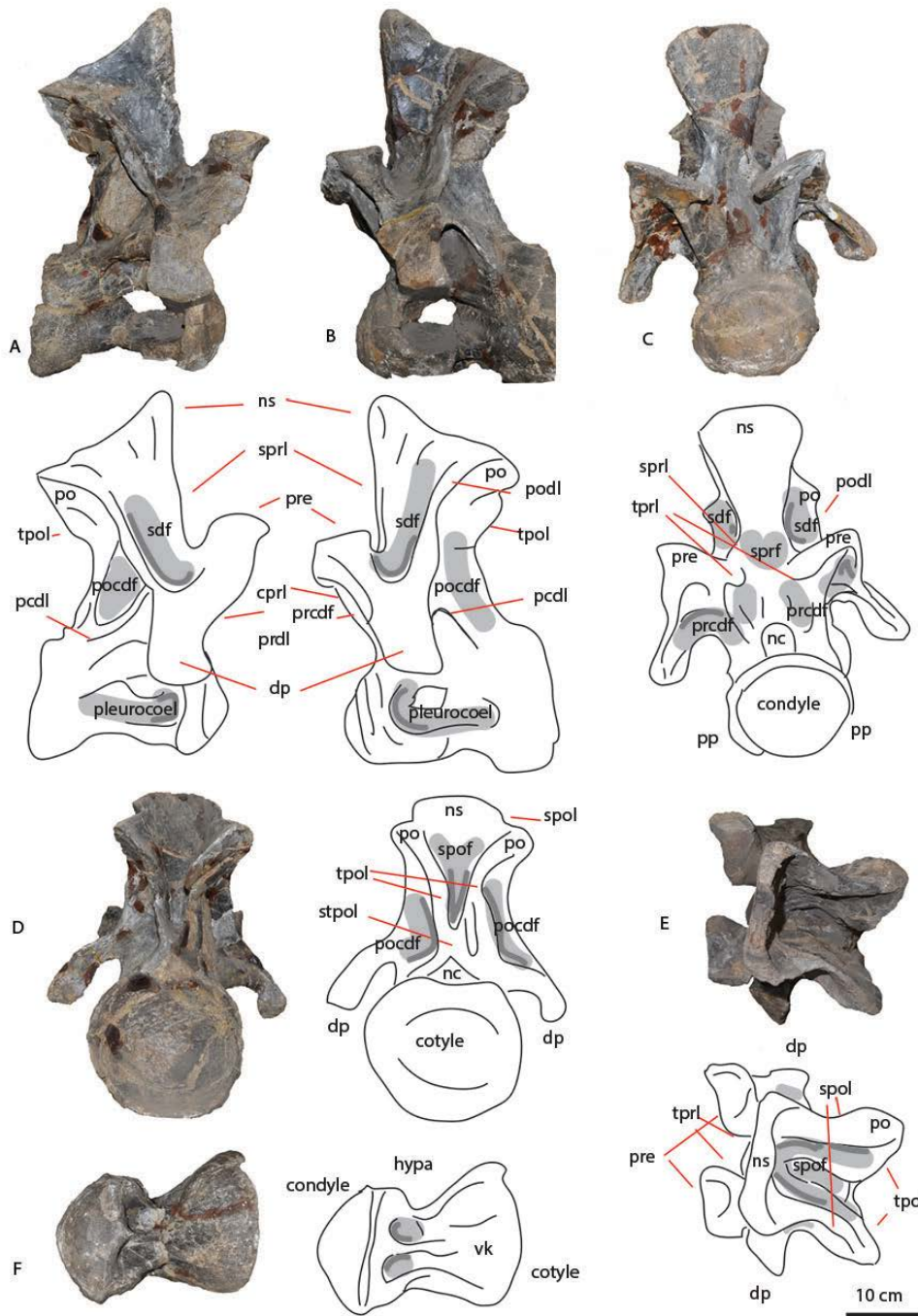
2928
 2929
 2930
 2931
 2932
 2933
 2934
 2935
 2936
 2937
 2938

Figure 7: Cervical PVL 4170 (6) in lateral (A,B), anterior (C), posterior (D), ventral (E) and dorsal (F) view. Abbreviations: acdl = anterior centrodiapophyseal lamina, cprl = centroprezygapophyseal lamina, cpol = centropostzygapophyseal lamina, dp = diapophysis, hypa = hypapophysis, nc = neural canal, ns = neural spine, pcdl = posterior centrodiapophyseal lamina, pp = parapophysis, po = postzygapophysis, prcdf = prezygapophyseal centrodiapophyseal fossa, pocdf = postzygapophyseal centrodiapophyseal fossa, prdl = prezygapophyseal diapophyseal lamina, pre = prezygapophysis, sdf = spinodiapophysal fossa, spof = spinopostzygapophyseal fossa, spol = spinopostzygapophyseal lamina, sprl = spinoprezygapophyseal lamina, tprl = intraprezygapophyseal lamina, vk = ventral keel.



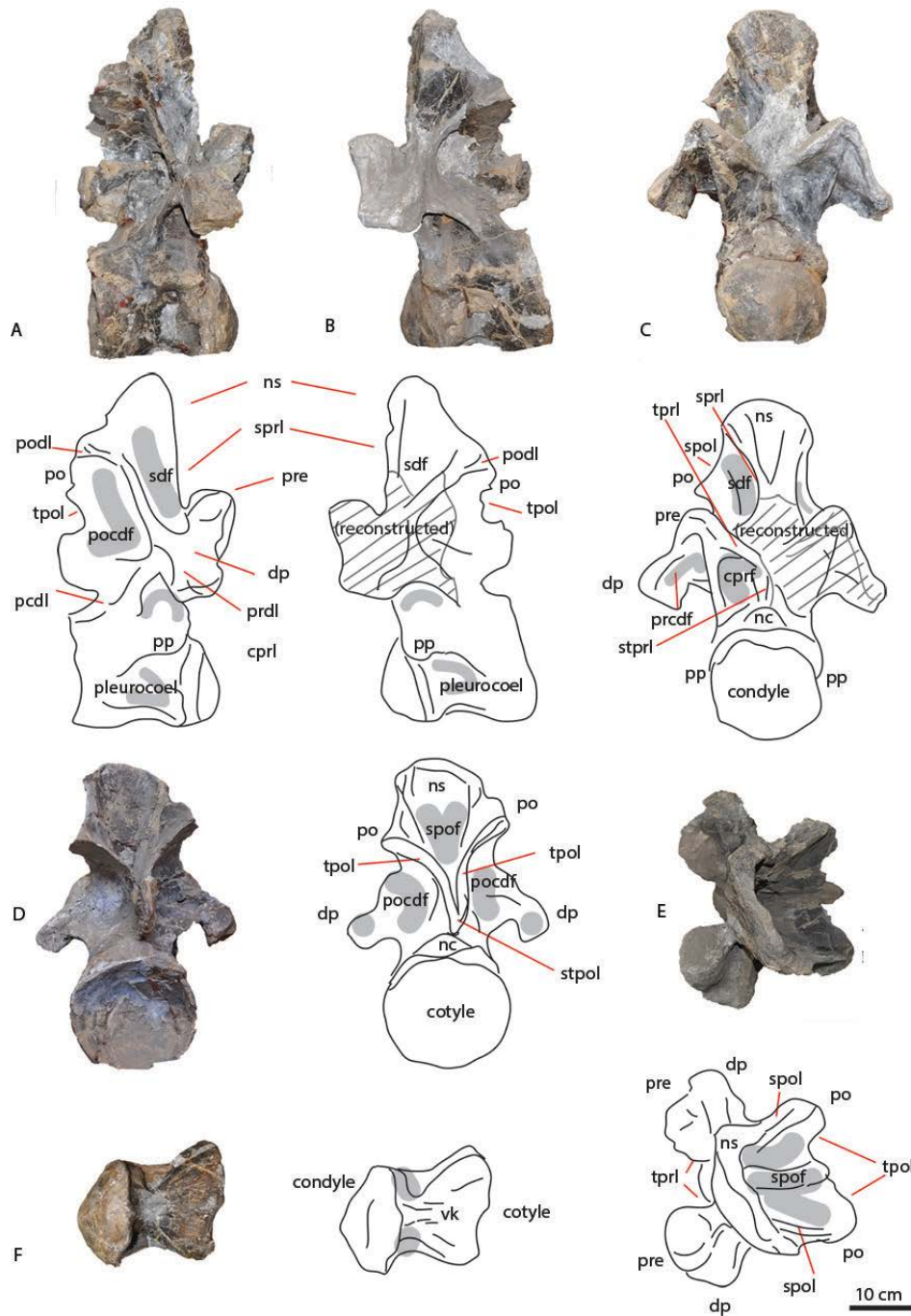
2939
 2940
 2941
 2942
 2943
 2944
 2945
 2946
 2947
 2948
 2949
 2950

Figure 8: Cervical PVL 4170 (7) in lateral (A,B), ventral (C), dorsal (D), anterior (E) and posterior (F) views. Abbreviations: acdl = anterior centrodiapophyseal lamina, cpri = centroprezygapophyseal lamina, cpol = centropostzygapophyseal lamina, dp = diapophysis, hypa = hypapophysis, nc = neural canal, ns = neural spine, pp = parapophysis, po = postzygapophysis, prcdf = prezygapophyseal centrodiapophyseal fossa, pocdf = postzygapophyseal centrodiapophyseal fossa, prdl = prezygapophyseal diapophyseal lamina, pre = prezygapophysis, sdf = spinodiapophysal fossa, spof = spinopostzygapophyseal fossa, spol = spinopostzygapophyseal lamina, sprf = spinoprezygapophyseal fossa, sprl = spinoprezygapophyseal lamina, tprl = intraprezygapophyseal lamina, tpol = intrapostzygapophyseal lamina, stpol = single intrapostzygapophyseal lamina, vk = ventral keel.



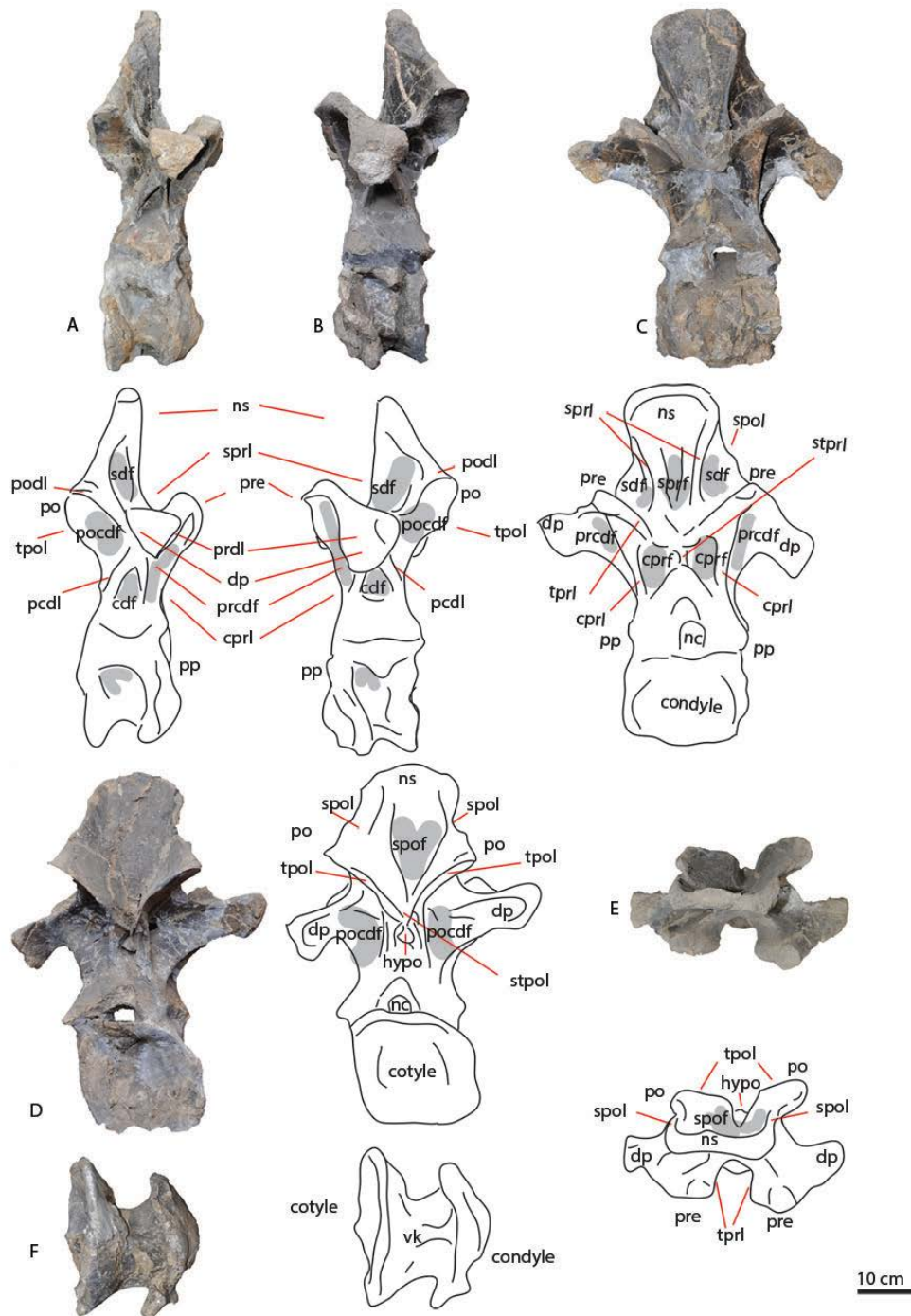
2951
 2952
 2953
 2954
 2955
 2956
 2957
 2958
 2959
 2960
 2961
 2962
 2963

Figure 9: Cervicodorsal PVL 4170 (8) in lateral (A,B), anterior (C), posterior (D), dorsal (E) and ventral(F) views. Abbreviations: acdl = anterior centrodiapophyseal lamina, cprl = centroprezygapophyseal lamina, cpol = centropostzygapophyseal lamina, dp = diapophysis, hypa = hypapophysis, nc = neural canal, ns = neural spine, pp = parapophysis, po = postzygapophysis, prcdf = prezygapophyseal centrodiapophyseal fossa, pocdf = postzygapophyseal centrodiapophyseal fossa, prdl = prezygapophyseal diapophyseal lamina, pre = prezygapophysis, sdf = spinodiapophysal fossa, spof = spinopostzygapophyseal fossa, spol = spinopostzygapophyseal lamina, sprf = spinoprezygapophyseal fossa, sprl = spinoprezygapophyseal lamina, tprl = intraprezygapophyseal lamina, tpol = intrapostzygapophyseal lamina, stpol = single intrapostzygapophyseal lamina, vk = ventral keel.



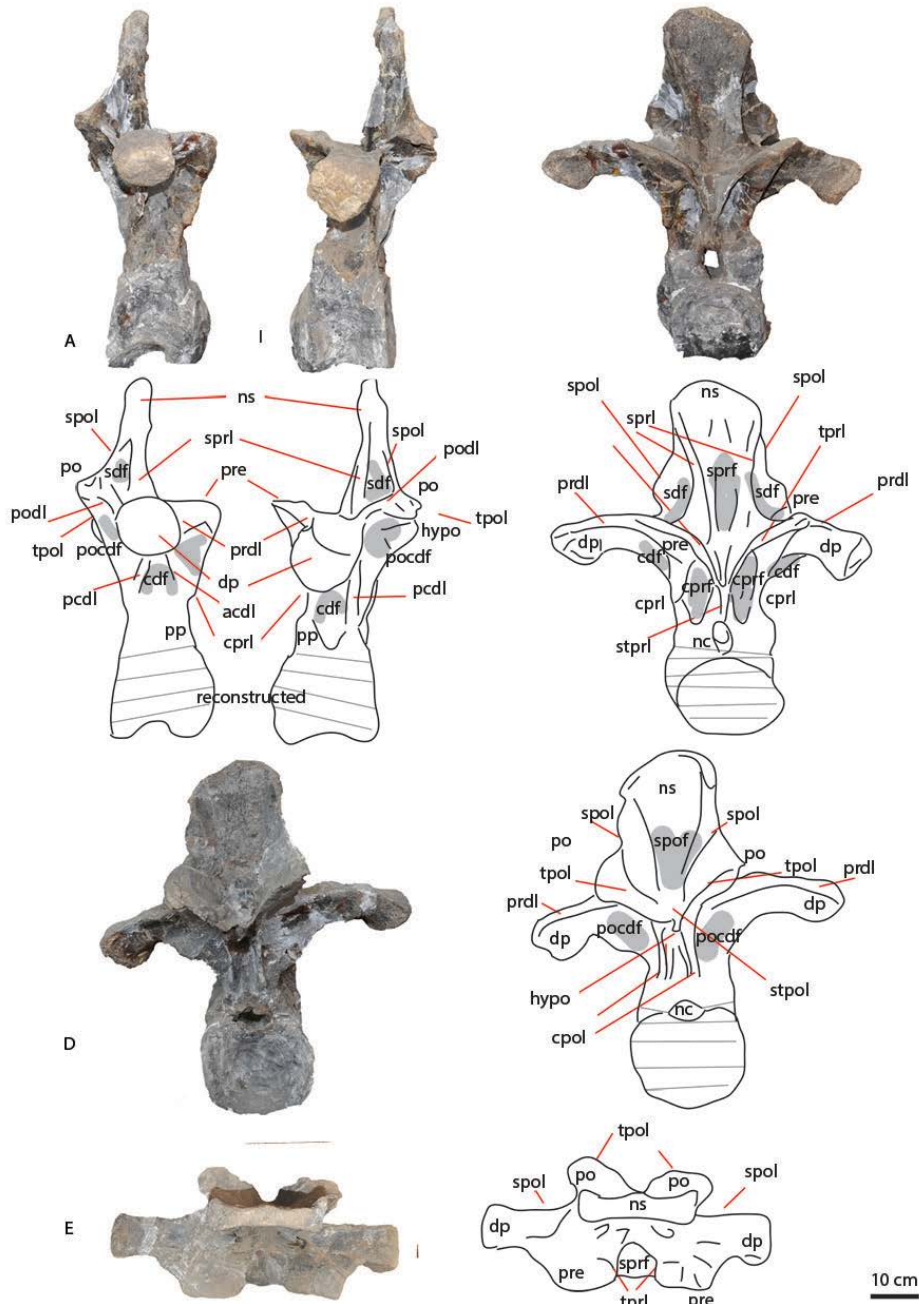
2964
 2965
 2966
 2967
 2968
 2969
 2970
 2971
 2972
 2973
 2974
 2975
 2976
 2977

Figure 10: Dorsal PVL 4170 (9) in lateral (A,B), anterior (C), posterior (D), dorsal (E) and ventral (F) views. Note part of this vertebra is reconstructed. Abbreviations: acdl = anterior centrodiapophyseal lamina, cprl = centroprezygapophyseal lamina, cpol = centropostzygapophyseal lamina, dp = diapophysis, hypa = hypapophysis, nc = neural canal, ns = neural spine, pcdl = posterior centrodiapophyseal lamina, pp = parapophysis, po = postzygapophysis, prcdf = prezygapophyseal centrodiapophyseal fossa, pocdf = postzygapophyseal centrodiapophyseal fossa, prdl = prezygapophyseal diapophyseal lamina, pre = prezygapophysis, sdf = spinodiapophysal fossa, spof = spinopostzygapophyseal fossa, spol = spinopostzygapophyseal lamina, sprf = spinoprezygapophyseal fossa, sprl = spinoprezygapophyseal lamina, tprl = intraprezygapophyseal lamina, tpol = intrapostzygapophyseal lamina, stpol = single intrapostzygapophyseal lamina, stprl = single intrapostzygapophyseal lamina, vk = ventral keel.



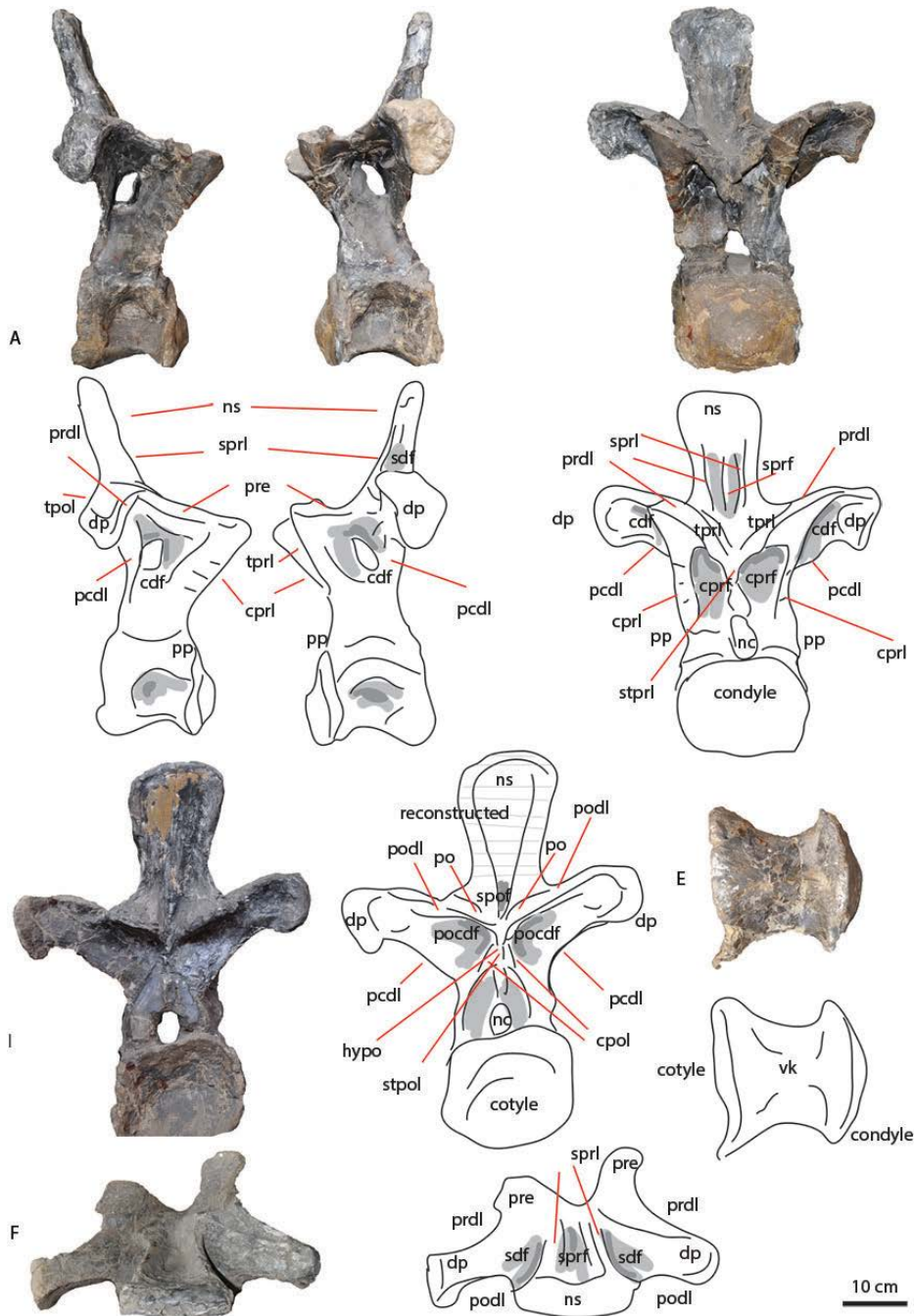
2978
 2979
 2980
 2981
 2982
 2983
 2984
 2985
 2986
 2987
 2988
 2989
 2990

Figure 11: MACN-CH 4170 (10) dorsal vertebra in lateral (A,B) anterior (C), posterior (D), dorsal (E) and ventral (F) views. Abbreviations: acdl = anterior centrodiapophyseal lamina, cdf = centrodiapophyseal fossa, cpri = centroprezygapophyseal lamina, dp = diapophysis, hypa = hypapophysis, nc = neural canal, ns = neural spine, pcdi = posterior centrodiapophyseal fossa, pp = parapophysis, po = postzygapophysis, prcdf = prezygapophyseal centrodiapophyseal fossa, pocdf = postzygapophyseal centrodiapophyseal fossa, prdl = prezygapophyseal diapophyseal lamina, pre = prezygapophysis, sdf = spinodiapophysal fossa, spof = spinopostzygapophyseal fossa, spol = spinopostzygapophyseal lamina, sprf = spinoprezygapophyseal fossa, sprl = spinoprezygapophyseal lamina, tprl = intraprezygapophyseal lamina, tpol = intrapostzygapophyseal lamina, stpol = single intrapostzygapophyseal lamina, stprl = single intrapostzygapophyseal lamina, vk = ventral keel.



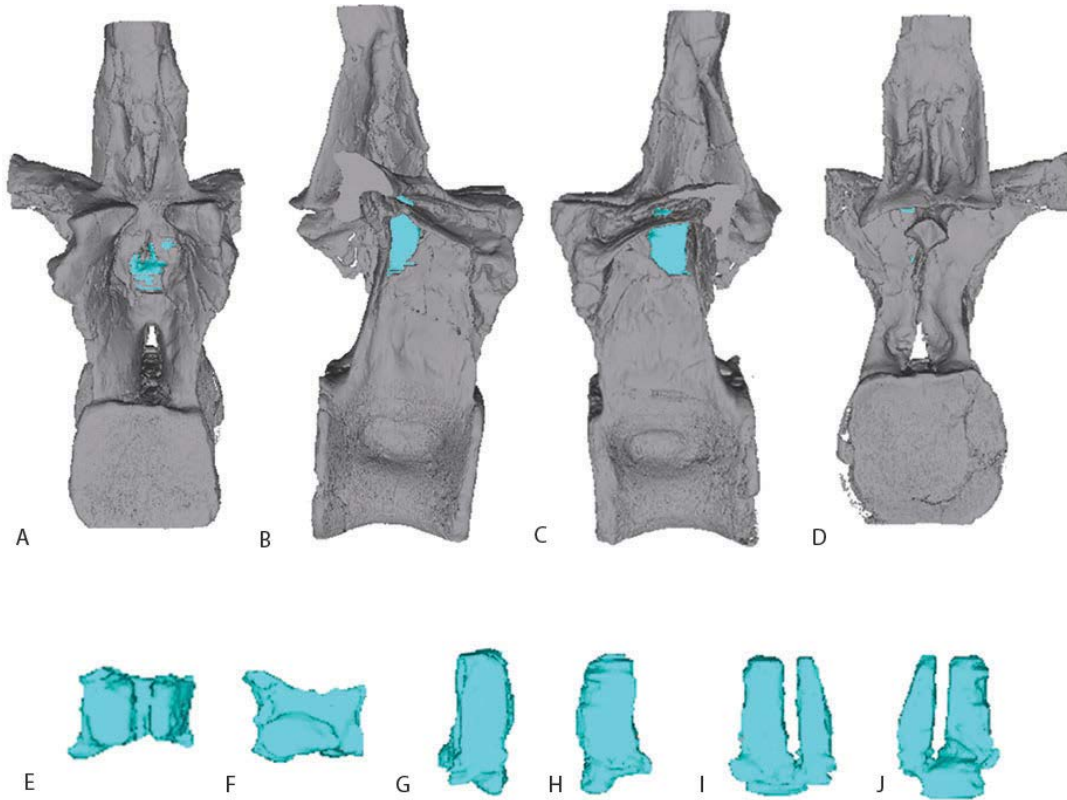
2991
 2992
 2993
 2994
 2995
 2996
 2997
 2998
 2999
 3000
 3001
 3002
 3003
 3004

Figure 12: Dorsal MACN-CH 4170 (11) in lateral (A,B) anterior (C), posterior (D), and dorsal (E) views. Note that the centrum is reconstructed, and a ventral view is therefore not given. Abbreviations: acdl = anterior centrodiapophyseal lamina, cdf = centrodiapophyseal fossa, cpol = centropostzygapophyseal lamina, cprl = centroprezygapophyseal lamina, dp = diapophysis, hypa = hypapophysis, nc = neural canal, ns = neural spine, pcdl = posterior centrodiapophyseal lamina, pp = parapophysis, po = postzygapophysis, prcdf = prezygapophyseal centrodiapophyseal fossa, pocdf = postzygapophyseal centrodiapophyseal fossa, prdl = prezygapophyseal diapophyseal lamina, pre = prezygapophysis, sdf = spinodiapophysal fossa, spof = spinopostzygapophyseal fossa, spol = spinopostzygapophyseal lamina, sprf = spinoprezygapophyseal fossa, sprl = spinoprezygapophyseal lamina, tprl = intraprezygapophyseal lamina, tpol = intrapostzygapophyseal lamina, stpol = single intrapostzygapophyseal lamina, stprl = single intrapostzygapophyseal lamina, vk = ventral keel.



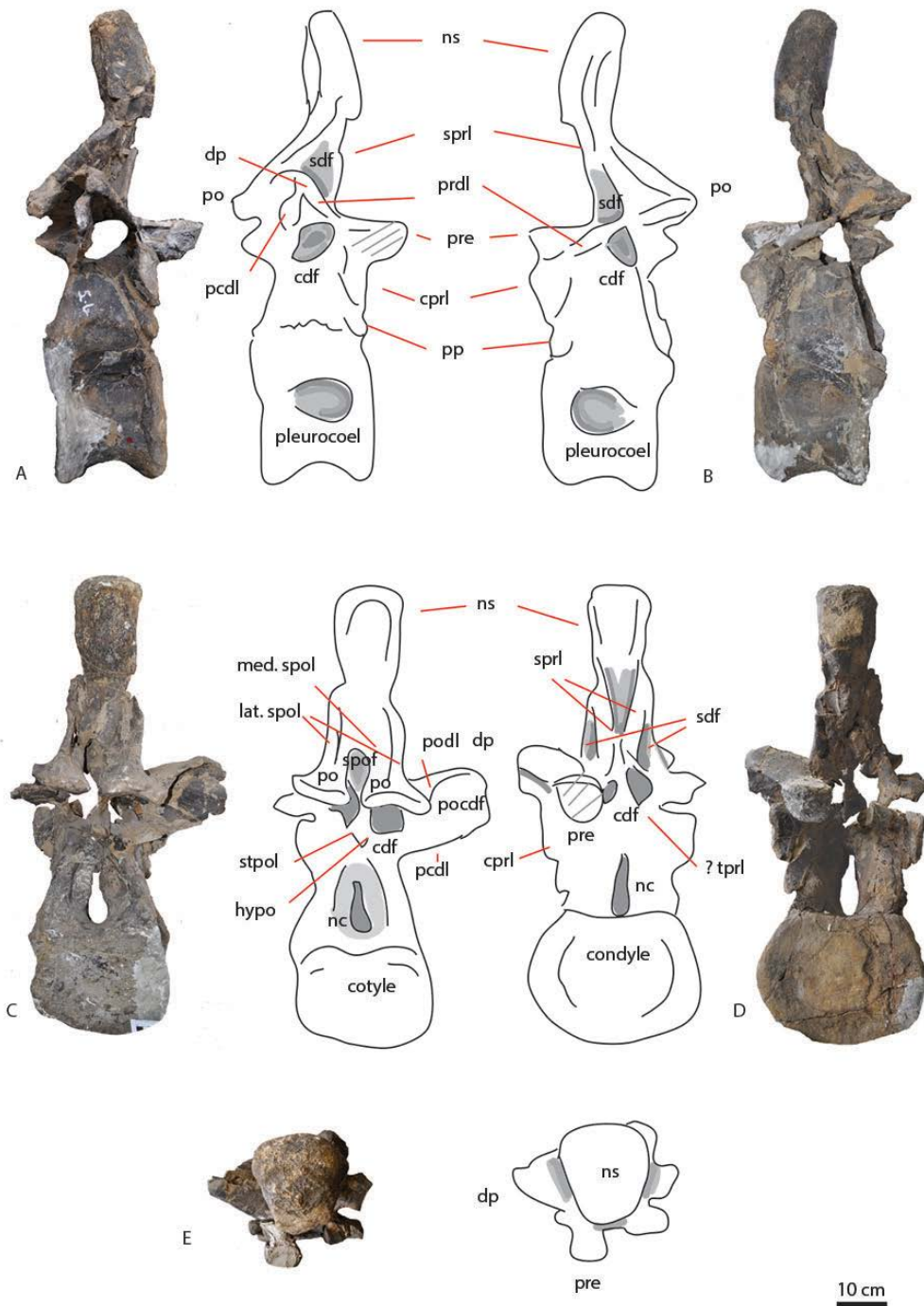
3005
 3006
 3007
 3008
 3009
 3010
 3011
 3012
 3013
 3014
 3015
 3016
 3017
 3018

Figure 13: Dorsal MACN-CH 4170 (12) in lateral (A,B) anterior (C), posterior (D), ventral (E) and dorsal (F) views. Note that a large part of the posterior neural arch and spine is reconstructed. Abbreviations: acdl = anterior centrodiapophyseal lamina, cpri = centroprezygapophyseal lamina, dp = diapophysis, hypa = hypapophysis, nc = neural canal, ns = neural spine, pccl = posterior centrodiapophyseal lamina, pp = parapophysis, po = postzygapophysis, prcdf = prezygapophyseal centrodiapophyseal fossa, pocdf = postzygapophyseal centrodiapophyseal fossa, prdl = prezygapophyseal diapophyseal lamina, pre = prezygapophysis, sdf = spinodiapophysal fossa, spof = spinopostzygapophyseal lamina, sprf = spinoprezygapophyseal fossa, sprl = spinoprezygapophyseal lamina, tprl = intraprezygapophyseal lamina, tpol = intrapostzygapophyseal lamina, stpol = single intrapostzygapophyseal lamina, stprl = single intrapostzygapophyseal lamina, vk = ventral keel.

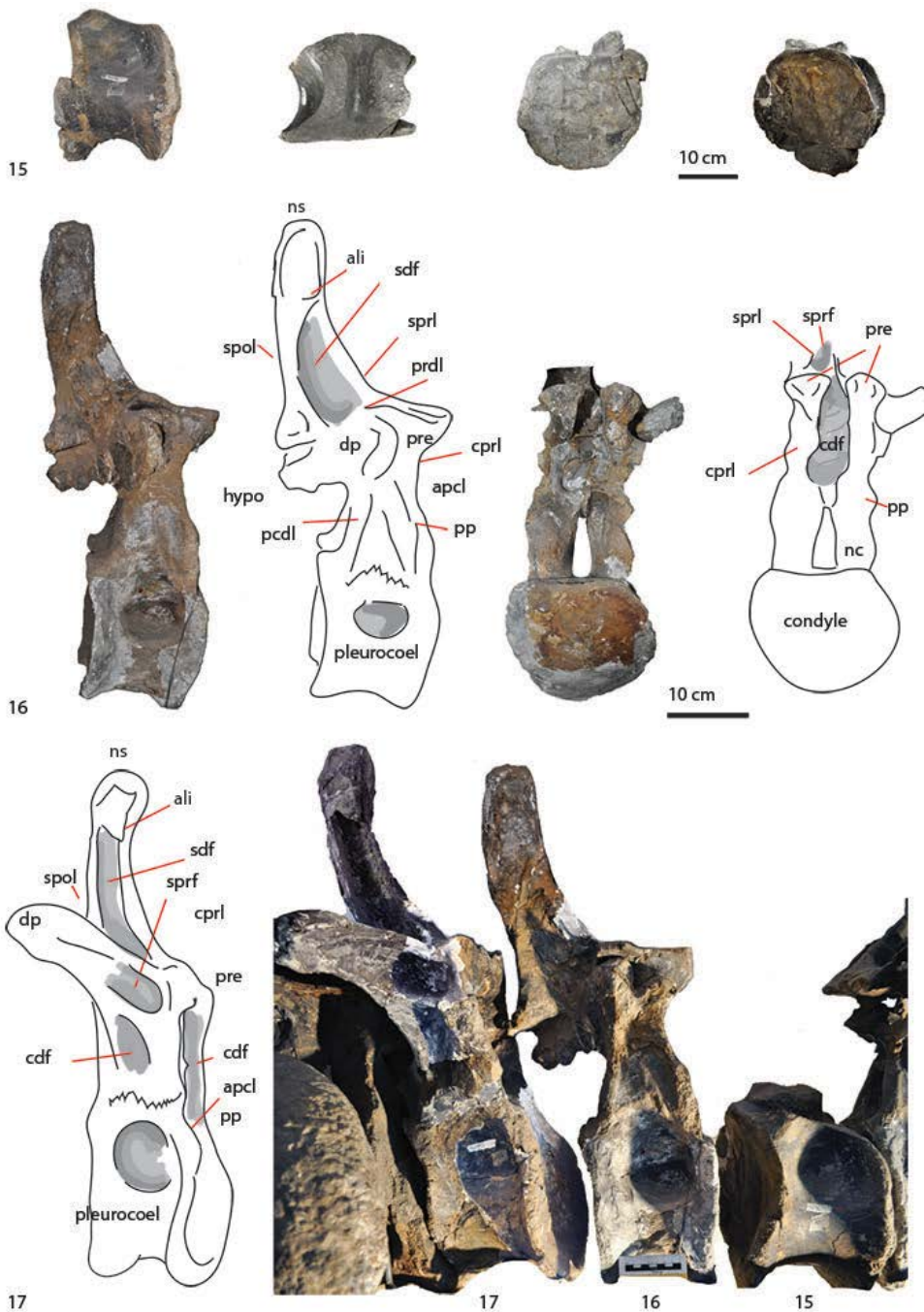


3019
3020
3021
3022

Figure 14: CT scan of PVL 4170 (13) in anterior (A), lateral (B,C) and posterior (D) views, with the shape of the internal pneumatic feature highlighted in light blue, in dorsal (E), ventral (F) lateral (G,H), anterior (I) and posterior (J) views.

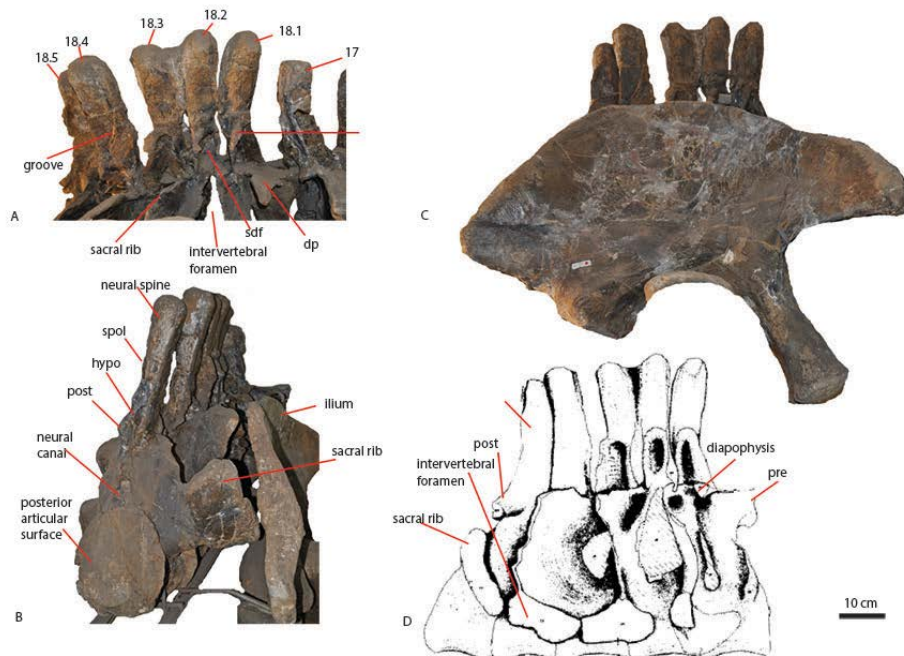


3036
 3037 Figure 16: Dorsal MACN-CH 4170 (14) in lateral (A,B), posterior (C), anterior (D), and dorsal
 3038 (E) views. Abbreviations: acdl = anterior centrodiapophyseal lamina, cpri =
 3039 centroprezygapophyseal lamina, dp = diapophysis, hypo = hypapophysis, nc = neural canal,
 3040 ns = neural spine, pp = parapophysis, po = postzygapophysis, prcdf = prezygapophyseal
 3041 centrodiapophyseal fossa, pocdf = postzygapophyseal centrodiapophyseal fossa, prdl =
 3042 prezygapophyseal diapophyseal lamina, pre = prezygapophysis, sdf = spinodiapophyseal
 3043 fossa, spof = spinopostzygapophyseal fossa, spol = spinopostzygapophyseal lamina, sprl =
 3044 spinoprezygapophyseal fossa, sprl = spinoprezygapophyseal lamina, tprl =
 3045 intraprezygapophyseal lamina, tpol = intrapostzygapophyseal lamina, lat.spol/med.spol =
 3046 lateral/medial spinopostzygapophyseal lamina, stpol = single intrapostzygapophyseal
 3047 lamina, stprl = single intraprezygapophyseal lamina, vk = ventral keel.
 3048



3049
 3050
 3051
 3052
 3053
 3054
 3055
 3056
 3057
 3058
 3059
 3060
 3061
 3062

Figure 17: Dorsals PVL 4170 (15,16,17). PVL 4170 (15) in lateral, dorsal, anterior, posterior (oblique) view. PVL 4170 (16) in lateral and anterior view. PVL 4170 (17) in lateral view. Abbreviations: acdl = anterior centrodiapophysal lamina, ali = aliform process, cprl = centroprezygapophysal lamina, cpol = centropostzygapophysal lamina, dp = diapophysis, hypa = hypapophysis, nc = neural canal, ns = neural spine, pp = parapophysis, po = postzygapophysis, prcdf = prezygapophysal centrodiapophysal fossa, pocdf = postzygapophysal centrodiapophysal fossa, prdl = prezygapophysal diapophysal lamina, pre = prezygapophysis, sdf = spinodiapophysal fossa, spof = spinopostzygapophysal fossa, spol = spinopostzygapophysal lamina, sprf = spinoprezygapophysal fossa, sprl = spinoprezygapophysal lamina, tprl = intraprezygapophysal lamina, tpol = intrapostzygapophysal lamina, stpol = single intrapostzygapophysal lamina, stprl = single intrapostzygapophysal lamina, vk = ventral keel.



3063
 3064 Figure 18: Upper row: All presacral vertebrae of MACN-CH 4170 (1-17) in left lateral view
 3065 (not to scale). Lower row: all sacral vertebrae of PVL 4170 (18) sacrum. A: PVL 4170 (18.1-5)
 3066 sacral neural arches and spines in right lateral view with dorsal PVL 4170 (17) on the right. B:
 3067 PVL 4170 (18) in posterior view. C: PVL 4170 (18) associated with ilium PVL 4170 (34). D:
 3068 Original drawing of PVL 4170 (Bonaparte, 1986b). Abbreviations: hypo = hyposphene, pre =
 3069 prezygapophysis, post = postzygapophysis, spol = spinopostzygapophyseal lamina.

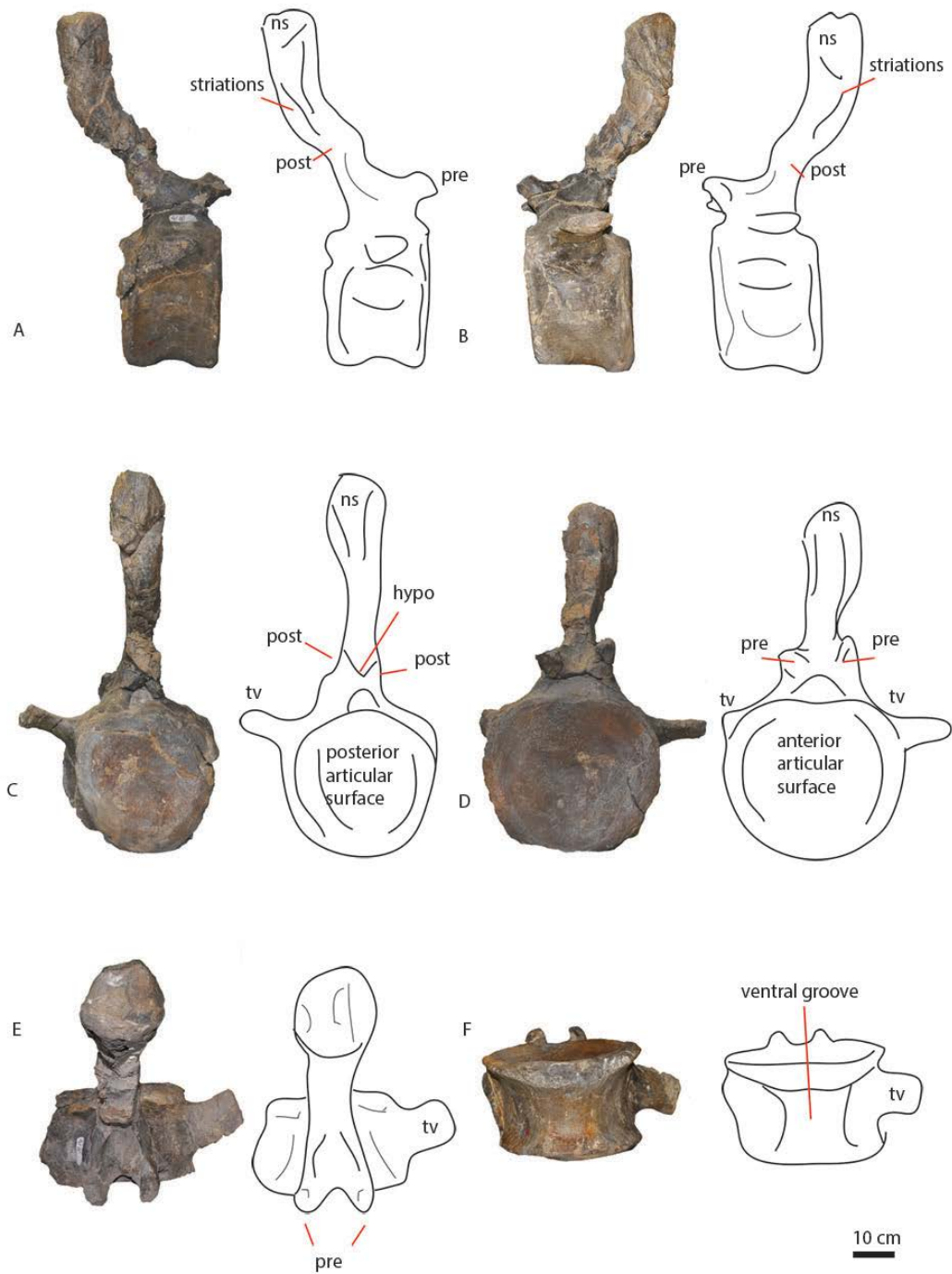


3070
 3071 Figure 19: Anterior Caudals PVL 4170 (19-20-21) in lateral view.



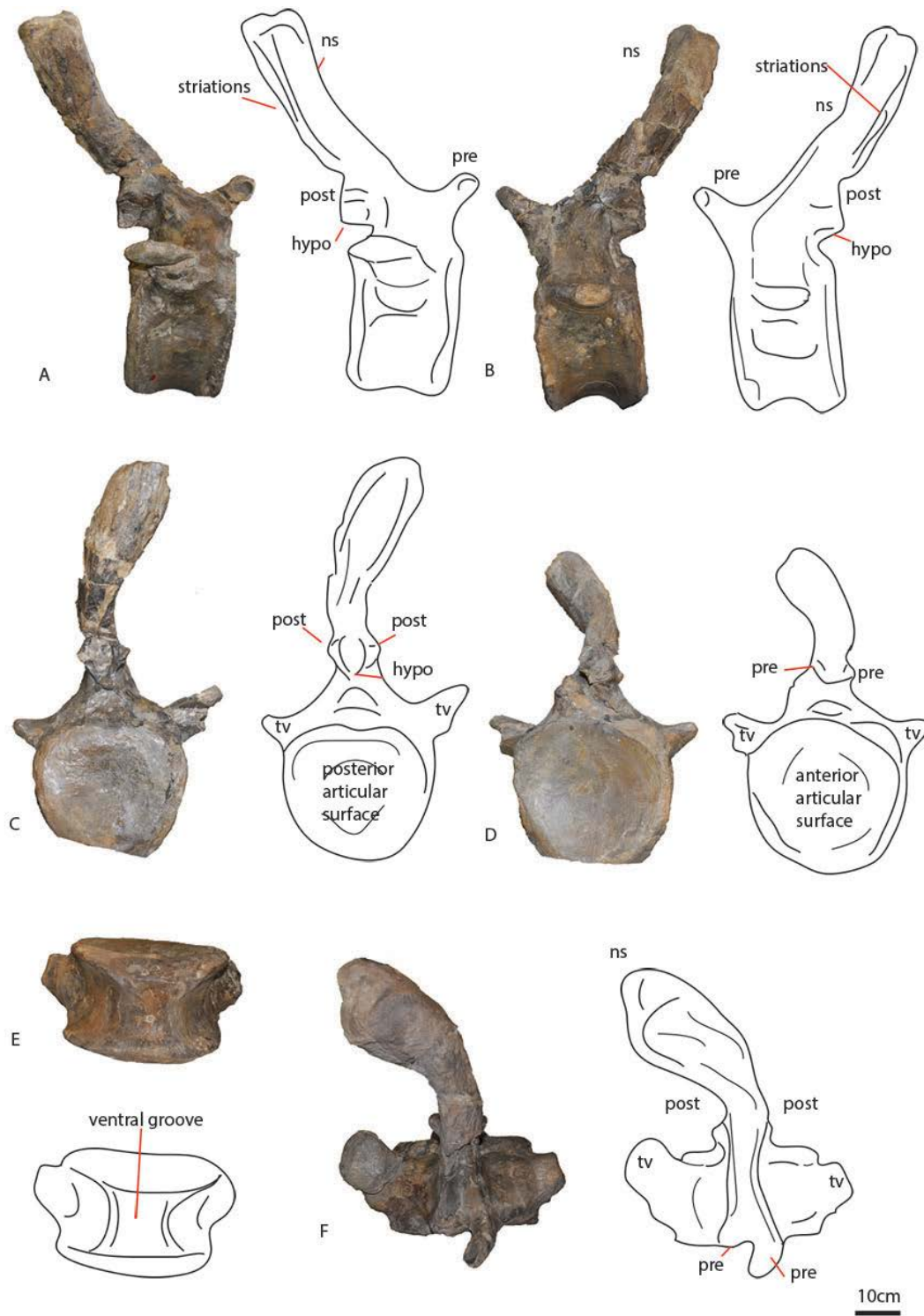
3072
3073

Figure 20: Middle Caudals PVL 4170 (22-23-24) in lateral view.



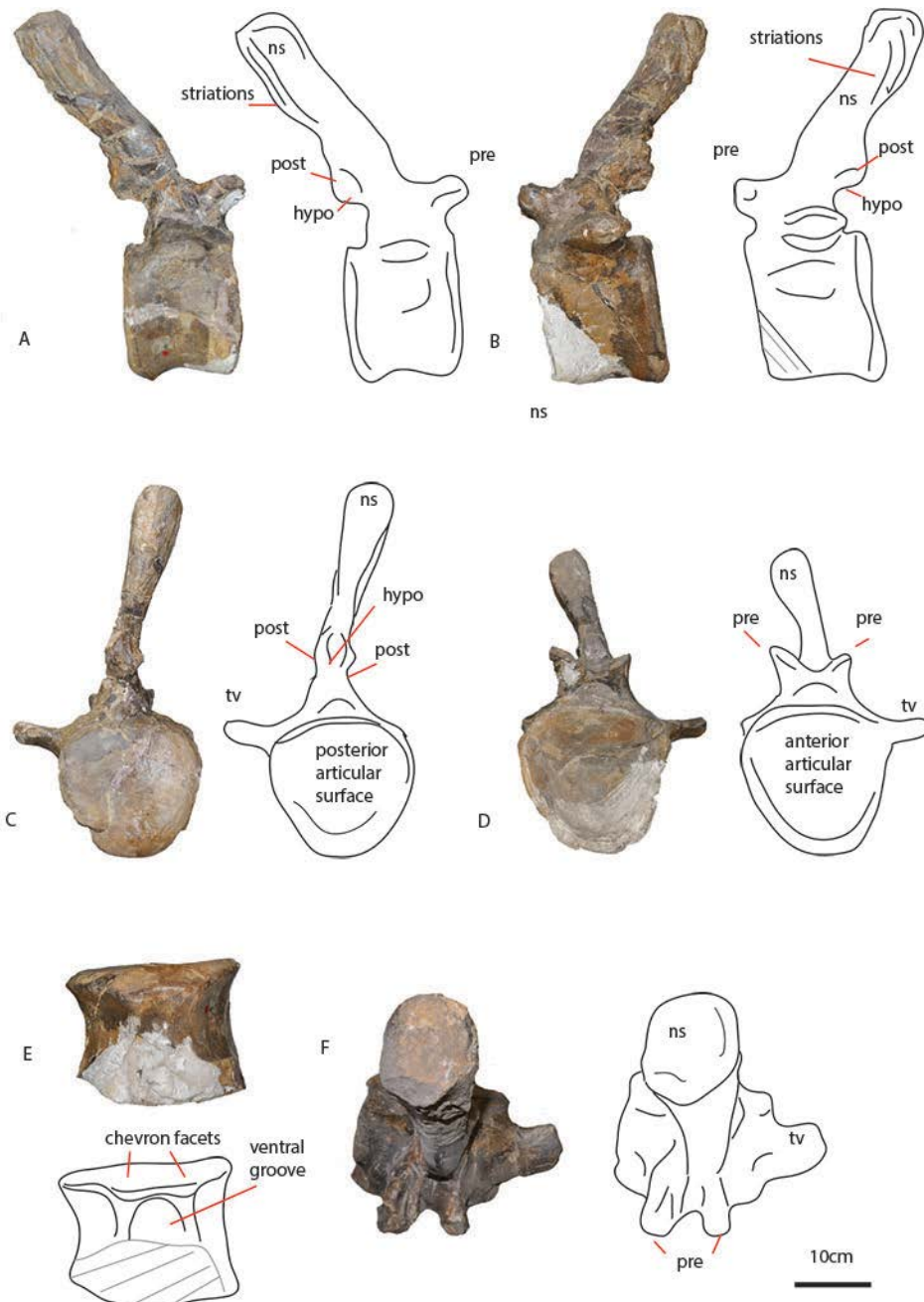
3074
 3075
 3076
 3077

Figure 21: Caudal PVL 4170 (19) in lateral (A,B), posterior (C), anterior (D) and ventral (E) and dorsal (F) views. Abbreviations: hypo = hyposphene, ns = neural spine, post = postzygapophysis, pre = prezygapophysis, tv = transverse process.



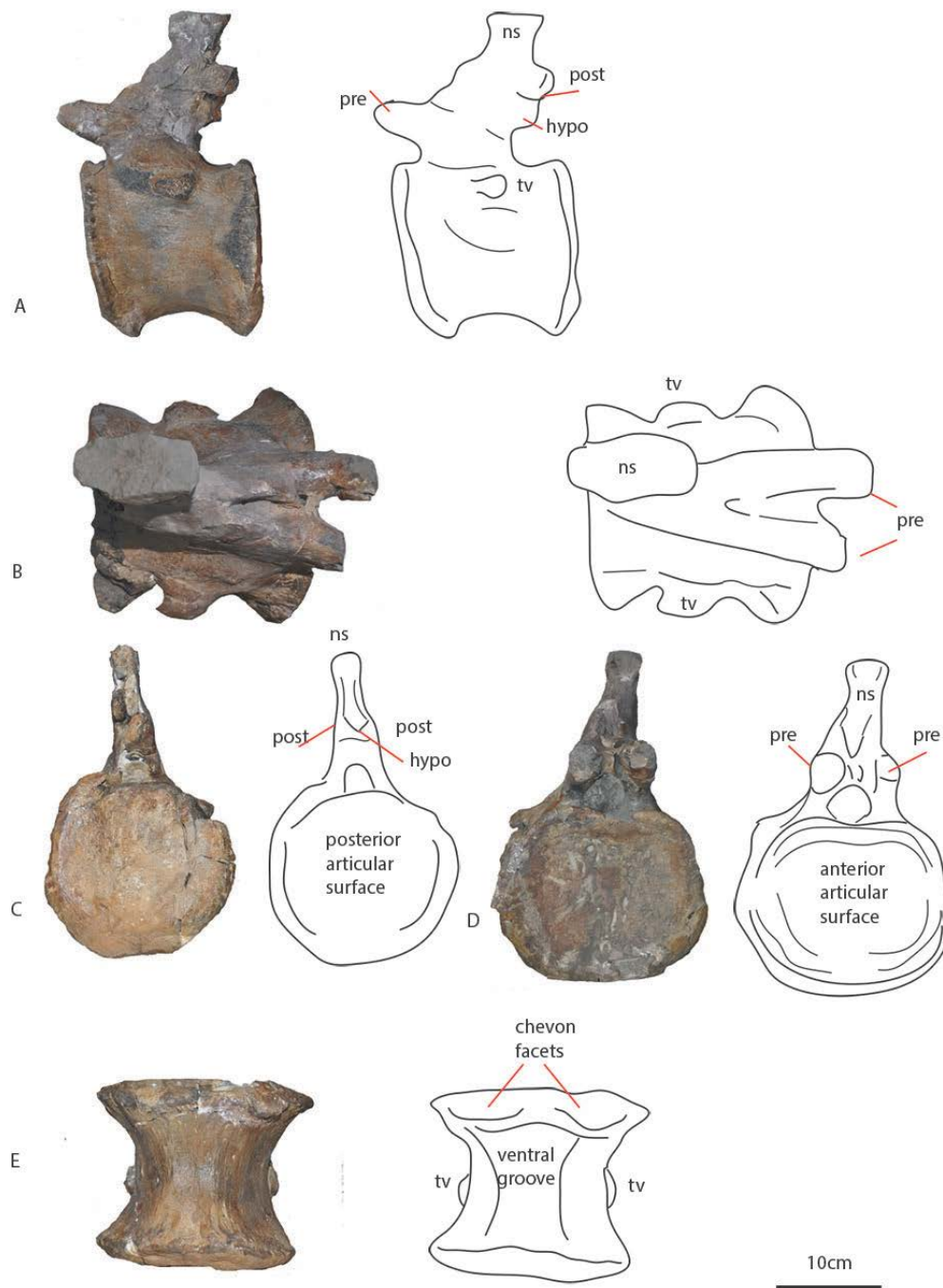
3078
 3079
 3080
 3081

Figure 22: Caudal PVL 4170 (20) in lateral (A,B), posterior (C), anterior (D), dorsal (E) and ventral (F) views. Abbreviations: hypo = hyosphene, ns = neural spine, post = postzygapophysis, pre = prezygapophysis, tv = transverse process.



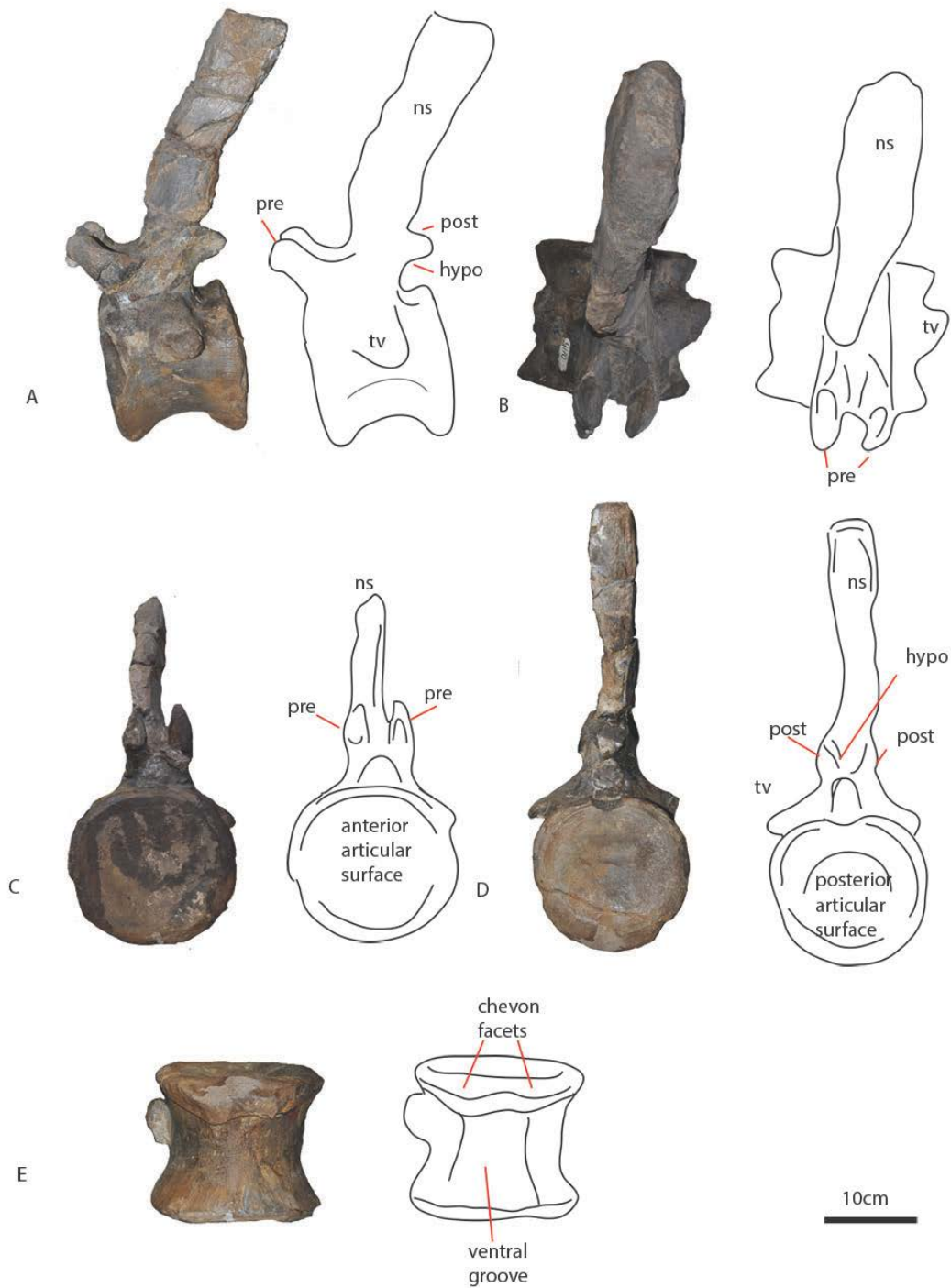
3082
 3083
 3084
 3085
 3086

Figure 23: Caudal PVL 4170 (21) in lateral (A,B), posterior (C), anterior (D), ventral (E) and dorsal (F) views. Abbreviations: hypo = hyposphene, ns = neural spine, post = postzygapophysis, pre = prezygapophysis, tv = transverse process.



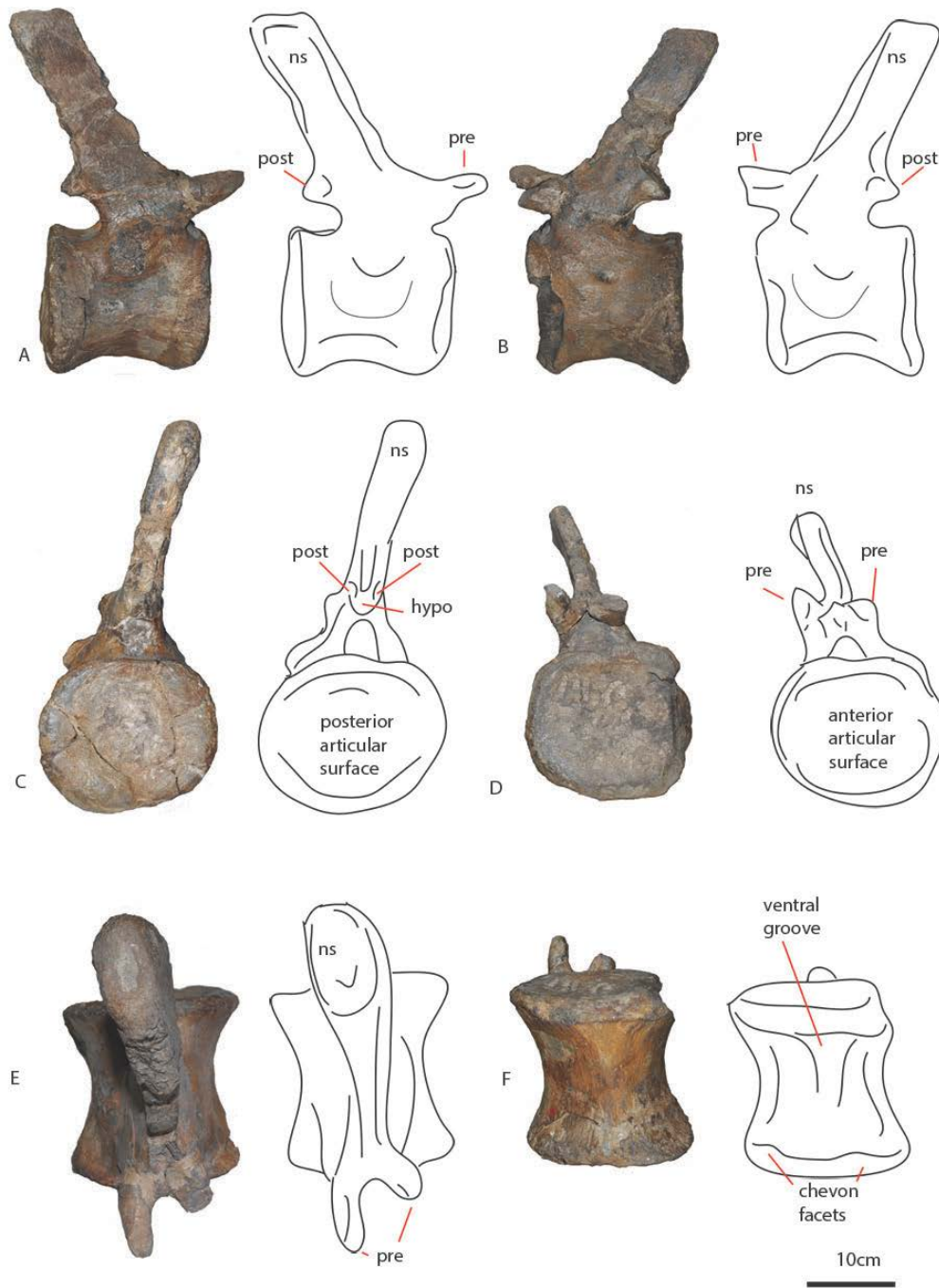
3087
 3088
 3089
 3090
 3091

Figure 24: Caudal PVL 4170 (22) in lateral (A), dorsal (B), posterior (C), anterior (D) and ventral (E) views. Abbreviations: hypo = hyposphene, ns = neural spine, post = postzygapophysis, pre = prezygapophysis, tv = transverse process.



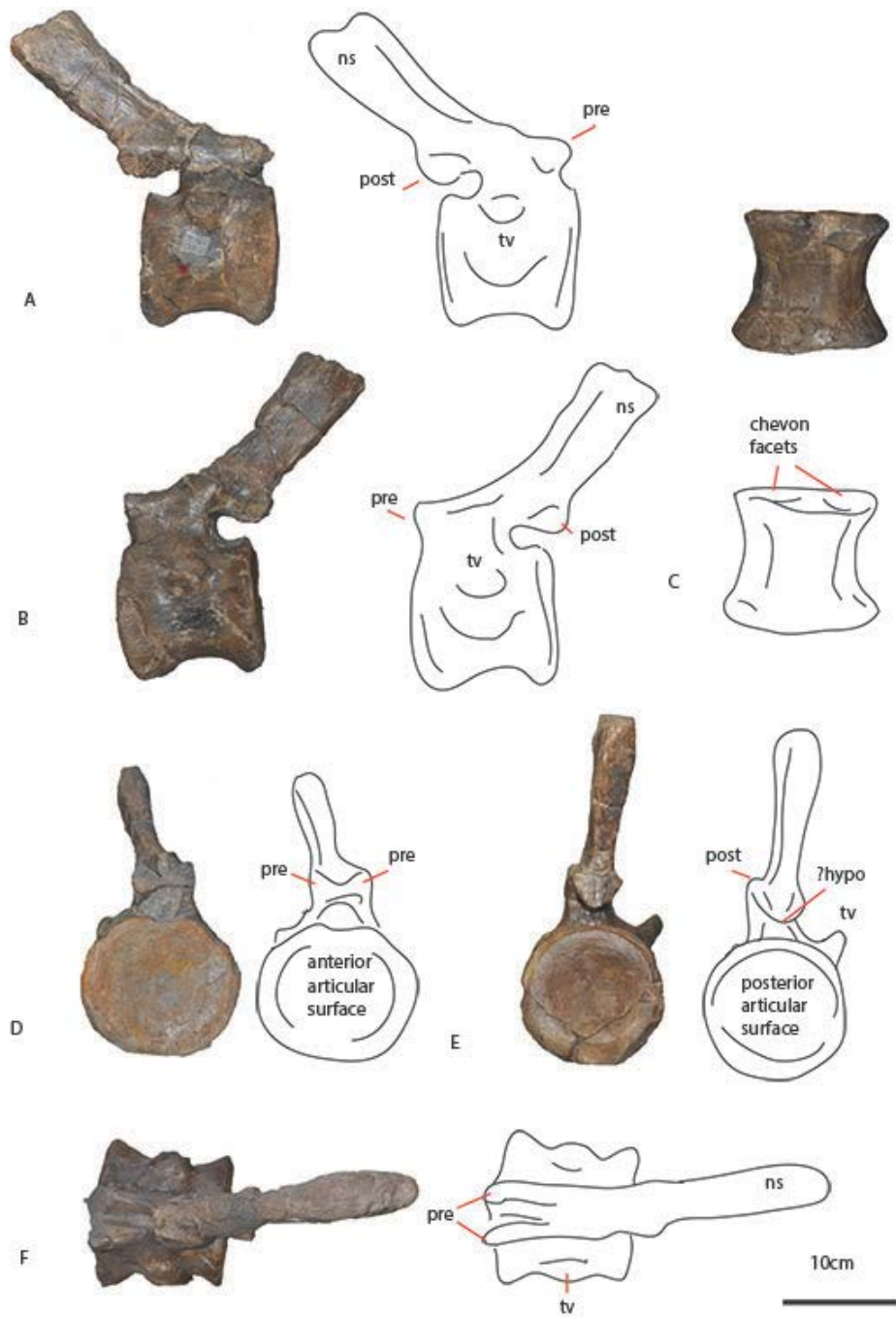
3092
 3093
 3094
 3095
 3096

Figure 25: Caudal PVL 4170 (23) in lateral (A), dorsal (B), anterior (C), posterior (D) and ventral (E) views. Abbreviations: hypo = hyposphene, ns = neural spine, post = postzygapophysis, pre = prezygapophysis, tv = transverse process.



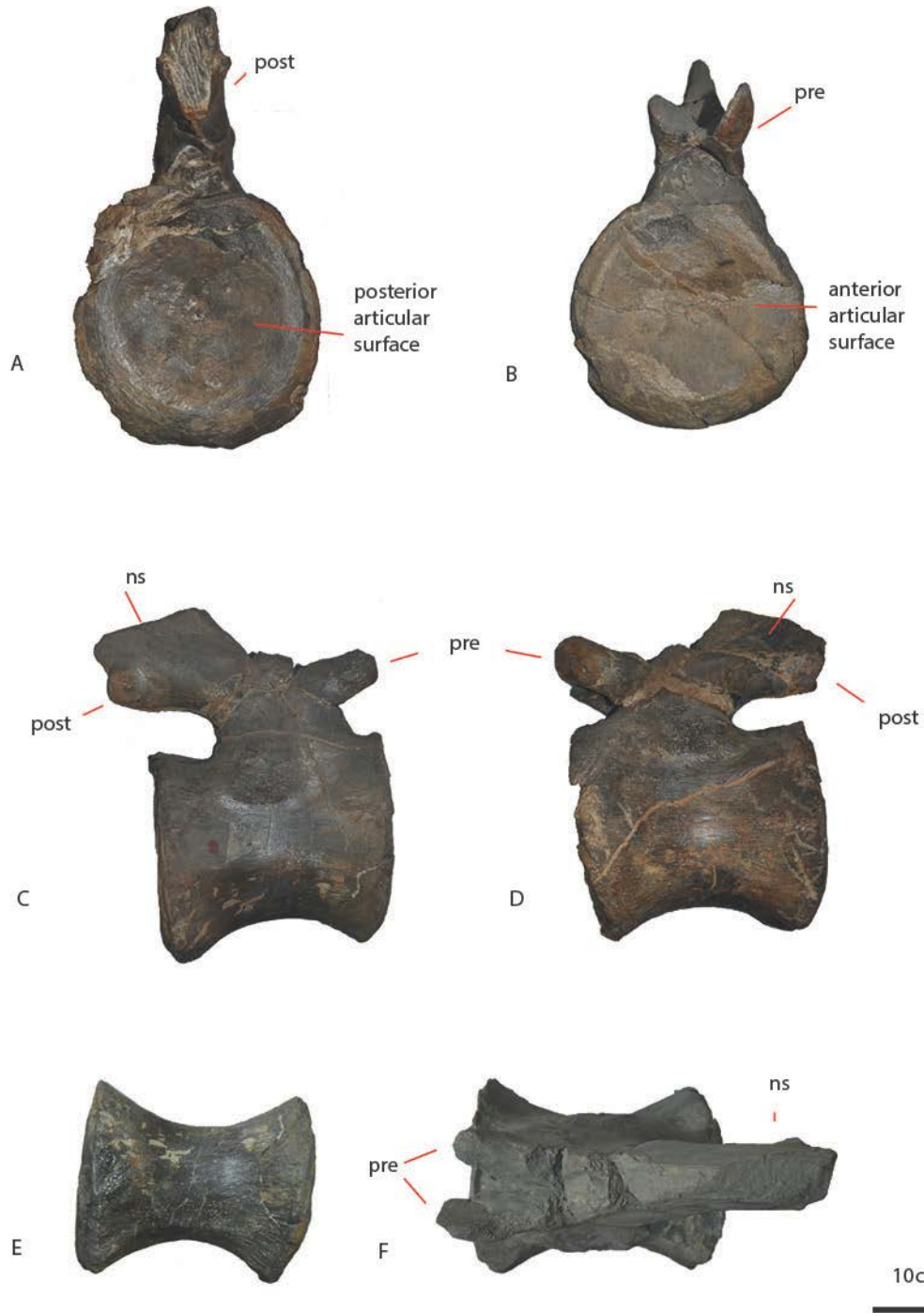
3097
 3098
 3099
 3100
 3101

Figure 26: Caudal PVL 4170 (24) in lateral (A,B), posterior(C), anterior (D), dorsal (E) and ventral (F) views. Abbreviations: hypo = hyposphene, ns = neural spine, post = postzygapophysis, pre = prezygapophysis, tv = transverse process.



3102
 3103
 3104
 3105
 3106

Figure 27: Caudal PVL 4170 (25) in lateral (A,B), ventral (C), anterior (D), posterior (E), and dorsal (F) views. Abbreviations: hypo = hyposphene, ns = neural spine, post = postzygapophysis, pre = prezygapophysis, tv = transverse process.



3107
 3108
 3109
 3110
 3111

Figure 28: Caudal PVL 4170 (26) in posterior (A), anterior (B), lateral (C,D), ventral (E), and dorsal (F) views. Abbreviations: ns = neural spine, post = postzygapophysis, pre = prezygapophysis, tv = transverse process.



3112
3113
3114
3115

Figure 29: Caudal PVL 4170 (27) in dorsal (A), ventral (B), lateral (C,D), posterior (E), anterior (F) views.



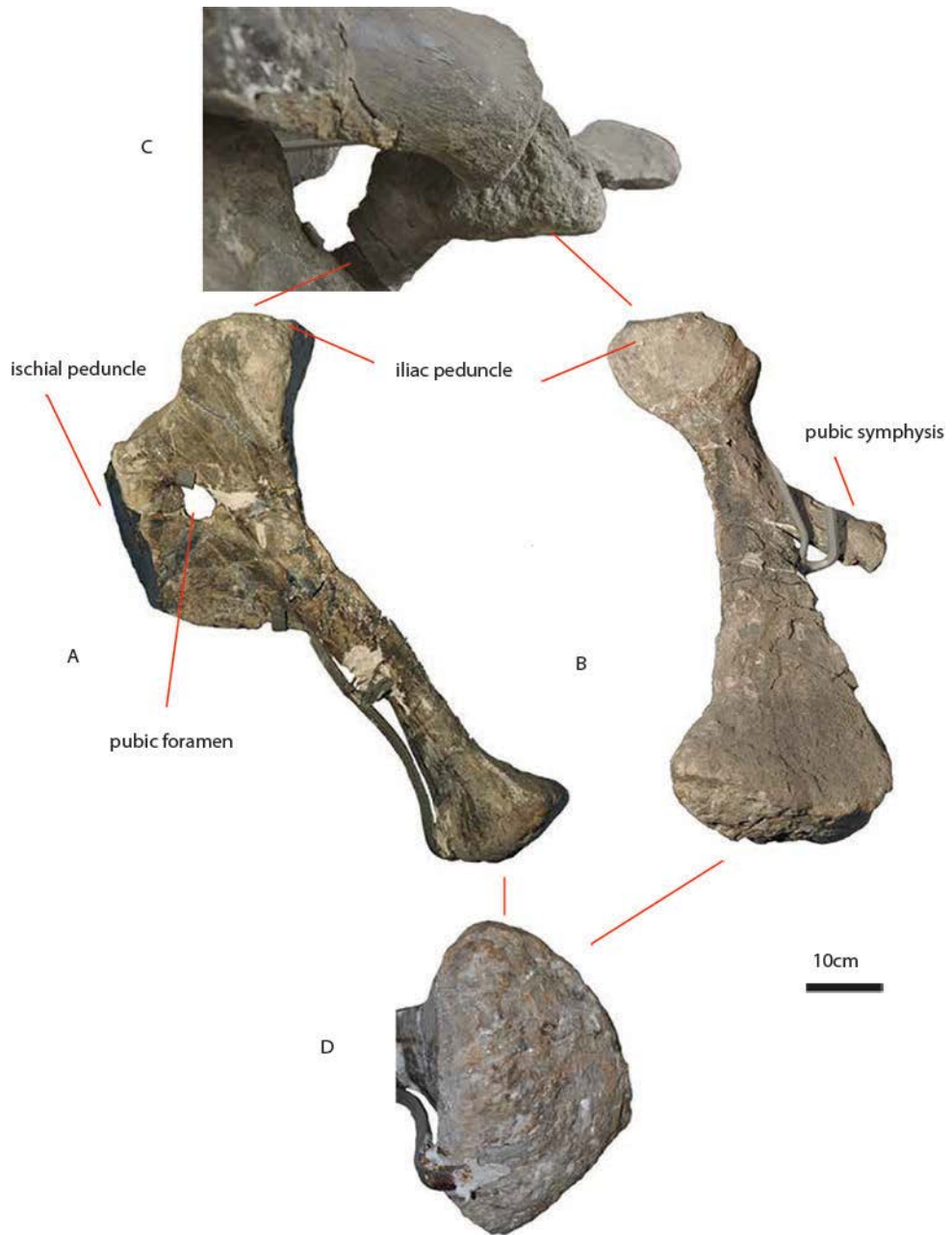
3116
3117
3118
3119

Figure 30: Caudal PVL 4170 (30) in anterior (A), posterior (B), ventral (C), dorsal (D), lateral (E,F) views.



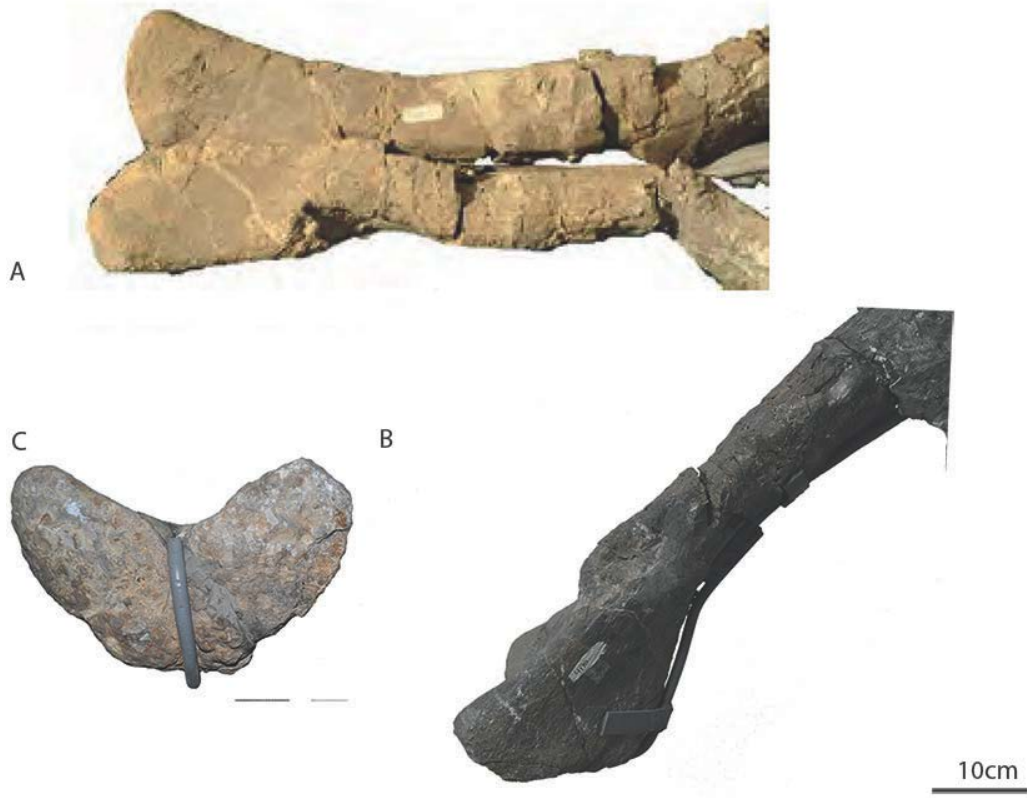
3120
3121
3122

Figure 31: PVL 4170 (34) ilium in anterior (A) posterior (B) and lateral (C) view.



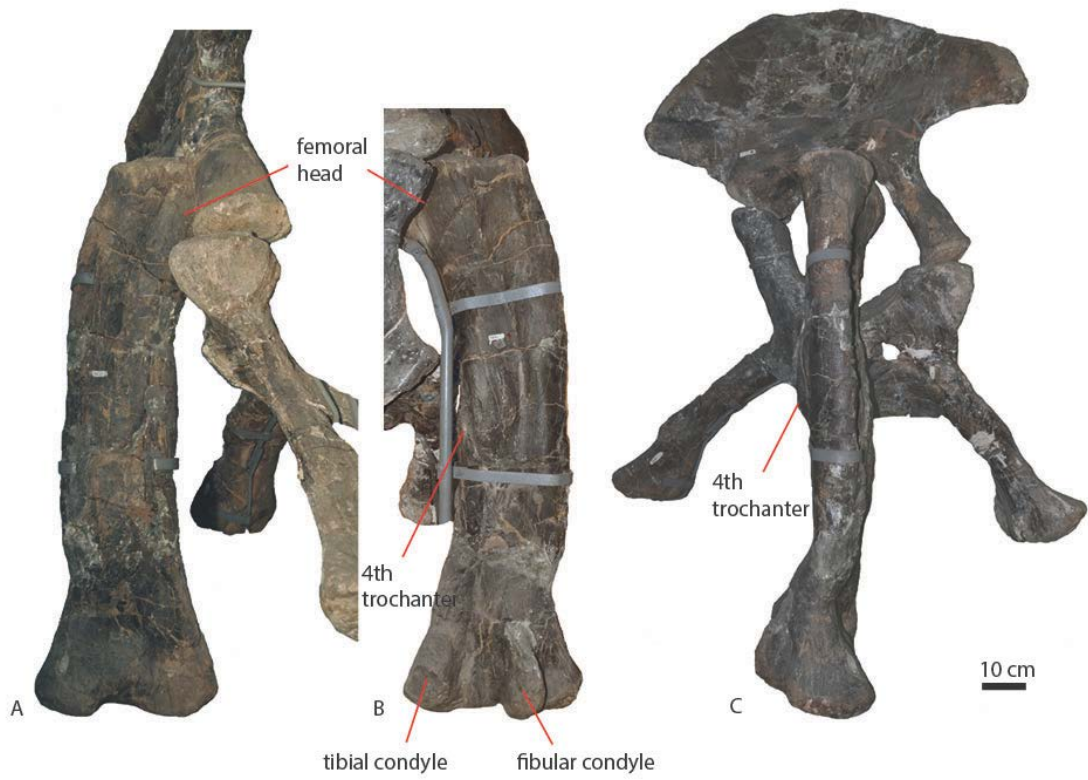
3123
3124
3125
3126

Figure 32: PVL 4170 (35) Pubis in lateral (A), distal (B), dorsal (C) and distal-most (D) view. Note that D is not to scale.



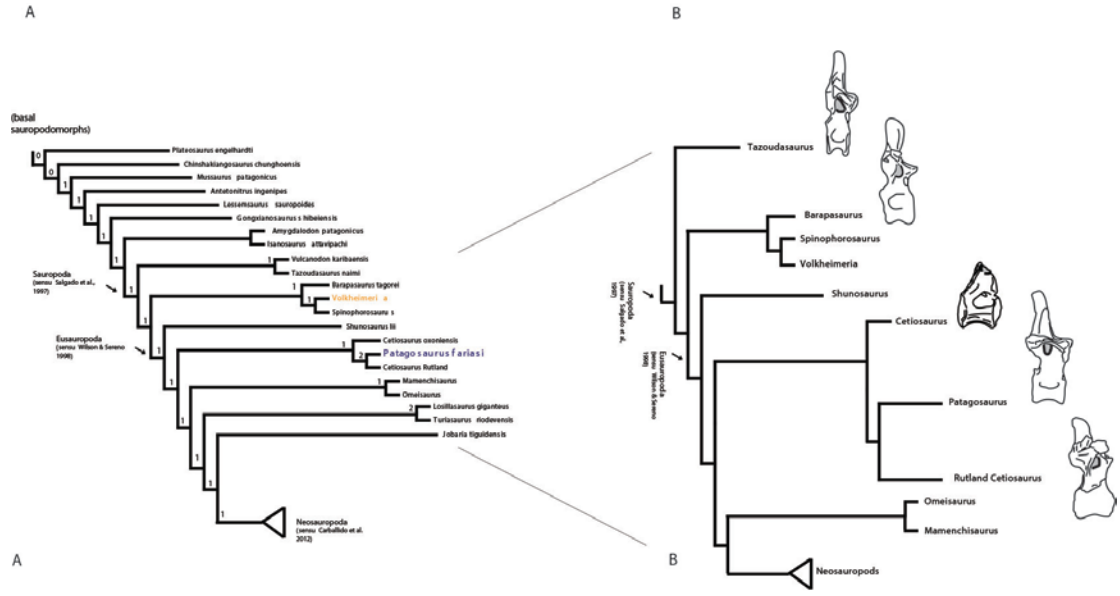
3127
3128
3129

Figure 33: PVL 4170 (36) ischia in dorsal (A) view, distal (B) view, and lateral (C) view.



3130
3131

Figure 34: PVL 4170 (37) Femur in (A) posterior, (B) anterior, and (C) lateral view.



3133
 3134
 3135
 3136
 3137
 3138
 3139
 3140
 3141
 3142
 3143
 3144
 3145
 3146
 3147
 3148
 3149
 3150

Figure 35: Simplified phylogenetic tree based on Holwerda & Pol, (2018) (A), with posterior dorsal vertebrae of *Tazoudasaurus*, *Barapasaurus*, *Cetiosaurus oxoniensis* and the Rutland *Cetiosaurus* showing possible analogous pneumatic features with *Patagosaurus* highlighted in grey (B).

Tables

- Table 1: EI and aEI for several sauropod cervicals
- Table 2: measurements of all presacral (1-17, blue), sacral (18, red), and caudal (19-30, green) vertebrae.
- Table 3: Measurements on appendicular elements of PVL 4170.